

Understanding Variability of Stream Productivity at Different Scales and Consequences for
Aquatic Food Webs

A Dissertation

Presented in Partial Fulfillment of the Requirements for the

Degree of Doctorate of Philosophy

with a

Major in Natural Resources

in the

College of Graduate Studies

University of Idaho

by

Francine H. Mejia

Major Professor: Alexander K. Fremier, Ph.D.

Committee Members: Colden V. Baxter, Ph.D., James R. Bellmore, Ph.D.,
Christopher C. Caudill, Ph.D.

Department Chair: Lisette Waits, Ph.D.

April 2016

Authorization to Submit Dissertation

This dissertation of Francine H. Mejia, submitted for the degree of Doctorate of Philosophy with a major in Natural Resources and titled “Understanding Variability of Stream Productivity at Different Scales and Consequences for Aquatic Food Webs,” has been reviewed in final form. Permission, as indicated by the signatures and dates given below, is now granted to submit final copies to the College of Graduate Studies for approval.

Major Professor: _____ Date: _____
Alexander K. Fremier, Ph.D.

Committee Members: _____ Date: _____
Colden V. Baxter, Ph.D.

_____ Date: _____
James R. Bellmore, Ph.D.

_____ Date: _____
Christopher C. Caudill, Ph.D.

Department

Administrator: _____ Date: _____
Lisette Waits, Ph.D.

Abstract

Streams and rivers are dynamic systems that vary over space and time. Understanding the relationship of spatial and temporal heterogeneity to ecosystem functions such as gross primary productivity, ecosystem respiration and growth is critical so we can understand and predict the consequences of human impacts on spatial and temporal patterns of lotic systems. These modifications have the potential effect of homogenizing and simplifying stream and river networks. I aimed to understand how the spatial organization and temporal patterns of a stream network affect stream productivity at different trophic levels. Chapter 2 focused on how the network spatial organization and temporal patterns influence groundwater inputs and subsequently how areas of active groundwater-surface water exchange increased stream productivity of multiple trophic levels (i.e. post emergent salmon, benthic invertebrates, and periphyton biomass). In Chapter 3, I used metabolic theory concepts to predict variation on the relationship between stream temperature and stream metabolism across the network. These findings highlight how stream networks may play a role in the global carbon cycle as increasing global surface temperatures have been associated with climate change. Lastly, in Chapter 4, I described the spatial and temporal patterns of stream metabolism at the reach and network scales. I found that stream metabolism increased with stream size and peaked asynchronously across the network with three main peaks observed (summer, winter and multiple). These findings underline the importance of sampling throughout the year and capturing the temporal variability of the system. My results suggest predictions derived solely from summer estimates can have the potential to either overestimate or underestimate metabolism depending on the location in the watershed. I also discussed the influences of these patterns on higher trophic levels and the

implications on management, conservation and restoration efforts. Each chapter focused on different temporal and spatial scales because to evaluate biological responses, ecological relevance must be taken into account to select the appropriate spatial and temporal scale. For example, post-emergent salmon operate at a smaller spatial and narrower temporal scale than stream metabolism. Thus, study designs reflected this to match the scale of observation with the scale of response.

Acknowledgements

This degree has indeed been a journey, and I have many people to thank for their support and encouragement. I have to first thank Dr. Alex Fremier for taking a chance on me. I am grateful for your mentorship and hope I didn't disappoint! I am also grateful to the thesis committee, Drs. Ryan Bellmore, Colden Baxter, and Chris Caudill. I am grateful for your guidance and insight. I also thank Dr. Joseph Benjamin for his invaluable help with the metabolism work and statistical analyses. Many thanks to the Fremier Lab – Dr. Kath Strickler, Aline Ortega, Adrienne Zuckerman (now Grimm), Rachel Hutchinson, Liza Mitchell, Cat Weichmann, Amanda Stahl, Laura Livingston, Joe Parzych, and John Jorgensen. Grace Watson of USGS (now Methow Salmon Recovery), was instrumental in the field; without her help, Chapters 3 and 4 would not have been possible. Last, but not least I want to thank Eric Berntsen. He is not only my life partner, but my best friend who helped me in many different aspects of this work, and without his support, I would not have embarked on this journey. This research was primarily supported by a grant from the Bureau of Reclamation, Portland, OR, Cooperative Agreement #R11 AC 17 061. Thanks to Michael Newsom for support of this work.

Dedication

This dissertation is dedicated to my mom. She has always put my success and happiness before hers, and for that I am eternally grateful

Table of Contents

Authorization to Submit Dissertation	ii
Abstract	iii
Acknowledgements	v
Dedication	vi
Table of Contents	vii
List of Tables	xi
List of Figures	xiii
CHAPTER 1: General Introduction	1
Background	1
Chapter 2	2
Chapter 3	3
Chapter 4	4
References	5
CHAPTER 2: Linking Groundwater-Surface Water Exchange to Food Production and Salmonid Growth	10
Introduction	10
Methods	12
Study Area and Site Selection	12
Multi-Trophic Level Responses	14
Growth of fish in enclosures	14
Observation of wild fish	15
Benthic invertebrates, gross primary production and periphyton biomass	16

Groundwater-Surface Water Exchange	18
Environmental Variables	18
Bioenergetics Simulations	19
Statistical Analyses	20
GW-SW exchange associations	20
Direct and indirect associations across trophic levels.....	22
Results.....	23
GW-SW Exchange and Associated Environmental Variables	23
Responses of Trophic Levels to GW-SW Exchange.....	24
Direct and Indirect Relationships Across Trophic Levels.....	25
Discussion.....	27
References.....	33
Tables.....	45
Figures.....	47
CHAPTER 3 – Understanding the Variability of Temperature Dependence of Stream Metabolism Across a Watershed	54
Introduction.....	54
Methods.....	56
Study Area	56
Periphyton Biomass, Physical and Chemical Measurements	57
Stream Metabolism Estimates	59
Statistical Analyses	60
Results.....	61

Stream Metabolism Estimates	61
Water Temperature and Periphyton Ash Free Dry Mass (AFDM)	61
Other Environmental Variables	62
Temperature Dependency of Stream Metabolism	63
Temperature Dependence Variability Across the Watershed.....	64
Discussion.....	65
References.....	69
Tables.....	75
Figures.....	79
CHAPTER 4: Stream Metabolism Increases with Drainage Area and Peaks Asynchronously Across a Stream Network	85
Introduction.....	85
Methods.....	88
Study Area	88
Study Design.....	89
Stream Metabolism Measures.....	90
Field methods.....	90
Metabolism estimation.....	90
Periphyton Biomass, Physical and Chemical Measurements	92
Statistical Analyses	94
Results.....	95
Does Stream Metabolism Increase with Drainage Area?	95
Does Heterotrophy Decrease with Drainage Area?.....	96

When are the Peaks and Troughs of Gross Primary Production and Ecosystem Respiration?	97
How Do Environmental Conditions Change Through the Year?	97
What are the Potential Drivers of GPP and ER?	98
Discussion	99
References	107
Tables	118
Figures	122
Appendix 1	129
Appendix 2	130
Appendix 3	134

List of Tables

- Table 2.1: Parameters used in the Bioenergetics model. We estimated diet composition from stomach contents and used prey energy density values from Cummins and Wuycheck (1971) and Beauchamp et al. (2004). We estimated predator energy density (ED) using study's percent dry weight data and an energy density equation that relates energy density and percent dry weight for juvenile Chinook Trudel et al. (2005). Chironomid pupae have considerably larger energy density than chironomid larvae ($3,400 \text{ J g}^{-1}$ vs $2,478 \text{ J g}^{-1}$) thus percentage consumed per chironomid life stages were entered separately in the model. 45
- Table 2.2: Effect size (coefficient estimates), standard errors, percent of the explained variance for fixed effects (R^2_m) and random and fixed effects combined (R^2_c) for a priori hypotheses driven models. Percentage increase or decrease for each trophic level when comparing losing sites to gaining sites. * degrees of freedom based on Satterthwaite approximation (Kuznetzova et. al. 2015). 46
- Table 3.1: Monthly average estimates for gross primary production (GPP) and ecosystem respiration (ER) in the Methow River basin. Empty cells represent months when sites were not sampled (i.e. high flows, or frozen) or sondes malfunctioned. Sites are organized by drainage area. 75
- Table 3.2: Average of biological and physical characteristics of sampled sites in the Methow River basin. Chl-a = Chlorophyl-a, AFDM=ash free dry biomass, PAR= photosynthetically active radiation, TEMP= temperature, DIN= dissolved inorganic nitrogen, SRP= soluble reactive phosphorus, Q=discharge, CON= channel confinement, DA=drainage area. 76
- Table 3.3: Estimates of the coefficient estimates, standard errors, p values, and R_m and R_c from the linear mixed models of the relationship between ln-transformed gross primary productivity and ln-transformed ecosystem respiration and $1/kT$, where k is the Boltzmann constant ($8.61 \times 10^{-5} \text{ eV/K}$; $1 \text{ eVK} = 1.6 \times 10^{-19} \text{ J}$) and T is temperature (K). Both rates were measured in $\text{mg O}_2 \text{ m}^{-2} \text{ d}^{-1}$. Sites in bold are considered temperature dependent. 77

Table 3.4: Estimates of the coefficient estimates, standard errors, p values, and R_m and R_c from the linear mixed models of the relationship between ln-transformed AFDM specific GPP and ln-transformed AFDM specific ER and $1/kT$, where k is the Boltzmann constant (8.61×10^{-5} eV/K; $1 \text{ eV} = 1.6 \times 10^{-19}$ J) and T is temperature (K). Both rates were measured in $\text{mg O}_2 [\text{g AFDM}] \text{ d}^{-1}$. Sites in bold are considered temperature dependent.	78
Table 4.1: Annual average metabolic rates and average of biological and physical characteristics of the 10 sampled stream reaches in the Methow River basin. Standard deviations are in parentheses. GPP=gross primary production, ER=ecosystem respiration, NEP=net ecosystem production, Chl-a =Chlorophyll-a, AFDM=ash free dry biomass, PAR=photosynthetically active radiation, TEMP=temperature, DIN=dissolved inorganic nitrogen, SRP=soluble reactive phosphorus, CON=channel confinement, DA=drainage area, Q=discharge.	118
Table 4.2: Coefficient estimates, standard errors, percent of the explained variance for fixed (R^2_m) and random and fixed effects combined (R^2_c) for GPP models for each site (all dates combined).	119
Table 4.3: Coefficient estimates, standard errors, percent of the explained variance for fixed effects (R^2_m) and random and fixed effects combined (R^2_c) for ER models for for each site (all dates combined).	120
Table 4.4: Coefficient estimates, standard errors, percent of the explained variance for fixed effects (R^2_m) and random and fixed effects combined (R^2_c) for across sites GPP and ER models.	121
Appendix 1 -Table 1: Correlation matrix for untransformed mean annual GPP, ER, and covariates. Pearson correlation coefficients and p- values. GPP=gross primary production, ER =absolute value of ecosystem respiration, NEP=net ecosystem production, Chl-a =Chlorophyll-a, AFDM=ash free dry biomass, PAR=photosynthetically active radiation, TEMP=temperature, DIN=dissolved inorganic nitrogen, SRP=soluble reactive phosphorus, CON=channel confinement, DA=drainage area, Q=discharge. Bold represents significant correlations.	129

List of Figures

- Figure 2.1: Map of the Methow River basin. The six sites, main tributaries and Columbia River are identified by name. The inset indicates the location of the Methow River in Washington state, USA..... 47
- Figure 2.2: Vertical hydraulic gradient (VHG) for each site versus segment scale surface water-groundwater exchange (two losing sites, two transient sites and two gaining sites) in the Methow River basin, Washington, USA. VHG data was measured at bed topography breaks. VHG readings from losing and transient sites were significantly lower than VHG readings from gaining sites. Surface water-groundwater exchange categories were based on the surface water-groundwater exchange analysis in Konrad (2006)..... 48
- Figure 2.3: Probability density distributions of surface water temperature recorded during fish growth experiment from March 1, 2014 to April 4, 2014 at all six sites (losing mean temperature of 4.27 ± 2.74 , transient mean temperature of 5.24 ± 2.06 , and gaining mean temperature of 6.33 ± 1.27 . Surface water-groundwater exchange categories were based on the surface water-groundwater exchange analysis in Konrad (2006). 49
- Figure 2.4: (a) Nitrate and nitrite and (b) soluble reactive phosphorus (SRP) concentrations (mg L^{-1}) from surface and hyporheic water samples for each segment scale surface-groundwater exchange. Reporting limits are 0.001 mg L^{-1} for SRP and 0.01 mg L^{-1} for ammonia, nitrate and nitrite. All ammonia samples were below the reporting limit. 50
- Figure 2.5: For each SW-GW category: estimated specific fish growth rate (a), percent fish dry weight (b), invertebrate benthic biomass (c), chironomid biomass (d), gross primary production (e), and chlorophyll-a biomass (f). Each figure shows associated p-value. . 51
- Figure 2.6: Daily growth simulations (a) and simulated weight accrued over the course of the experiment (b) for post-emergent fish growth under the six site conditions observed in the field. G1 and G2 are gaining sites, T1 and T2 are transient sites and L1 and L2 are losing sites. 52

- Figure 2.7: Wild post-emergent Chinook salmon length-weight relationships obtained for four of the six sites included in the study. Wild fish were not captured at G1 and L2 even after extensive sampling..... 53
- Figure 3.1: Map of the Methow River basin. The 10 stream reaches, main tributaries and Columbia River are identified by name. The inset indicates the location of the Methow River in Washington State, USA. Black star represents location of PAR sensor. 79
- Figure 3.2: (a) Temperature of profile and (b) monthly measured AFDM biomass of the 10 study sites in the Methow River basin. Sites are organized by drainage area from small to large. 80
- Figure 3.3: (a) Temperature dependence of gross primary production (E_p , originally measured in $\text{mg O}_2 \text{ m}^{-2} \text{ d}^{-1}$) plotted as the relationship between ln-transformed GPP rate and inverse temperature ($1/kT$). (b) Temperature dependence of ecosystem respiration (E_r , originally measured in $\text{mg O}_2 \text{ m}^{-2} \text{ d}^{-1}$) plotted as the relationship between ln-transformed ER rate and inverse temperature ($1/kT$). k is the Boltzmann constant ($8.61 \times 10^{-5} \text{ eV/K}$; $1 \text{ eVK} = 1.6 \times 10^{-19} \text{ J}$) and T is temperature (K). The canonical expectation of GPP and ER are -0.32 and -0.65, respectively. Sites are organized by drainage area from small to large. 81
- Figure 3.4: (a) Temperature dependence (E_{mp}) of AFDM specific gross primary production (GPP, originally measured in $\text{mg O}_2 [\text{AFDM}] \text{ d}^{-1}$) plotted as the relationship between ln-transformed GPP rate and inverse temperature ($1/kT$). (b) Temperature dependence (E_{mr}) of AFDM specific ecosystem respiration (ER, originally measured in $\text{mg O}_2 [\text{AFDM}] \text{ d}^{-1}$) plotted as the relationship between ln-transformed ER rate and inverse temperature ($1/kT$). k is the Boltzmann constant ($8.61 \times 10^{-5} \text{ eV/K}$; $1 \text{ eVK} = 1.6 \times 10^{-19} \text{ J}$) and T is temperature (K). The canonical expectation of GPP and ER are -0.32 and -0.65, respectively. Sites are organized by drainage area from small to large. 82
- Figure 3.5: Relationship of temperature dependence estimated for individual sites for gross primary production (E_p) vs. (a) drainage area and (b) channel confinement, and ecosystem respiration (E_r) vs. (c) drainage area and (d) channel confinement. * E_r for EW site was not included. 83

- Figure 3.6: Relationship of temperature dependence estimated for individual sites for AFDM specific gross primary production (Emp) vs. (a) drainage area and (b) channel confinement, and AFDM specific ecosystem respiration (Emr) vs. (c) drainage area and (d) channel confinement. * Emp and Emr for EW site were not included. 84
- Figure 4.1: Map of the Methow River basin. The 10 stream reaches, main tributaries and Columbia River are identified by name. The inset indicates the location of the Methow River in Washington State, USA. Black star represents location of PAR sensor. 122
- Figure 4.2: Seasonal patterns of GPP (a),ER (b),NEP (c). Stream reaches were ordered from smallest to largest drainage area. 123
- Figure 4.3: Plots of daily gross primary productivity (GPP) vs. daily ecosystem respiration (ER) for our ten stream reaches. Line is $GPP = ER$. Net ecosystem production (NEP) is average NEP for the entire sampling period June 2013-May 2014. 124
- Figure 4.4: Generalized curves of observed patterns of gross primary production (GPP) and ecosystem respiration (ER) across the stream network. Mean monthly metabolism values were standardized by calculating mean z-scores for each site. Groups were classified according to their peaks: summer, winter and multiple for GPP (a), and AFDM specific GPP (b), and fall and winter for ER (c). The red line crosses 0 representing the mean. 125
- Figure 4.5: Mean environmental conditions for the three temporal patterns observed in GPP. Summer group includes stream reaches that peak in the summer. Winter group includes stream reaches that peak in the winter. Multiple peaks group has multiple peaks. 126
- Figure 4.6: Conceptual model of environmental drivers of GPP for streams that peak in the summer (a), peak in the winter (b) and multiple peaks (c). 127
- Figure 4.7: Conceptual model of environmental drivers of ecosystem respiration for streams that peak in the fall (a) and winter (b). 128
- Appendix 2-Figure 1: Daily gross primary production (GPP) measured across 10 sites within the Methow River network. GPP are in $mg\ O_2\ m^{-2}\ d^{-1}$. Gray line represents moving

average. Stream reaches, BD, EW, C2 and T2 were partially frozen from mid December to mid February. 130

Appendix2-Figure 2: Daily AFDM specific gross primary production measured across 10 sites within the Methow River network. GPP are in $\text{mg O}_2 \text{ g[AFDM] d}^{-1}$. Gray line represents moving average. Stream reaches, BD, EW, C2 and T2 were partially frozen from mid December to mid February. 131

CHAPTER 1: General Introduction

Background

Food webs and river networks are dynamic hierarchical systems that interact with gradients of productivity, disturbance and habitat structure to impose a spatial and temporal organization (Power and Dietrich 2002, Benda et al. 2004). Stream productivity is an integrated response that incorporates abiotic and biotic processes that take place at different spatial and temporal scales (Poff and Huryn 1998, Warnars et al. 2007), thus multiple insights can be gained from examining stream productivity at different scales across a river network. For example, at the reach scale, stream metabolism is driven by light availability, nutrient concentration, organic matter quantity and quality and hydrology. These factors are in turn controlled by larger scale features such as climate, soil, vegetation and disturbance (Bernot et al. 2010). Using whole-stream metabolism estimates combined with key physical habitat characterizations of the entire basin can inform us about the overall potential for a system to support fish and identify hot spots of productivity. Given that stream metabolism measures production and use of organic carbon, it provides an estimate of the food base, how subsidies are used and how energy is transferred through the food web (Young et al. 2008, Marcarelli et al. 2011).

Numerous approaches have been used to identify what types of habitat improvements or restorations are likely to yield the best results, with fish production being the ultimate goal (Feist et al. 2003, McGarvey and Johnston 2011, Naiman et al. 2012). Although the majority of food web studies have focused on small spatial scales (Thompson et al. 2012, Naiman et al. 2012), a food web approach at the watershed level used to examine the efficacy of the

restoration activities can reveal insights into supporting ideas regarding system carrying capacity and resilience that cannot be gained from the more traditional habitat-focus approaches routinely used in basins like the Columbia River. The food web approach emphasizes the concept that available energy in river ecosystems is produced through local primary production and resources subsidies from outside the system, be it from lateral, vertical, upstream or marine sources (Wipfli and Baxter 2010) and that given the fluid nature of temperate rivers, energy sources available to stream biota are highly spatially and temporally variable, and driven by an array of environmental factors (Bilby et al. 2003). This variability in energy production is a key determinant in fish assemblages, and therefore vital to understand in river restoration efforts.

In this dissertation I aimed to understand how the spatial and temporal organization of the network affects stream productivity at different trophic levels. Each chapter focused on different temporal and spatial scales because ecological relevance must be taken into account when selecting spatial and temporal scale to evaluate biological responses (Torgersen et al. 2012). Post-emergent salmon were more likely to operate at a smaller (spatial) narrower (temporal) scale than stream metabolism. Thus, study designs reflected this to match the scale of observation with the scale of response.

Chapter 2

Production and transfer of energy across ecological systems is spatially and temporally heterogeneous (Vanni et al. 2004). This cross-systems view emphasizes energy dependence of communities (termed donor-controlled) on subsidies of resources from adjacent systems (Pimm 1982, Polis and Hurd 1996). Materials, energy, and organisms from groundwater

serve as resource subsidies to streams and rivers. These resource subsidies influence energetic conditions and production of food for rearing fish through nutrient inputs and water temperature changes. I tested the hypothesis that upwelling flows in gaining sites cause higher growth rates in rearing salmon. To examine this, I conducted an enclosure experiment using post-emergent Chinook salmon across a gradient of groundwater-surface water exchange in the Methow River, Washington. I also measured periphyton, benthic invertebrates and wild salmon, and applied a bioenergetics model to simulate fish growth trajectories. Results from the experiment with hatchery fish and surveys of wild fish revealed fish grew almost twice as fast in gaining ($2.7\% \text{ g d}^{-1}$) than in losing sites ($1.5\% \text{ g d}^{-1}$). Fish from transient sites grew as much as gaining sites, but their condition was significantly lower (18.3% compared to 20.7%). My results suggest direct and indirect pathways by which groundwater inputs may affect fish growth and energetic condition. I showed that elevated nitrogen concentrations and consistently warmer water temperature associated with sites gaining groundwater have a strong effect on basal production with subsequent effects on invertebrate biomass and growth of post-emergent salmonids and their energetic status. These findings highlight the importance of groundwater-surface water exchange to rearing salmon in winter and early spring, emphasize the importance of vertical connectivity as a spatially and temporally dynamic source of resource subsidies, and may inform strategies for conserving and restoring critical fish rearing habitat.

Chapter 3

Metabolic theory (MTE) scales variation in gross primary production (GPP) and ecosystem respiration (ER) with biomass and temperature. Thus, it provides an approach to predict how

temperature influences ecosystem processes (Welter et al. 2015). I hypothesized that the degree to which GPP and ER are temperature dependent varies with drainage area and channel confinement. Here, I measured stream metabolism at 10 sites across a stream network for 11 months. I quantified the effects of temperature on GPP and ER, and examined potential landscape features (i.e. drainage area and channel confinement) driving these patterns. I found that the effects of temperature on GPP, mass specific GPP, and ER varied substantially throughout the river network and that these relationships not always fit the predictions of the MTE. We initially anticipated that GPP was strongly related to water temperature, but we found that not all sites were associated with temperature and when they were, GPP was more temperature dependent than ER at most sites. We also found that drainage area and channel confinement can influence GPP and ER response to temperature. In addition, because the temperature dependence of GPP is larger than that of ER, our findings suggest that that carbon emissions in open canopied floodplain rivers although larger than carbon emissions in forested headwaters, could still lead to increased carbon sequestration under future global warming scenarios because in larger streams, most CO₂ emissions are produced directly in the stream itself derived from autochthonous production (Hotchkiss et al. 2015).

Chapter 4

My overall objective with this chapter was to describe the spatial and temporal patterns in stream metabolism across a stream network and examine potential drivers. To investigate these patterns, I measured dissolved oxygen continuously for 11 months to derive estimates of stream metabolism at 10 stream reaches across a temperate stream network. Here, I

hypothesized: (1) GPP and ER increase with stream size and streams become less heterotrophic; and (2) GPP and ER were highest when available light and temperature were highest after the high stream flows (summer months); but potential co-limiting environmental conditions, that vary by site, drive seasonal patterns in GPP and ER. I found that there was substantial variation in GPP and ER across the network and throughout the year, and that spatial variability was greater than temporal variability, but within the range reported in other studies in temperate streams (Hoellein et al. 2013, Hall et al. 2015). I confirmed that GPP and ER increased with drainage area as predicted by the River Continuum Concept RCC (Vannote et al. 1980) and that the stream network was largely heterotrophic except for few days in the spring and summer. I also determined three main seasonal patterns for GPP and two for ER. For some stream reaches, GPP peaked in the summer, others in the winter and some had multiple peaks. ER peaked either in the fall or in the winter. The spatial arrangement and temporal patterns of discharge, temperature, light and nutrients and their relative importance resulted in asynchrony of the peaks of GPP and ER despite consistent regional climatic conditions across the stream network.

References

Acuña V, Wolf A, Uehlinger U, Tockner K. 2008. Temperature dependence of stream benthic respiration in an Alpine river network under global warming. *Freshwater Biology* 53:2076–88.

Benda L, Poff NL, Miller D, Dunne T, Reeves G, Pess G, Pollock M. 2004. The network dynamics hypothesis: How channel networks structure riverine habitats. *Bioscience* 54: 413-27.

Bernot MJ, Sobota DJ, Hall RO, Mulholland PJ, Dodds WK, Webster JR, Tank JL, Ashkenas LR, Cooper LW, Dahm CN, Gregory S V., Grimm NB, Hamilton SK, Johnson SL, McDowell WH, Meyer JL, Peterson B, Poole GC, Maurice Valett HM, Arango C, Beaulieu JJ, Burgin AJ, Crenshaw C, Helton AM, Johnson L, Merriam J, Niederlehner BR, O'Brien JM, Potter JD, Sheibley RW, Thomas SM, Wilson K. 2010. Inter-regional comparison of land-use effects on stream metabolism. *Freshwater Biology* 55:1874–90.

Bilby RE, Reeves GH, Dolloff CA. 2003. Sources of variability in aquatic ecosystems: factors controlling biota production and diversity. R.C. Wissmar RC, Bisson PA, editors. *Strategies for restoring river ecosystems: Sources of variability and uncertainty in natural and managed systems*. Bethesda, Maryland: American Fisheries Society. p. 129-48

Brown JH, Gillooly JF, Allen AP, Savage VM, West GB. 2004. Toward a metabolic theory of ecology. *Ecology* 85:1771–89.

Cross WF, Hood JM, Benstead JP, Hury AD, Nelson D. 2015. Interactions between temperature and nutrients across levels of ecological organization. *Global Change Biology* 21:1025–40. <http://doi.wiley.com/10.1111/gcb.12809>

Feist BE, Steel EA, Pess GR, Bilby RE. 2003. The influence of scale on salmon habitat restoration priorities. *Animal Conservation* 6:271-82.

Finlay JC. 2011. Stream size and human influences on ecosystem production in river networks. *Ecosphere* 2:art87. doi:10.1890/ES11-00071.1

Fisher SG, Welter JR. 2005. Flowpaths as integrators of heterogeneity in streams and landscapes. Lovett GM, Jones CG, Turner MG, Weathers KG, editors. Ecosystem function in heterogeneous landscapes. New York. Springer. p. 311-28.

Hotchkiss ER, Hall Jr RO, Sponseller RA, Butman D, Klaminder J, Laudon H, Rosvall M, Karlsson J. 2015. Sources of and processes controlling CO₂ emissions change with the size of streams and rivers. *Nature Geoscience* 8:696–9.

<http://dx.doi.org/10.1038/ngeo2507>
<http://www.nature.com/ngeo/journal/v8/n9/abs/ngeo2507.html#supplementary-information>
<http://www.nature.com/doi/10.1038/ngeo2507>

Jankowski K, Schindler DE, Lisi PJ. 2014. Temperature sensitivity of community respiration rates in streams is associated with watershed geomorphic features. *Ecology* 95:2707–14.
<http://doi.wiley.com/10.1890/14-0608.1>

Marcarelli AM, Baxter CV, Mineau MM, Hall RO. 2011. Quantity and quality: Unifying food web and ecosystem perspectives on the role of resource subsidies in freshwaters. *Ecology* 92:1215–25.

McGarvey DJ, Johnston JM. 2011. A simple method to predict regional fish abundance: an example in the McKenzie River Basin, Oregon. *Fisheries* 36:534-46.

Naiman RJ, Alldredge JR, Beauchamp DA, Bisson PA, Congleton J, Henny CJ, Huntly N, Lamberson R, Levings C, Merrill EN, Percy WG, Rieman BE, Ruggerone GT, Scarnecchia D, Smouse PE, Wood CC. 2012. Developing a broader scientific foundation for river restoration: Columbia River food webs. *Proceedings of the National Academy of Sciences of*

the United States of America; 109:21201-207.

Poff NL, Huryn AD. 1998. Multi-scale determinants of secondary production in Atlantic salmon streams. *Canadian Journal of Fisheries and Aquatic Sciences* 55 (Suppl. 1): 201-17.

Poole GC. 2002. Fluvial landscape ecology: Addressing uniqueness within the river discontinuum. *Freshwater Biology* 47:641–60.

Power ME, Dietrich WE. 2002. Food webs in river networks. *Ecological Research* 17:451-71.

Thompson RM, Brose U, Dunne JA, Hall RO, Hladyz S, Kitching RL, Martinez ND, Rantala H, Romanuk TN, Stouffer DB, Tylianakis JM. 2012. Food webs: Reconciling the structure and function of biodiversity. *Trends in Ecology and Evolution* 27:689–97.

<http://dx.doi.org/10.1016/j.tree.2012.08.005>

Torgersen CE, Baxter CV, Ebersole JL, Gresswell RE. 2012. Incorporating spatial context into the analysis of salmonid-habitat relations. Church M., Biron P., Roy AG., editors, *Gravel bed rivers: Processes, tools, environments*: Chichester, UK: John Wiley and Sons, p. 216-24.

Warnaars TA, Hondzo M, Power ME. 2007. Abiotic controls on periphyton accrual and metabolism in streams: Scaling by dimensionless numbers. *Water Resources Research* 43. W08425, doi:10.1029/2006WR005002.

Welter JR, Benstead JP, Cross WF, Hood JM, Huryn AD, Johnson PW, Williamson TJ. 2015. Does N₂ fixation amplify the temperature dependence of ecosystem metabolism? *Ecology* 96:603–10. <http://doi.wiley.com/10.1890/14-1667.1>

Wipfli MS, Baxter CV. 2010. Linking ecosystems, food webs, and fish production: Subsidies in salmonid watersheds. *Fisheries* 35:373-87.

Young, RG, Matthaei CD, Townsend CR. 2008. Organic matter breakdown and ecosystem metabolism: functional indicators for assessing river ecosystem health. *Journal of the North American Benthological Society* 27: 605–25.

CHAPTER 2: Linking Groundwater-Surface Water Exchange to Food Production and Salmonid Growth

Chapter 2 is written in the plural “we” because it was submitted to the Canadian Journal of Fisheries and Aquatic Sciences with co-authors Colden V. Baxter, Eric K. Berntsen, and Alexander K. Fremier.

Introduction

Fluxes of materials, energy, and organisms across habitat boundaries, referred to as resource subsidies, are ubiquitous ecological phenomena that link land and water (Polis et al. 1996, Vanni et al. 2004). Stream food webs, because of close connections to their watersheds and the constant downstream movement of materials and organisms, are often strongly influenced by subsidies of resources from adjacent habitats (Baxter et al. 2005, Richardson et al. 2009). Subsidies from terrestrial, tributary, marine, and hyporheic habitats can be important to sustaining populations of stream fishes like salmonids (Wipfli and Baxter 2010, Nelson and Reynolds 2015). However, the importance of subsidies created by either hyporheic flows or groundwater-surface water exchange (GW-SW exchange) to fish has received less investigation.

An abundant body of literature indicates GW-SW exchange as a significant transport process of materials and nutrients, which can enrich basal production in lotic ecosystems (Valett et al. 1994, Jones et al. 1995, Wyatt et al. 2008). In this paper, we refer to the combined subsurface flows (which may include, shallow hyporheic flow) as GW-SW exchange, because of the complex interaction between groundwater and subsurface flows

(Larned et al. 2015, Boano et al. 2014). Studies of GW-SW influence on fishes have principally focused on physical habitat conditions, especially as it relates to spawning habitat and egg survival (Curry and Noakes 1995, Malcolm et al. 2003, Bowerman et al. 2014), but less so for its influence on the energetic conditions for growth (Power et al. 1999, Whitledge et al. 2006, French et al. 2014), and rarely for its possible direct and indirect influences on prey resources (but see French et al. 2014).

Several mechanisms exist by which GW-SW exchange may directly and indirectly influence the energetic conditions for fish growth and prey resources. GW-SW exchange flows can affect energetic conditions for growth by stabilizing water temperature and providing thermal refugia (Power et al. 1999, Whitledge et al. 2006), increasing metabolic rates (Brown et al. 2004) and increasing primary production and invertebrate production in the absence of other limiting factors such as light and nutrients (McCullough et al. 2009). GW-SW exchange in upwelling areas that are rich in nutrients may influence prey resources. Nutrients in upwelling water can directly stimulate primary production and primary producers in these habitats may recover quickly from disturbance (Valett et al. 1994, Wyatt et al. 2008). In turn, higher primary production may influence invertebrate biomass (Pepin and Hauer 2002). Fluxes of invertebrates derived from the hyporheic zone also provide prey to stream fishes (Wissmar et al. 1997). In this light, we view materials, energy and organisms provided by GW-SW exchange flows as a resource subsidy that is both temporally and spatially dynamic in a watershed.

Locations of GW-SW exchange are often associated with unconstrained stream reaches (floodplains), and this exchange is often cited as part of the basis for the high productivity and fish use of these habitats (Stanford et al. 2005). Stream reaches with GW-

SW exchange are actively selected by adult salmonids during spawning (Geist and Dauble 1998, Baxter and Hauer 2000, Hall and Wissmar 2004) and have been shown to be important sites for salmonid rearing (Sommer et al. 2001, Bellmore et al. 2013, Malison et al. 2015). Areas of GW-SW exchange may also be critical habitat for post-emergent salmonid growth and survival, though this has received less study. As post-emergent salmonids transition from endogenous to exogenous feeding, their bodies contain minimal energy reserves after yolk absorption (Armstrong and Nislow 2006). This transition occurs in Chinook salmon in late winter or early spring when input of terrestrial prey resources may be low (Baxter et al. 2005). GW-SW resource contributions delivered during critically low food periods may maintain fish growth at higher levels than in the absence of this subsidy. However, evidence from experimental studies regarding the causal connections between GW-SW exchange and fish growth are lacking.

In this study, we investigated the influence of GW-SW exchange on post-emergent fish growth and prey resources. In particular, we tested the overarching hypothesis that post-emergent fish grow faster in gaining sites due to the effects of a consistent water temperature regime on fish bioenergetics, and in response to nutrient and temperature influences that contribute to increased invertebrate food availability.

Methods

Study Area and Site Selection

The Methow River watershed in the Columbia River basin in Washington, USA has a catchment area of 4,462 km² and elevations ranging from 2,700 m in the Cascade Mountains to 240 m near the confluence with the Columbia River. The Methow River basin has a

snowmelt driven hydrology with high-altitude areas on the western side of the basin receiving approximately 2000 mm in precipitation annually and areas in the lower river valley receiving 300 mm (Konrad 2006). The river has no major impoundment, and a typical snowmelt hydrograph - high flows in late spring (May –June) and early summer and low flows in late summer and winter (August-January). Discharge (Q) during the duration of the study was representative of discharge within the historic flow record. Groundwater discharge from the floodplain aquifer (comprised of alluvium and glacio-fluvial sediments) is the primary source of base flow in the Methow and Twisp Rivers and is highest during the summer and lowest in the late winter and early spring (Konrad 2006).

The Methow River basin, with its low nutrient levels and cool water temperatures, supports among other native and non-native fish species populations of spring and summer Chinook salmon (*Oncorhynchus tshawytscha*) runs, steelhead (*Oncorhynchus mykiss*), bull trout (*Salvelinus confluentus*) and Coho salmon (*Oncorhynchus kisutch*) (Willms and Kendra 1990, Konrad et al. 2006, Bellmore et al. 2013). Despite the relatively intact, connected river-floodplain segments in the basin, native salmonid populations have decreased considerably. These declines have led to numerous restoration efforts to improve habitat for juvenile salmonids, including efforts to improve habitat of floodplain side channels, providing additional motivation for our study.

We classified and selected our study sites according to large-scale groundwater discharge and recharge areas identified by Konrad (2006) as gaining, losing and transient. To classify streams in the Methow River basin, Konrad (2006) used a mass-balance budget of inflows and outflows and attributed gains in streamflow to ground-water discharge, and losses to ground-water recharge. Transient sites were located in neutral areas. We selected

six accessible sites across a gradient of GW-SW exchange; two of each classified as gaining, losing or transient, including low velocity habitats used by post-emergent salmonids such as alcoves, side channels or springs (Figure 2.1). The selected sites had similar instream and riparian cover, water velocity and water depth. We conducted the study for five weeks from March 1 to April 5 in 2014 and measured environmental conditions and biota at the beginning and end of the study.

Multi-Trophic Level Responses

Growth of fish in enclosures

We conducted an enclosure experiment to compare growth rates among sites spanning the range of GW-SW exchange conditions (gaining, transient and losing exchange) encompassed by the selected sites. We built enclosures with PVC pipes of 4 m² and 0.5 m high, and mesh walls (3 mm). We added boulders or large woody debris to each enclosure to provide fish refugia and to better mimic natural conditions. The mesh allowed movement (e.g., drift) of aquatic invertebrates and insects but prevented fish from moving in or out of the enclosure. We measured dissolved oxygen at each enclosure with a handheld YSI multiprobe (Yellow Springs, Ohio, USA) at the beginning and end of experiment and monitored fish behavior every other day to ensure enclosures were not placed under anoxic conditions.

We constructed four separate enclosures at each site, into which we placed ten un-fed, recently emerged Chinook salmon fry ($0.36\text{g} \pm 0.02\text{g}$) obtained from the Winthrop National Fish Hatchery. We weighed fish at the beginning and end of the experiment and estimated specific growth rates for each site. Specific growth rate (SGR) is the difference between the

natural logarithm of successive weights over a unit of time and expressed as a percentage.

$$SGR = \frac{\ln(w_f) - \ln(w_i)}{days} \times 100$$

Where w_f is the final weight and w_i is the initial weight and days is the total number of days between weight measurements. At the end of the experiment, we euthanized the fish with a buffered solution of 10mL of tricaine methane sulfonate (MS222) per liter of water. We froze fish carcasses to estimate percent dry weight (DW) to infer energetic status. We also removed and froze their stomachs to later identify their contents to the lowest practical taxon using a dissecting microscope and weight to the nearest 0.001 g. We estimated energy density (ED) by relating ED to DW (Trudel et al. 2005). Gut contents and ED were subsequently used in the bioenergetics model. Hatchery post-emergent Chinook salmon were weighed wet (± 0.001 g) and oven dried to constant weight at 70°C. We weighed each fish and calculated the percent dry weight. One enclosure at a gaining site (G2; see Figure 2.1) was removed due to dewatering. We assumed the constrained movement of fry in experimental enclosures did not yield erroneous results. Although few studies of post-emergent Chinook salmon exist, we used an enclosure size based upon the range of movement observed while fish in this post-emergent life stage rear within a given habitat (e.g., 2-26 m for Atlantic salmon, Einum et al. 2011).

Observation of wild fish

We complemented our experimental approach with field surveys (Power et al. 1998) of wild post-emergent salmon during the five-week experiment. We dip netted, snorkeled

and electrofished wild post-emergent Chinook salmon to obtain lengths and weights, and record evidence of yolk sac for the first 30 wild post-emergent Chinook salmon collected at each site. We did not keep wild fish for stomach analysis as spring Chinook salmon are protected under the Endangered Species Act. We continued fish surveys until recently emerged fry were observed at all sites, except for sites Losing Site 2 (L2) and Gaining Site 1 (G1) where no fish were observed. We conducted extensive electrofishing at G1 in March and April, after which, we deemed reasonable to assume fry did not emerge from the gravel. At least one recently-built spawning nest (redd) had been previously identified in G1 near where sampling took place. At L2, we snorkeled and dip netted multiple occasions; the closest redds identified near this site were approximately nine kilometers upstream and 0.6 kilometers downstream. Because of the difference in emergence dates among redds, we only used weights from the first set of surveys to compare among sites, as incorporation of new sibling groups made discerning growth patterns difficult. Lastly, we drew inferences about the fish growth trajectories by comparing their length-weight distributions among the sites we were able to sample.

Benthic invertebrates, gross primary production and periphyton biomass

We sampled benthic invertebrate biomass, gross primary production (GPP) and periphyton biomass to examine food availability for post-emergent Chinook salmon, more specifically, whether gaining sites produced more food. We sampled benthic substrates for invertebrates at each site at the beginning and end of the experiment. On each sampling date, we collected two benthic samples using a standard Hess sampler (sample area of 0.086 m², 250-um mesh, Wildlife Supply Company, Yulee, Florida) at the most downstream area of the

sampling site, near the enclosures. One person held the sampler in place, while disturbing substrate to a depth of 10 cm. Our sampling technique would only have reached invertebrates inhabiting the shallow hyporheic zone, or perhaps those in motion from deeper areas. We sorted samples and identified invertebrates to family. We counted all invertebrates, then combined and dried at 60°C for 24 hours, and weighed them to 0.001 g. Because Chironomidae was the most common family of prey item in spring Chinook salmon stomachs, the first 30 Chironomidae of each sample were measured. Chironomid weights were based on published length weight relationships (Benke et al. 1999).

We measured gross primary production (GPP) to determine whether increased primary production in gaining sites might drive a “bottom-up” increase in food availability responsible for any response observed in post-emergent fish growth. We measured GPP and ER via the open channel, single-station, diel O₂ method by recording dissolved oxygen (DO) concentrations and water temperatures in each site every 10 minutes for at least a week with an YSI sonde (Yellow Springs, Ohio, USA) outfitted with an optical oxygen probe. We used the BAYesian Single-station Estimation (BASE) program (Grace et al. 2015) to generate estimates of metabolism from the diel DO curves. We used the average of the daily GPP estimates for the statistical analysis.

The open channel method provided an estimate of GPP, integrated over a scale larger than that of enclosures (likely 10s of meters versus a few meters). Thus, we used standing periphyton biomass collected at the enclosure scale in our predictive models of fish growth. We collected periphyton to measure the standing biomass available to invertebrates by scrubbing the surface of three randomly selected rocks near enclosures at the beginning and end of the experiment. From the slurry of each rock, we collected two replicate samples. We

then traced the top surface of sampled substrate to determine planar surface area (Bergey and Getty 2006). We sent samples to the University of Idaho, Analytical Science Laboratory (Moscow, Idaho) where they followed standard APHA methods to determine chlorophyll-*a* (Chl-*a*) content. Chl-*a* biomass is the measurement most commonly used as a proxy for primary production, as it is a measure of the photosynthetically active biomass (Steinman et al. 2006).

Groundwater-Surface Water Exchange

We used piezometric measurements of vertical hydraulic gradient (VHG, cm cm^{-1}) and specific vertical discharge (Q_s , $\text{cm}^3 \text{ cm}^2 \text{ s}^{-1}$) as a proxy for groundwater discharge. VHG is a dimensionless ratio that estimates pressure differentials between hyporheic and surface waters (Baxter et al. 2003). VHG is positive in areas of hyporheic discharge and negative in areas of hyporheic recharge. Q_s is the vertical component of water flux in the streambed and K , is the hydraulic conductivity (cm s^{-1}). To measure VHG and Q_s and K at each site, we drove four PVC pipe piezometers (38.1mm diameter) with a sledgehammer approximately 30-35 cm deep during the fall preceding the experiment; this was done after salmon spawning occurred, to minimize disturbance to redds.

Environmental Variables

We measured a suite of environmental variables known to be influenced by groundwater-surface water exchange, and/or may influence invertebrate prey or the feeding and growth of salmonid fishes. We measured water depth (cm) inside the enclosures at each site at the beginning and end of the experiment. Water velocity (m s^{-1}) was measured in front

of each enclosure at the beginning and end of experiment. We also measured substrate size at each site before enclosures were placed by randomly selecting one hundred rocks and determining each rock diameter using a gravelometer (Wolman 1954). We estimated the median grain size (D_{50} ; mm) at each enclosure location.

Because GW-SW exchange is known to positively influence primary production via delivery of available forms of nutrients (Valett 1994, Jones et al. 1995), we collected samples of surface and hyporheic water at each site at the beginning and end of the experiment for chemistry analysis. For the hyporheic samples, water was drawn from piezometers with a peristaltic pump (Pegasus Athena, Mississauga, Ontario, Canada), the first 500 ml were discarded, and then water was directly pumped and filtered into the sample bottles. Water samples intended for ammonium nitrogen ($\text{NH}_4\text{-N}$), nitrate nitrogen ($\text{NO}_3\text{-N}$), nitrite nitrogen ($\text{NO}_2\text{-N}$) and soluble reactive phosphorus (SRP) analyses were frozen immediately after collection, while dissolved organic carbon, (DOC) was kept refrigerated and later sent for analysis to the IEH Aquatic Research Laboratory and Consulting Services (Seattle, Washington, USA).

Water temperature ($^{\circ}\text{C}$) and light intensity (Lux) data were recorded at each site on an hourly basis throughout the study using Onset HOB0 data loggers (Pocasset, Massachusetts, USA). Water temperature data were used to verify areas of groundwater discharge, as an input to bioenergetics simulations, and in the multivariate analysis to investigate which factors were most important for predicting growth of post-emergent Chinook salmon.

Bioenergetics Simulations

After empirically estimating daily growth of post-emergent Chinook salmon, we

simulated the effects of water temperature and diet on the Chinook salmon growth trajectory under the different site conditions (Stewart and Ibarra 1991). Bioenergetic models can be used to estimate rates of consumption using data on observed growth and physiological parameters. This approach requires site-specific data on initial and final fish weights, diet composition, energy density (ED) of predator and prey and thermal distribution (Table 2.1). Energy density (ED) is not only a measure of fish condition that integrates the history of the fish feeding environment (Fergusson et al. 2010), but is also necessary to provide an accurate estimate of consumption. EDs for prey items were obtained from the literature (Cummins and Wuycheck 1971, Beauchamp et al. 2004). We used several bioenergetic model output variables, including proportion of maximum consumption (P , 0 to 1), specific consumption rates (C , $\text{g g}^{-1} \text{d}^{-1}$) and percent gross conversion efficiencies (GCE) to examine fish consumption and how fish growth trajectories differed under different sets of diet and temperature regimes.

Statistical Analyses

GW-SW exchange associations

To evaluate the direct effect of GW-SW exchange on each trophic level, we used repeated measures mixed-effects models in R (R Development Core Team 2013) using lme4 (Bates et al. 2015) package for the log and squared root transformed data (Chl-*a*, GPP, total invertebrate and chironomid biomass, SGR and percent fish dry weight). The models included random intercept terms (grouped by site and cage) to account for non-independence of repeated measurements. The random effects structure for the models was selected by using the restricted maximum likelihood approach (REML). Throughout the paper, we refer

to these models as treatment-effects models. We tested normality with the Shapiro–Wilk test and deemed results significant if $p < 0.05$ and marginally significant if p was between 0.05 and 0.1 but of potential ecological importance, given the low sample size and statistical power of our study. We used this graded approach because p -values are a continuous measure of evidence and are influenced by small sample size (Gelman 2013). P -values were generated using the lmerTest package (Kusnetzova et al. 2015) based on Satterthwaite 's approximations. $R^2_{\text{GLMM}(m)}$, marginal R^2 for fixed factors and $R^2_{\text{GLMM}(c)}$ conditional R^2 for both fixed and random factors $R^2_{\text{GLMM}(m)}$ were estimated with the R function 'r.squaredGLMM' from the package 'MuMIn' (Bartoń 2015).

Comparisons among GW- SW exchange categories were also carried out for each of the environmental variables using linear mixed models, with the exception of nutrient chemistry measures. All of these models included a random intercept term grouped by site to account for non-independence of repeated measurements. For nutrients, we used the nonparametric method for non-detects in the NADA package (Lopaka 2013) to test for treatment effects because measurements of stream water ammonia and SRP contained many values at or below method detection limits (0.001 mg L^{-1} for SRP and 0.01 mg L^{-1} for ammonia). In addition, we also carried out Kruskal-Wallis test using substitution of one-half of reporting limit. Both analyses yielded similar results. Thus, we decide to use substitution of one-half of reporting limit for subsequent multivariate analysis. Additionally, surface water and hyporheic stream water samples were not significantly different, so they were grouped and their mean values used for further multivariate analysis.

Direct and indirect associations across trophic levels

To investigate direct and indirect associations between specific fish growth rates and water temperature and food availability, we developed complementary linear mixed models based on a priori causal hypotheses (Benjamin et al. 2013). We fit a multivariate model of periphyton as a function of light, temperature, SRP, N, and water velocity, which are all factors known to mechanistically influence streambed periphyton (Larned 2010). Similarly, we fit a multivariate model of invertebrate biomass as a function of water temperature, Chl-*a* biomass and D_{50} because these are factors that have been identified to affect invertebrate biomass, particularly grazers (Lamberti et al. 2006). Lastly, specific fish growth rate was estimated as a function of water temperature and invertebrate biomass (Sommer et al. 2001). We also included D_{50} , water velocity and water depth in the multivariate fish model to account for potential energetic costs associated with habitat characteristics because post-emergent fish seek out shallow, slow habitats (Power et al. 1999, Einum et al. 2011). When detecting and quantifying indirect effects in a study, researchers traditionally use statistical methods such as path analysis or structural equation modelling. However, as described by Benjamin et al. (2013), small number of replicates and potential confounding influences of covariates make these statistical approaches impracticable. We tested models for collinearity using the function `vif` (variance inflation factor) from the `car` package (Fox and Weisberg 2011). Variables were considered collinear if `vif` values were greater than three and they were subsequently removed from the model. Finally, we estimated for each trophic level the percent increase or decrease attributed to each explanatory variable in the multivariate models after combining the influence of the treatment effect models.

Results

GW-SW Exchange and Associated Environmental Variables

We chose sites to control variation in environmental variables other than GW-SW exchange. As a result, water velocity ($F_{2,5,6}=0.766$, $p=0.5082$), median substrate (D_{50} , $F_{2,6}=0.668$, $p=0.547$) and light intensity ($F_{2,2443}= 1.622$, $p= 0.198$) did not differ significantly among GW-SW exchange categories. On average losing sites tended to be deeper (25.6 cm) than gaining and transient sites (17.2 and 15.2), though this difference was marginally significant ($F_{2,6}= 3.92$, $p =0.083$).

Local field measurements of vertical hydraulic gradient (VHG) and specific vertical discharge (Q_s) matched groundwater discharge and recharge segments per Konrad's (2006) classifications. The mean values for both VHG ($F_{2,23} =20.22$, $p < 0.0001$, Figure 2.2) and Q_s ($F_{2,16} = 3.47$, $p = 0.056$) were significantly lower for losing sites and transient sites, than for gaining sites, but there were no differences between losing sites and transient sites.

Measurements of water temperature and nutrients showed variation across sites and GW- SW classes (Figures 2.3, 2.4a, and 2.4b) As expected, mean water temperature was highest (6.3 °C) in the gaining sites, lowest in the losing sites (4.3 °C) and transient sites had intermediate values, 5.2 °C ($F_{2,6} = 6.00$, $p < 0.038$; Figure 2.3). Mean inorganic nitrogen was also approximately twice as high in transient, 0.120 mg L⁻¹ and gaining sites, 0.112 mg L⁻¹ as in losing sites, 0.058 mg L⁻¹ ($H= 19.6$, $p<0.0001$; Figure 2.4b). In contrast to our expectations, the point estimate of the mean SRP was not significantly different due to the high variation in samples ($H= 2.9$, $p=0.229$; Figure 2.4a).

Responses of Trophic Levels to GW-SW Exchange

For each GW-SW category, we estimated average specific fish growth and percent fish dry biomass, benthic invertebrate biomass, chironomid biomass, chlorophyll *a* biomass and GPP (Figure 2.5a-f). We found that for each trophic level, the biomass or growth, was generally higher in the gaining sites (G1, G2) and/or transient sites (T1, T2) than in losing sites (L1, L2) (Figure 2.5a-f). Post-emergent Chinook salmon in the enclosures ate mostly chironomids (77% to 98% biomass of gut contents). Fish stomachs also contained stoneflies, mayflies and caddisflies but in much lower proportions (Table 2.1) and there were no empty stomachs. Enclosed fish in gaining sites gained mass almost twice as fast as fish in losing sites, with a specific growth rate of 2.7 percent d^{-1} compared to 1.5 percent d^{-1} (Figures 2.5a, $F_{2,6}= 6.42$, $p= 0.032$). Percent dry weight and energy density (as estimated from percent dry weight) were also greater in gaining sites than in losing sites and transient sites, 20.7%, 18.8% and 18.3%, respectively (Figure 2.5b, $F_{2,6}= 9.31$, $p= 0.014$). Although fish in T2 grew as much as those in G1 and G2, their average percent dry weight was considerably lower than those of the gaining sites, 18.6%.

Invertebrate biomass in gaining sites and transient sites was approximately 7 and 10 times higher than in losing sites, respectively, but variability was high across sites of the same exchange category, thus differences were not significant at the 0.05 level (Figure 2.5c, $F_{2,6}= 4.16$, $p= 0.067$). Specifically, chironomid biomass, the most important prey item for post-emergent Chinook salmon, was also six and 11 times higher in the gaining and transient sites than in losing sites, but due to the high variability among sites, these differences were not significant (Figure 2.5d, $F_{2,6}= 1.199$, $p= 0.361$).

GPP in gaining sites was approximately seven times higher than that of losing sites and

two times higher than that of transient sites (Figure 2.5e, $F_{2,6} = 4.81$, $p = 0.055$). Chl-*a* biomass was also seven times greater in gaining sites than losing sites and two times greater than in transient sites (Figure 2.5f, $F_{2,6} = 6.50$, $p = 0.032$).

Bioenergetics model simulations revealed that fish ate at a relatively moderate proportion (0.63 to 0.76) of maximum consumption regardless of the GW-SW exchange category. Post-emergent fish grew steadily in the gaining sites. In contrast, fish in the losing and transient sites lost weight at the beginning of the experiment when temperatures were colder, their growth generally fluctuated more, and as water temperature rose fish grew faster (Figures 2.6a and 2.6b). Percent gross conversion efficiencies (GCEs) associated with these growth trajectories also increased with rising temperatures as expected; median GCE values ranged from 7.1% in the losing sites to 14.6% in the transient sites. Overall, GCE variance was much higher for losing sites (60% and 128%) and transient sites (16% and 86%) than for gaining sites (8.7% and 13.4%) as a result of the rapid temperature increases in the losing and transient sites.

Similar to the observed weights of the enclosed fish, length-specific weights from wild post-emergent Chinook salmon in G2, a gaining site, were higher (0.563 g) than mean weights from T2, a transient site, and L1, a losing site, (0.384g and 0.375g, respectively). This is despite our having sampled and recorded G2 wild fish weights at least a week earlier than fish from T2 and L1 (Figure 2.7). However, we acknowledge that these differences may be within the error margin of our measurements.

Direct and Indirect Relationships Across Trophic Levels

The linear mixed models used to examine potential mechanisms determining post-

emergent fish growth were consistent with our hypothesis that higher growth rates in gaining areas were due to elevated water temperatures and increased food production (Table 2.2).

First, the model for fish growth revealed that water temperature was the most important variable explaining fish growth, followed by invertebrate biomass (Table 2.2). Second, the model for invertebrate biomass showed that Chl-*a* biomass explained most of the variability in invertebrate biomass (Table 2.2). Third, the model for Chl-*a* biomass indicated that water temperature; SRP and N were all significant variables explaining Chl-*a* biomass (Table 2.2).

By combining the multivariate model results with the treatment-effect models that accounted solely for GW-SW exchange effects, we examined how GW-SW exchange interacted with the environmental variables considered important predictors of post-emergent fish growth, invertebrate biomass and Chl-*a* biomass (Table 2.2). We calculated that water temperature increased fish growth by 64.1 % in gaining sites compared to losing sites. Invertebrate biomass increased fish growth by 10.8 % in gaining sites compared to losing sites. In contrast, variables deemed to correlate with energetic costs, substrate size (D_{50}), water velocity and water depth decreased post-emergent fish growth marginally (0.4% to 5.7%, Table 2.2). We also calculated that Chl-*a* biomass increased invertebrate biomass by 80.6% in gaining sites compared to losing sites. Moreover, although effects of water temperature and D_{50} on invertebrate biomass were not significant, they both increased invertebrate biomass by about 10%, on average, in gaining sites compared to losing sites. Lastly, water temperature increased Chl-*a* biomass the most, by 42.9% in gaining sites compared to losing sites, followed by N (26.7%). In contrast to our expectations, we observed a negative association between SRP and Chl-*a* biomass (49.8%), likely owing to high phosphorus uptake in the gaining sites. Light and water velocity had marginal effects

on Chl-*a* biomass (0.9% to 3.1%).

Discussion

The findings of our study demonstrate that groundwater inputs can positively influence growth of post-emergent salmon fry, and point to direct and indirect pathways by which these inputs may affect their growth and energetic condition. This illustrates how groundwater-surface water exchange of materials, energy, and organisms may serve as another cross-boundary subsidy of potential importance to stream fishes. Although our experiment did not explicitly determine causal mechanisms, we showed that the elevated nitrogen concentrations and consistently warmer water temperature associated with sites gaining groundwater have a strong effect on basal production, which has subsequent effects on invertebrate biomass and growth of post-emergent salmonids and their energetic status. Our use of a manipulative field experiment and replicated enclosures helped distinguish effects of groundwater-surface water exchange character from other sources of environmental variation. The experiment also aided in separating direct and indirect effects associated with post-emergent salmon growth. Moreover, results of concurrent sampling of wild fish confirmed the patterns we observed in the experimental setting, while the growth trajectories from bioenergetics simulations informed interpretation of the consumption patterns in reaches that were gaining, losing, or transient with respect to groundwater exchange.

Prior studies have shown that nutrient contributions from groundwater inputs can positively impact biomass of algae and invertebrates (Valett et al. 1994, Pepin and Hauer 2002, Wyatt et al. 2008), but they have not directly shown an effect on fish. Here, we

demonstrated that in gaining sites, exchange can affect the energetic conditions for post-emergent salmonid growth directly through increased temperature and increased prey availability, and indirectly through increased nitrogen concentrations and temperature, that then stimulated prey biomass. Because we aimed to control conditions that affected energetic costs to the fish, as expected factors associated with energetic costs such as water velocity and substrate size did not explain the variation we observed among sites with variable groundwater-surface water exchange characteristics. We determined that stable, higher winter water temperatures and increased invertebrate prey availability in gaining sites had a direct GW-SW exchange effect on post-emergent Chinook salmon growth and energetic condition.

Our bioenergetics model results showed that fish growth was steady and consistent in gaining sites, whereas it fluctuated widely at the transient and losing sites. The highest estimated growth rates also occurred towards the end of the experiment at the losing and transient sites where fish had initially been starving, which suggests that these fish exhibited compensatory feeding. Kennedy et al. (2008) determined that juvenile Atlantic salmon exhibited compensatory feeding, as sites with the highest late-season consumption were the sites that had the lowest mid-season consumption and a majority of starving individuals in the early season. Low temperatures, feeding from yolk sack remains and poor swimming ability may have decreased feeding in the early part of the experiment. As a result, energetic status paralleled growth except for fish in one transient site (T2) where compensatory growth and consumption were highest. The occurrence of compensatory growth, the accelerated growth after a period of resource limitation, may reduce energy reserves, survival probability, delay maturation, and reduce physical performance and cognitive function (Ab

Ghani et al. 2014). We reason that as water temperatures continue to rise at all sites, fish in the losing and transient streams are likely to experience higher growth rates than fish in the gaining sites as experienced in T2. However, we cannot speculate as to whether or not fish condition in losing and transient sites would be the same as in gaining sites. This would likely depend on whether the temperature fluctuations experienced in these areas are outside their energetic optimum or preference (Jobling 1997).

We determined that higher N concentrations and warmer water temperatures in transient and gaining sites stimulated chlorophyll-*a* biomass and primary production. Upwelling groundwater is often enriched in labile forms of inorganic nitrogen (Dent et al. 2001), and we found that in gaining and transient sites this appeared to indirectly affect invertebrates by subsidizing periphyton production, which, in turn, increased prey availability for post-emergent Chinook salmon. Although we initially expected higher SRP concentrations in gaining sites, we did not observe this. Instead, a large proportion of SRP samples were under the detection limit, and the negative associations we found between SRP and our periphyton model suggested high phosphorus demand. Lower SRP concentrations in gaining sites may have been attributable to higher uptake rates in upwelling areas due to high availability of labile carbon, high microbial demand in the hyporheic zone and warmer temperatures at this time of year typical of upwelling areas (D'Angelo et al. 1991, Mulholland et al. 1997). High concentrations of SRP in T2, a transient site that had been newly restored, may be the result of rewetting of previously isolated sediments in the floodplain (Valett et al. 2005, Schönbrunner et al. 2012). Whereas a bottom-up, benthic mechanism appears most consistent with our findings, it is also possible, and even likely, that some component of the invertebrate prey subsidy to post-emergent salmon was at least

indirectly derived from the hyporheic zone itself, particularly because the chironomid prey we found to be most prevalent in their stomachs are well known to utilize hyporheic habitats for portions of their life cycle (Stanford and Gauvin 1974, Brunke and Gonser 1999, Reynolds and Benke 2012). In addition, top-down processes may have influenced our results as well. For instance, in one gaining site (G2) we observed relatively low invertebrate biomass that may have been due to high prey demand by wild post-emergent Chinook salmon that were abundant at this site. In sum, our findings point to a variety of pathways by which groundwater-derived resources may be incorporated into the food web that sustains rearing salmonid fishes.

Areas of GW-SW exchange introduce heterogeneity in stream water temperature, energy resources, and organisms into surface river environments. Understanding how this patchiness in productivity originates from the heterogeneity caused by the GW-SW exchange is important to effective conservation and restoration of habitat complexity, as this spatial complexity can promote community stability and the maintenance of biodiversity (Bellmore et al. 2015). Our findings are consistent with the hyporheic corridor and the shifting habitat mosaic concepts (Stanford and Ward 1993, Stanford et al. 2005) that the convergence of surface and groundwater in areas of active exchange (i.e., floodplains) is important to determining biological production by responding to spatially and temporally dynamic vertical and lateral processes rather than longitudinal processes (Stanford et al. 2005, Poole 2002). However, our study was limited to one study area and the strength of our inferences may be limited by the geomorphic, hydrologic and land use context that mediate the influence of GW-SW interactions on the ecology of streams (e.g., Wright et al. 2005).

For post-emergent fish rearing in active GW-SW exchange areas like floodplains, the

strength and duration of groundwater-derived subsidies may not be as important as the timing of their delivery. During critically low food periods in winter and early spring, even subsidies of small magnitude may maintain growth and abundance of animal populations (e.g., Nakano and Murakami 2001). Nevertheless, the consequences of these subsidies for growth at the post-emergence life stage of Chinook salmon may or may not translate into consequences at the scale of populations or overall fitness. Because the weeks following emergence may be a critical period for survival, larger early emerging juveniles may have an advantage competing for available territories (Skoglund et al. 2012). Alternatively, post-emergent salmonids may be subject to strong maternal effects that can conceal the connection between habitat and growth and survival (Kennedy et al. 2008). As juveniles rear in the stream in late spring and summer, losing or transient sites that exhibit higher water temperatures than juvenile Chinook salmon optimum temperatures may pose energetic bottlenecks that potentially limit their growth as a result of food limitation increased with fish size due to temperature-induced metabolic cost (Myrvold and Kennedy 2015). Moreover, any benefits realized at these early life stages of Pacific salmon may be overshadowed by limiting factors that manifest at later stages and in other habitats; in this case, processes that occur in the mainstem Columbia River, its estuary, or the marine environments used by these fish (impacts of dams, reservoirs, predators, ocean conditions, etc.).

Rivers are interacting, hierarchical mosaics of habitat heterogeneity, and in such a context understanding differences between losing and gaining areas in floodplains has important implications for planning conservation and restoration efforts to enhance rearing habitat for salmonids. At the watershed scale, the cumulative thermal and flow regimes of a stream and nutrient contributions are influenced by the arrangement and size of groundwater

inputs in gaining and losing floodplain segments (Jones et al. 1995, Baxter and Hauer 2000, Dent et al. 2001). This is most clearly seen in winter, when gaining areas have less ice cover because of groundwater influence.

Anthropogenic disturbances lead to habitat simplification and loss of habitat heterogeneity (Tockner et al. 2010, Peipoch et al. 2015). This habitat simplification can decrease vertical connectivity directly by reducing in-channel and planform complexity through channel modifications such as straightening, dredging, and floodplain disconnection and indirectly through land use changes where increased sedimentation disconnects surface water-groundwater exchange (Hester and Gooseff 2011). Traditionally, a goal of floodplain restoration has been to re-establish lateral connectivity (Roni et al. 2008). However, as evidenced in this study, restoring the dynamic processes that create and maintain GW-SW connectivity can be an equally important goal (Kondolf et al. 2006, Boulton et al. 2010). Restoration of river-floodplain connectivity (especially focused on side-channels) is being conducted along the Methow River and elsewhere in the Columbia Basin and Pacific Northwest with the aim of improving habitat for rearing salmon and steelhead. Though, it is uncertain whether these conditions limit populations, and mechanisms assumed to underpin population responses to such restoration and mitigation activities remain largely untested (Bellmore et al. 2013, Collins et al. 2015). Our findings suggest restoration or construction of a floodplain side-channel in the context of a losing or transient reach would likely result in a habitat with markedly different conditions for salmonid rearing than if either were conducted within a gaining reach. Yet, this context is rarely accounted for in planning or prioritization of such projects. Thus, our findings highlight the need for understanding groundwater-surface water exchange as a key component to context-based conservation and

restoration, particularly for rearing salmon.

References

- Ab Ghani, N.I., and Merilä, J. 2014. Cross-generational costs of compensatory growth in nine-spined sticklebacks. *Oikos* **123**(12): 1489–1498.
- Armstrong, J.D., and Nislow, K.H. 2006. Critical habitat during the transition from maternal provisioning for freshwater fishes. *J. Zool.* **269**(4): 403 – 413. Available from <http://www.jstor.org/stable/10.1086/680024> (Accessed 8 November 2015).
- Bartoń, K. 2015. MuMIn: Multi-Model Inference. R package version 1.15.1.
- Bates, D., Maechler, M., Bolker, B., and Walker S. 2015. Fitting Linear Mixed-Effects Models Using lme4. *Journal of Statistical Software*, 67(1), 1-48.
doi:10.18637/jss.v067.i01.
- Baxter, C. V., Fausch, K. D., and Saunders, W. C. 2005. Tangled webs: reciprocal flows of invertebrate prey link streams and riparian zones. *Freshw. Biol.* **50**(2):201-220
- Baxter, C., Hauer, F.R., and Woessner, W.W. 2003. Measuring groundwater–stream water exchange: new techniques for installing minipiezometers and estimating hydraulic conductivity. *Trans. Am. Fish. Soc.* **132**(3): 493–502.
- Baxter, C.V., and Hauer, F.R. 2000. Geomorphology, hyporheic exchange and selection of spawning habitat by bull trout (*Salvelinus confluentus*). *Can. J. Fish. Aquat. Sci.* **57**(7): 1470-1481.

- Beauchamp, D. A., Sergeant, C. J., Mazur, M. M., Scheuerell, J. M., Schindler, D. E., Scheuerell, M. D., Fresh, K. L., Seiler, D. E., and Quinn, T. P. 2004. Spatial-temporal dynamics of early feeding demand and food supply by sockeye salmon fry in Lake Washington. *Trans Am. Fish. Soc.* **133**(4): 1014-1032.
- Bellmore, J.R., Baxter, C.V, Connolly, P.J., and Martens, K. 2013. The floodplain mosaic: a study of its importance to production of salmon and steelhead. *Ecol. Appl.* **23**(1): 189–207.
- Bellmore J.R., Baxter, C.V., and Connolly, P.J. 2015. Spatial complexity reduces interaction strengths in the meta-food web of a river floodplain mosaic. *Ecology* 96(1): 274-283.
- Benjamin, J.R., Lepori, F., Baxter, C.V., and Fausch, K.D. 2013. Can replacement of native by non-native trout alter stream-riparian food webs? *Freshw. Biol.* 58(8): 1694-1709. doi: 10.1111/fwb.12160:
- Benke A.C., Huryn A.D., Smock L.A., and Wallace J.B. 1999. Length-mass relationships for freshwater macroinvertebrates in North America with particular reference to southeastern United States. *J. N. Am. Benthol. Soc.* 18(3): 308–343.
- Bergey, E.A., and Getty, G.M. 2006. A review of methods for measuring the surface area of stream substrates. *Hydrobiologia* **556**(1): 7–16.
- Boano, F., Harvey, J. W., Marion, A., Packman, A. I., Revelli, R., Ridolfi, L., and Wörman, A. 2014. Hyporheic flow and transport processes: Mechanisms, models, and biogeochemical implications, *Rev. Geophys.*, **52**, 603–679,

doi:10.1002/2012RG000417.

- Boulton, A. J., Datry, T., Kasahara, T., Mutz, M., & Stanford, J. A. 2010. Ecology and management of the hyporheic zone: stream-groundwater interactions of running waters and their floodplains. *J. N. Am. Benthol. Soc.* **29**(1), 26-40.
- Bowerman, T., Neilson, B.T., and Budy. P. 2014. Effects of fine sediment, hyporheic flow, and spawning site characteristics on survival and development of bull trout embryos. *Can. J. Fish. Aquat. Sci.* **71**(7): 1059-1071. doi: 10.1139/cjfas-2013-0372
- Brown, J.H., Gillooly, J.F., Allen, A.P., Savage, V.M., and West, G.B. 2004. Toward a metabolic theory of ecology. *Ecology* **85**(7): 1771–1789. doi: 10.1890/03-9000.
- Brunke, M., and Gonser, T. 1999. Hyporheic invertebrates: the clinal nature of interstitial communities structured by hydrological exchange and environmental gradients. *J. N. Am. Benthol. Soc.* **18**(3): 344-362.
- Collins, S. F., Marcarelli, A. M., Baxter, C. V., and Wipfli, M. S. 2015. A critical assessment of the ecological assumptions underpinning compensatory mitigation of salmon-derived nutrients. *Environ Manage.* **56**(3):571-586. doi: 10.1007/s00267-015-0538-5
- Cummins, K.W., and Wuycheck, J.C. 1971. Caloric equivalents for investigations in ecological energetics. International Association of Theoretical and Applied Limnology, Stuttgart, Germany.
- Curry, R.A., and Noakes, D.L.G. 1995. Groundwater and spawning site selection by brook charr (*Salvelinus fontinalis*). *Can. J. Fish. Aquat. Sci.* **52**(8): 1733–1740.

- D'Angelo, D.J., Webster, J.R., and Benfield, E.F. 1991. Mechanisms of stream phosphorus retention: an experimental study. *J. N. Am. Benthol. Soc.* **10**(3): 25-237.
- Dent, C.L., Grimm, N.B., and Fisher, S.G. 2001. Multiscale effects of surface-subsurface exchange on stream water nutrient concentrations. *J. N. Am. Benthol. Soc.* **20**(2): 162-181.
- Einum, S., Robertsen, G., Nislow, K.H., McKelvey, S., and Armstrong, J.D. 2011. The spatial scale of density-dependent growth and implications for dispersal from nests in juvenile Atlantic salmon. *Oecologia* **165**(4): 959–969.
- Fox, J., and Weisberg, S. 2011. *An {R} Companion to Applied Regression, Second Edition.* Thousand Oaks CA: Sage. URL:
<http://socserv.socsci.mcmaster.ca/jfox/Books/Companion>
- French, W.E, Vondracek, B., Ferrington, L.C., Finlay, J.C., and Dieterman, D.J. 2014. Winter feeding, growth and condition of brown trout (*Salmo trutta*) in a groundwater-dominated stream. *J. Freshwater Ecol.* **29**(2): 187-200.
doi:10.1080/02705060.2013.847868
- Geist, D. R., and Dauble, D.D, 1998. Redd site selection and spawning habitat use by fall Chinook salmon: the importance of geomorphic features in large rivers. *Environ. Manage.* **22**(5): 655-669. doi: 10.1007/s002679900137
- Gelman, A. 2013. Commentary: P Values and Statistical Practice. *Epidemiology* 24(1): 69–72. doi: 10.1097/EDE.0b013e31827886f7.

- Grace, M.R., Giling, D.P., Hladyz, S., Caron, V., Thompson, R.M., and McNally, R. 2015. Fast processing of diel oxygen curves : estimating stream metabolism with BASE (BAYesian Single-station Estimation). *Limnol. Oceanogr. Methods*. **13**(3): 103–114. doi: 10.1002/lom.10011
- Hall, J.L., and Wissmar, R.C. 2004. Habitat factors affecting sockeye salmon redd site selection in off-channel ponds of a river floodplain, *Trans. Am. Fish. Soc.*, **133**(6): 1480-1496. doi: 10.1577/T03-126.1
- Hester, E.T., and Gooseff, M.N. 2011. Hyporheic restoration in streams and rivers. *In Stream restoration in dynamic fluvial systems: Scientific approaches, analyses, and tools. Edited by A. Simon, S.J. Bennett, and J.M. Castro. American Geophysical Union, Washington, D.C. pp. 167-187. doi: 10.1029/2010GM000966*
- Jobling, M. 1997. Temperature and growth: modulation of growth rate via temperature change. *In Global warming: implications for freshwater and marine fish. Edited by C. M. Wood, and D. G. McDonald. Cambridge University Press, Cambridge, UK. pp. 225-253.*
- Jones, J.B., Fisher, S.G., and Grimm, N.B. 1995. Vertical hydrologic exchange and ecosystem metabolism in a Sonoran desert stream. *Ecology* **76**(3): 942-952. Available from <http://www.jstor.org/stable/1939358> (Accessed 8 November 2015).
- Kennedy, B.P., Nislow, K.H., and Folt., C.L. 2008. Habitat-mediated foraging limitations drive survival bottlenecks for juvenile salmon. *Ecology* **89**(9): 2529–2541.

- Kondolf, G. M., Boulton, A. J., O'Daniel, S., Poole, G. C., Rahel, F. J., Stanley, E. H., and Huber, H. 2006. Process-based ecological river restoration: visualizing three-dimensional connectivity and dynamic vectors to recover lost linkages. *Ecol Soc*, **11**(2), 5.
- Konrad, C.P. 2006. Location and timing of river-aquifer exchanges in six tributaries to the Columbia River in the Pacific Northwest of the United States. *J. Hydrol.* **329**(3-4): 444–470.
- Kuznetsova, A., Brockhoff, P., and Christensen, R.H.B. 2015. lmerTest: Tests in Linear Mixed Effects Models. R package version 2.0-29.
- Lamberti, G.A., Feminella, J.W., Pringle, C.M. 2006. Primary producer– consumer interactions. *In: Methods in Stream Ecology. Edited by Hauer, F.R. and Lamberti, G.A.* Academic Press. Oxford, UK. pp. 537–559.
- Larned, S.T. 2010. A prospectus for periphyton: recent and future ecological research. *J. N. Am. Benthol. Soc.* **29**(1):182–206. doi: 10.1899/08-063.1
- Larned, S. T., Gooseff, M. N., Packman, A. I., Rugel, K., and Wondzell, S. M. 2015. Groundwater–surface-water interactions: current research directions. *Freshw. Sci.*, **34**(1), 92–98. <http://doi.org/10.1086/679491>
- Lopaka L. 2013. NADA: Nondetects and data analysis for environmental data. R package version 1.5-6. <http://CRAN.R-project.org/package=NADA>
- Malcolm, I.A., Soulsby, C., Youngson, A.F., and Petry, J. 2003. Heterogeneity in ground

water–surface water interactions in the hyporheic zone of a salmonid spawning stream. *Hydrol. Process.* **17**(3): 601–617. doi: 10.1002/hyp.1156

Malison, R.L, Eby, L.A., and Stanford, J.A. 2015. Juvenile salmonid growth, survival, and production in a large river floodplain modified by beavers (*Castor canadensis*). *Can. J. Fish. Aquat. Sci.* **72**(11): 1639–165. doi:10.1139/cjfas-2015-0147

McCullough, D.A., Bartholow, J.M., Jager, H.I., Beschta, R.L., Cheslak, E.F., Deas, M.L., Ebersole, J.L., Foott, J.S., Johnson, S.L., Marine, K.R., Mesa, M.G., Petersen, J.H., Souchon, Y., Tiffan, K.F., and Wurtsbaugh, W.A. 2009. Research in thermal biology: Burning questions for coldwater stream fishes. *Rev. Fish. Sci.* **17**(1): 90-115.

Mulholland, P.J., Marzolf, E.R., Webster, J.R., Hart, D.R., and Hendricks, S.P. 1997. Evidence that hyporheic zones increase heterotrophic metabolism and phosphorus uptake in forest streams. *Limnol. Oceanogr.* **42**(3): 443-451.

Myrvold, K.M., and Kennedy, B.P. 2015. Interactions between body mass and water temperature cause energetic bottlenecks in juvenile steelhead. *Ecol. Freshw. Fish.* **24**(3): 373–383

Nakano, S., and Murakami, M. 2001. Reciprocal subsidies: dynamic interdependence between terrestrial and aquatic food webs. *Proc. Natl. Acad. Sci. U.S.A.* **98**(1), 166-170.

Nelson, M. C., and Reynolds, J.D. 2015. Effects of subsidies from spawning chum and pink salmon on juvenile coho salmon body size and migration timing. *Ecosphere*

6(10):209:1-14. doi: 10.1890/ES14-00162.1

- Peipoch, M., Brauns, M., Hauer, F.R., Weitere, M., and Valett, M. 2015. Ecological simplification: human influences on riverscape complexity. *BioScience* **65**(11): 1057–1065. doi:10.1093/biosci/biv120
- Pepin, D.M., and Hauer, F.R. 2002. Benthic responses to groundwater-surface water exchange in two alluvial rivers in northwestern Montana. *J. N. Am. Benthol. Soc.* **21**(3): 370-383.
- Polis, G. A., and Hurd, S.D. 1996. Linking marine and terrestrial food webs: allochthonous input from the ocean supports high secondary productivity on small island and coastal land communities. *Am. Nat.* **147**(3): 396-423.
- Poole, G.C. 2002. Fluvial landscape ecology: addressing uniqueness within the river discontinuum. *Freshwater Biol.* **47**(4), 641-660.
- Power, G., Brown, R.S., and Imhof, J.G. 1999. Groundwater and fish --insights from northern North America. *Hydrol. Process.* **13**(3): 401-422
- Power, M.E., Dietrich, W.E., and Sullivan, K.O. 1998. Experiment, observation, and inference in river and watershed investigations. *In* *Experimental ecology: Issues and perspectives*. Edited by W.J. Resetarits and J. Bernardo. Oxford Univ. Press, Oxford, UK. pp. 113-132
- R Development Core Team. 2013. R: A language and environment for statistical computing. R Foundation for Statistical Computing, Vienna, Austria. R 2.15.2 GUI

- Reynolds Jr, S. K., and Benke, A. C. 2012. Chironomid production along a hyporheic gradient in contrasting stream types. *Freshw. Sci.* **31**(1), 167-181.
- Richardson, J. S., Zhang, Y., and Marczak, L. B. 2009. Resource subsidies across the land–freshwater interface and responses in recipient communities. *River Research and Applications*, 26(1): 55-66.
- Roni, P., Hanson, K., and Beechie, T.J. 2008. Global review of the physical and biological effectiveness of stream habitat rehabilitation techniques. *N. Am. J. Fish. Manage.* **28**(3): 856-890. doi: 10.1577/M06-169.1
- Schönbrunner, I.M., Preiner, S., and Hein, T. 2012. Impact of drying and re-flooding of sediment on phosphorus dynamics of river- floodplain systems. *Sci. Total Environ.* **432**: 329–337.
- Skoglund, H., Einum, S., Forseth, T., and Barlaup, B. T. 2012. The penalty for arriving late in emerging salmonid juveniles: differences between species correspond to their interspecific competitive ability. *Funct. Ecol.* **26**(1): 104–111. doi:10.1111/j.1365-2435.2011.01901.x
- Sommer, T., Nobriga, M.L., Harrell, B., Batham, W., and Kimmerer, W.J. 2001. Floodplain rearing of juvenile Chinook salmon: evidence of enhanced growth and survival. *Can. J. Fish. Aquat. Sci.* **58**(2): 325-333.
- Stanford, J. A., and Gaufin, A. R. 1974. Hyporheic communities of two Montana rivers. *Science*, **185**(4152): 700-702.

- Stanford, J. A., and Ward, J. V. 1993. An ecosystem perspective of alluvial rivers: connectivity and the hyporheic corridor. *J. N. Am. Benthol. Soc.* **12**(1): 48-60.
- Stanford, J.A., Lorang, M.S., and Hauer, F.R. 2005. The shifting habitat mosaic of river ecosystems. *Verh. Int. Verein. Limnol.* **29**(1): 123–136.
- Steinman, A.D., Lamberti, G.A., and Leavitt, P.R. 2006. Biomass and pigments of benthic algae. *In: Methods in Stream Ecology. Edited by Hauer, F.R. and Lamberti, G.A.* Academic Press. Oxford, UK. pp. 357-379.
- Stewart, D.J., and Ibarra, M. 1991. Predation and production by salmonine fishes in Lake Michigan, 1978-1988. *Can. J. Fish. Aquat. Sci.* **48**(5): 909-922.
- Tockner, K., Lorang, M.S. and Stanford, J.A. 2010. River flood plains are model ecosystems to test general hydrogeomorphic and ecological concepts. *River. Res. Applic.* **26**(1): 76–86. doi: 10.1002/rra.1328
- Trudel, M., Tucker, S., Morris, J.F.T., Higgs, D., and Welch, D.W. 2005. Indicators of energetic status in juvenile coho salmon and Chinook salmon. *N. Am. J. Fish. Manage.* **25**(1): 374–390.
- Valett H.M, Baker, M.A, Morrice, J.A., Crawford, C.S., Molles, M.C., Dahm, C.N., Moyer, D.L., Thibault, J.R., and Ellis, L.M. 2005. Biogeochemical and metabolic responses to the flood pulse in a semiarid floodplain. *Ecology* **86**(1): 220–234
- Valett, M., Fisher, S.G., Grimm, N.B., and Camill, P. 1994. Vertical hydrologic exchange and ecological stability of a desert stream ecosystem. *Ecology* **75**(2): 548-560.

Available from <http://www.jstor.org/stable/1939557> (Accessed October 17, 2012).

Vanni, M.J., and Headworth, J.L. 2004. Cross-habitat transport of nutrients by omnivorous fish along a productivity gradient: Integrating watersheds and reservoir food webs. *In* Food webs at the landscape level. *Edited by* G.A. Polis, M.E. Power and G.R. Huxel. University of Chicago Press, Chicago, Ill. pp. 43-61.

Whitledge, G W., Rabeni, C. F., Annis, G. and Sowa, S.P. 2006. Riparian shading and groundwater enhance growth potential for smallmouth bass in Ozark streams. *Ecol. Appl.* **16**(4): 1461–1473. doi: 10.1890/1051-0761(2006)016[1461:RSAGEG]2.0.CO;2

Willms, R. and Kendra, W. 1990. Methow river water quality survey and assessment of compliance with water quality standards. Washington State Department of Ecology. Environmental Investigations and Laboratory Services Program. Olympia, Washington. USA. 37 pp. Available from <https://fortress.wa.gov/ecy/publications/publications/90e71.pdf> (Accessed 13 September 2015)

Wipfli, M.S., and Baxter, C.V. 2010. Linking ecosystems, food webs, and fish production: Subsidies in salmonid watersheds. *Fisheries* **35**(8): 373-387.

Wissmar, R. C., Stanford, J., and Ellis, B.K. 1997. 15N natural isotope tracing of nitrogen in insect food webs of hyporheic habitats. *In* Groundwater/surface water ecotones: Biological and hydrological interactions and management options. *Edited by* J. Gilbert, J. Mathieu and F. Fournier. International Hydrology Series, Cambridge University Press, Cambridge, UK. pp. 166-171.

Wolman, G.M. 1954. A method of sampling coarse river-bed material. *Trans. Am. Geophys. Union* **35**(6):951-956

Wright, K.K., Baxter, C.V., and Li, J.L. 2005. Restricted hyporheic exchange in an alluvial river system: implications for theory and management. *J. N. Am. Benthol. Soc.* **24**(3): 447-460. doi: <http://dx.doi.org/10.1899/04-090.1>

Wyatt, K. H., Hauer, F.R., and Pessoney, G.F. 2008. Benthic algal response to hyporheic-surface water exchange in an alluvial river. *Hydrobiologia.* **607**(1): 151–161. doi: 10.1007/s10750-008-9385-

Tables

Table 2.1: Parameters used in the Bioenergetics model. We estimated diet composition from stomach contents and used prey energy density values from Cummins and Wuycheck (1971) and Beauchamp et al. (2004). We estimated predator energy density (ED) using study's percent dry weight data and an energy density equation that relates energy density and percent dry weight for juvenile Chinook Trudel et al. (2005). Chironomid pupae have considerably larger energy density than chironomid larvae ($3,400 \text{ J g}^{-1}$ vs $2,478 \text{ J g}^{-1}$) thus percentage consumed per chironomid life stages were entered separately in the model.

Site	Exchange	Fish weight		Percent diet composition				Chinook salmon energy density (kJ g^{-1})
		Initial (g)	Final (g)	Chironomid larvae ($2,478 \text{ J g}^{-1}$)	Chironomid pupae ($3,400 \text{ J g}^{-1}$)	EPT ($4,700 \text{ J g}^{-1}$)	Other ($4,000 \text{ J g}^{-1}$)	
L1	Losing	0.364	0.642	0.0	82.0	13.3	4.7	3,705
L2	Losing	0.359	0.553	0.4	76.7	21.8	1.1	3,249
T1	Transient	0.355	0.633	3.7	93.7	1.1	1.4	3,255
T2	Transient	0.354	0.913	5.7	77.6	15.3	1.4	3,462
G1	Gaining	0.369	0.900	65.0	26.4	6.6	2.0	4,059
G2	Gaining	0.360	0.874	2.8	94.8	1.6	0.8	4,353

Table 2.2: Effect size (coefficient estimates), standard errors, percent of the explained variance for fixed effects (R^2_m) and random and fixed effects combined (R^2_c) for a priori hypotheses driven models. Percentage increase or decrease for each trophic level when comparing losing sites to gaining sites. * degrees of freedom based on Satterthwaite approximation (Kuznetzova et. al. 2015).

Model	Percent increase or decrease from losing to gaining	Estimate	SE	df*	t	p	R^2_m	R^2_c
<i>Fish growth</i>							0.89	0.93
Water temperature	64.1	0.0053	0.0008	2.6	6.991	0.009		
Invertebrate biomass	10.8	0.0011	0.0004	11.4	2.501	0.029		
D50	-1.8	0.0005	0.0004	13.9	1.151	0.269		
Water velocity	-0.4	-0.0183	0.0147	13.6	-1.246	0.234		
Water depth	-5.7	0.0002	0.0001	13.2	1.480	0.162		
<i>Invertebrate biomass</i>							0.50	0.50
Water temperature	11.1	0.1010	0.3373	17.0	0.299	0.768		
Chl- <i>a</i> biomass	80.6	0.7689	0.3019	17.0	2.546	0.021		
D50	10.4	-0.2540	0.2164	17.0	-1.173	0.257		
<i>Chl-<i>a</i> biomass</i>							0.75	0.75
Water temperature	42.9	0.6034	0.16780	18.0	3.596	0.0020		
SRP	-49.8	2.1977	0.47220	18.0	4.654	0.0002		
N	26.7	1.2391	0.47150	18.0	2.628	0.017		
Light	3.1	-0.4216	1.11730	18.0	-0.377	0.710		
Water velocity	0.9	3.9230	4.65100	18.0	0.843	0.410		

Figures

Figure 2.1: Map of the Methow River basin. The six sites, main tributaries and Columbia River are identified by name. The inset indicates the location of the Methow River in Washington state, USA

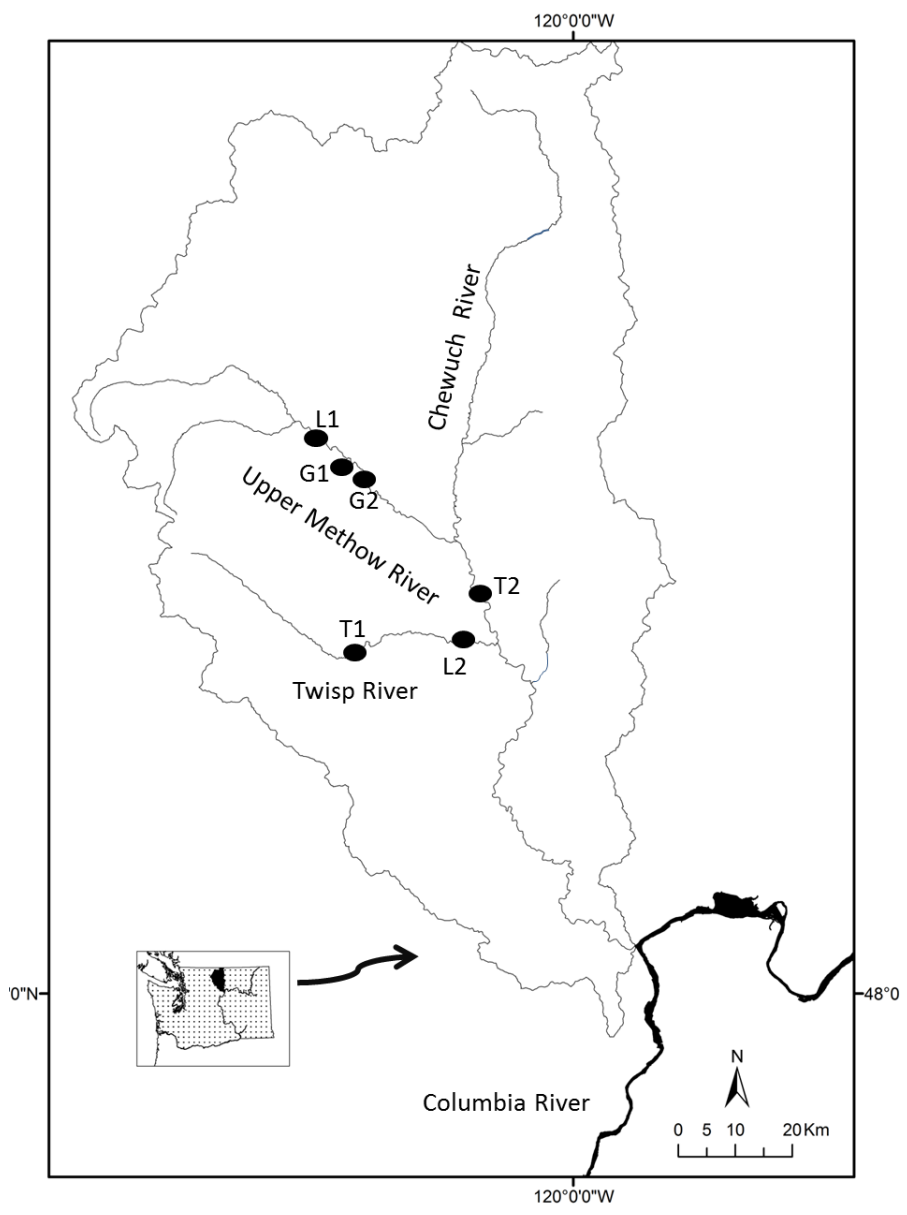


Figure 2.2: Vertical hydraulic gradient (VHG) for each site versus segment scale surface water-groundwater exchange (two losing sites, two transient sites and two gaining sites) in the Methow River basin, Washington, USA. VHG data was measured at bed topography breaks. VHG readings from losing and transient sites were significantly lower than VHG readings from gaining sites. Surface water-groundwater exchange categories were based on the surface water-groundwater exchange analysis in Konrad (2006).

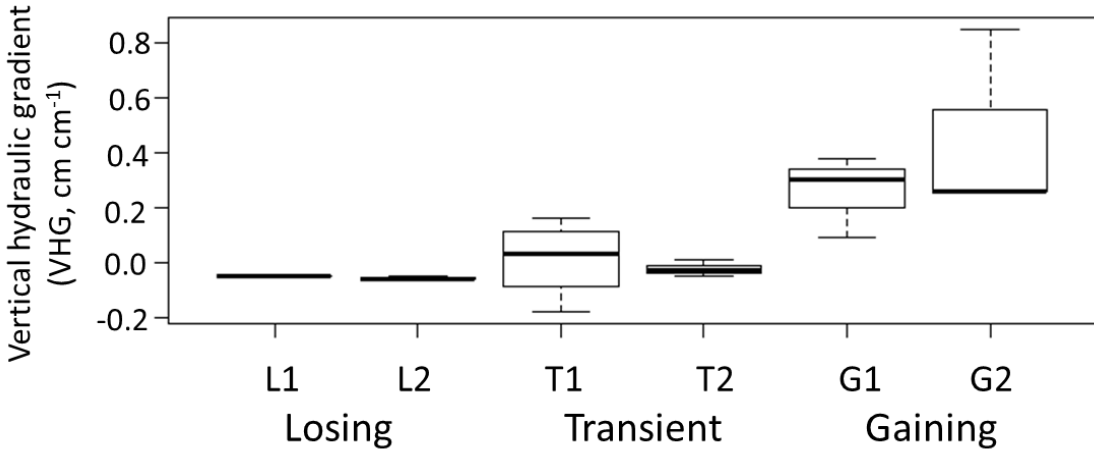


Figure 2.3: Probability density distributions of surface water temperature recorded during fish growth experiment from March 1, 2014 to April 4, 2014 at all six sites (losing mean temperature of 4.27 ± 2.74 , transient mean temperature of 5.24 ± 2.06 , and gaining mean temperature of 6.33 ± 1.27 . Surface water-groundwater exchange categories were based on the surface water-groundwater exchange analysis in Konrad (2006).

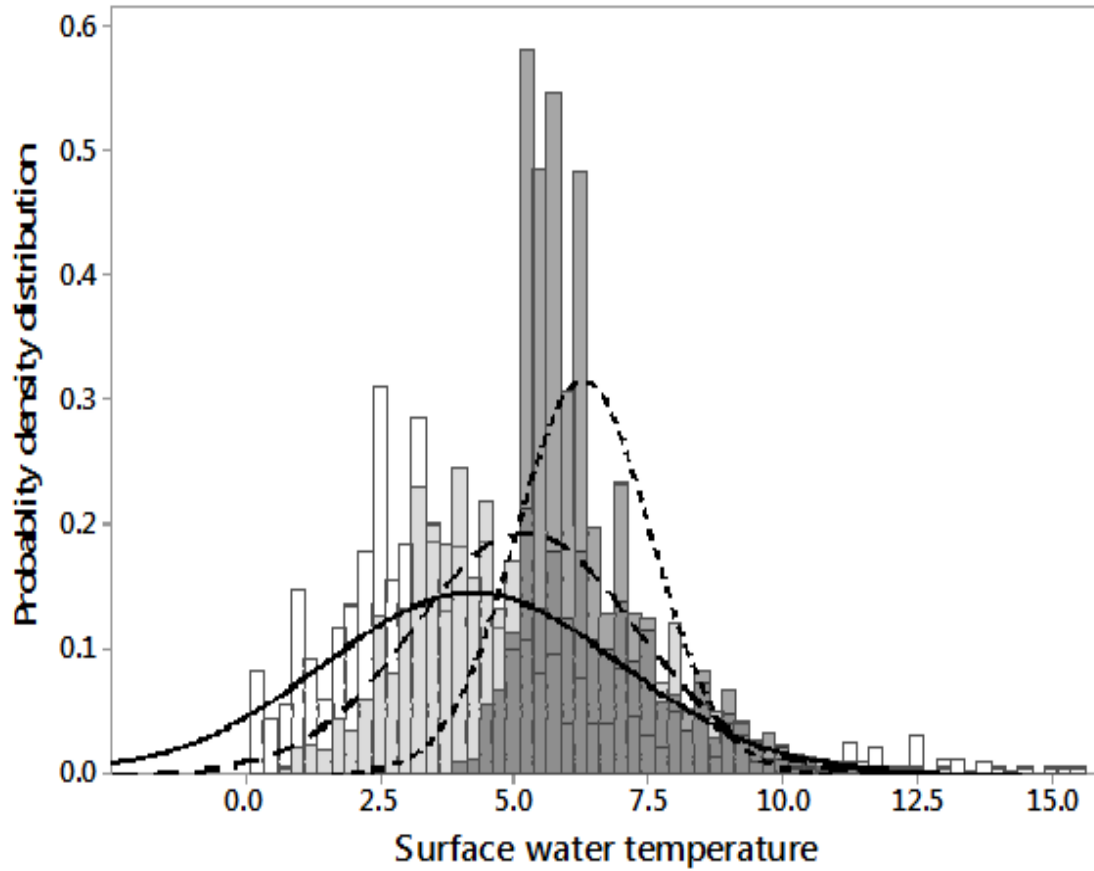


Figure 2.4: (a) Nitrate and nitrite and (b) soluble reactive phosphorus (SRP) concentrations (mg L^{-1}) from surface and hyporheic water samples for each segment scale surface-groundwater exchange. Reporting limits are 0.001 mg L^{-1} for SRP and 0.01 mg L^{-1} for ammonia, nitrate and nitrite. All ammonia samples were below the reporting limit.

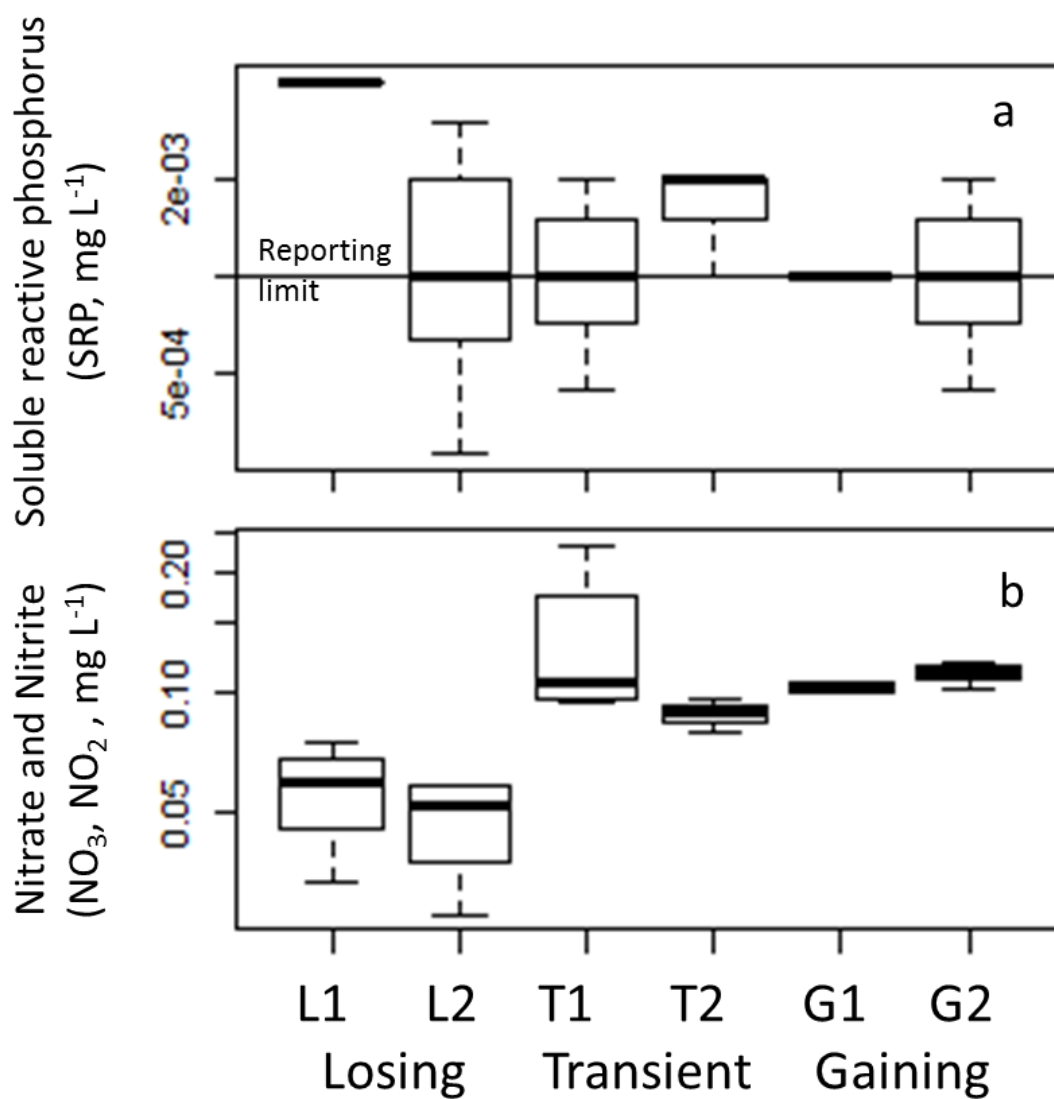


Figure 2.5: For each SW-GW category: estimated specific fish growth rate (a), percent fish dry weight (b), invertebrate benthic biomass (c), chironomid biomass (d), gross primary production (e), and chlorophyll-a biomass (f). Each figure shows associated p-value.

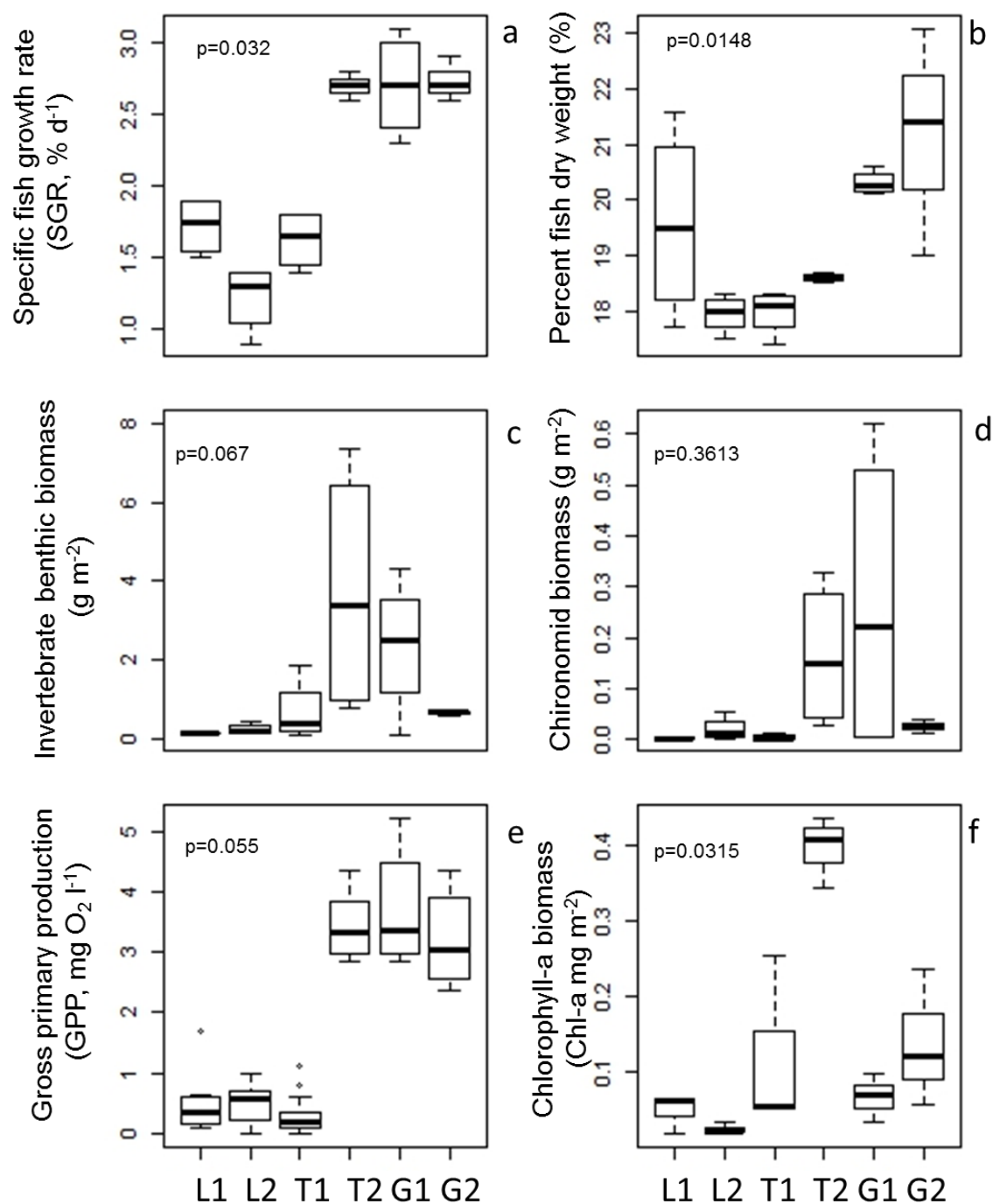


Figure 2.6: Daily growth simulations (a) and simulated weight accrued over the course of the experiment (b) for post-emergent fish growth under the six site conditions observed in the field. G1 and G2 are gaining sites, T1 and T2 are transient sites and L1 and L2 are losing sites.

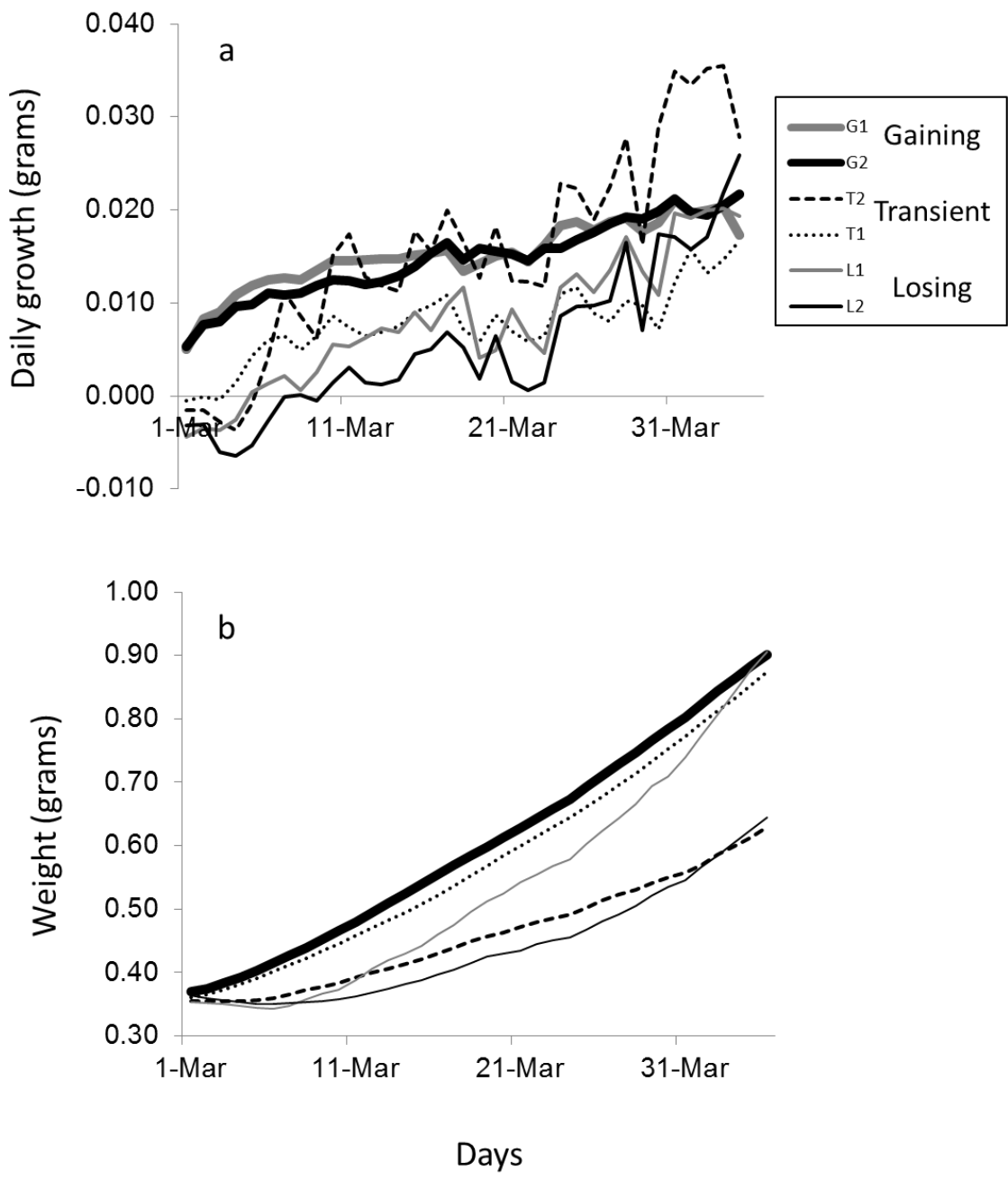
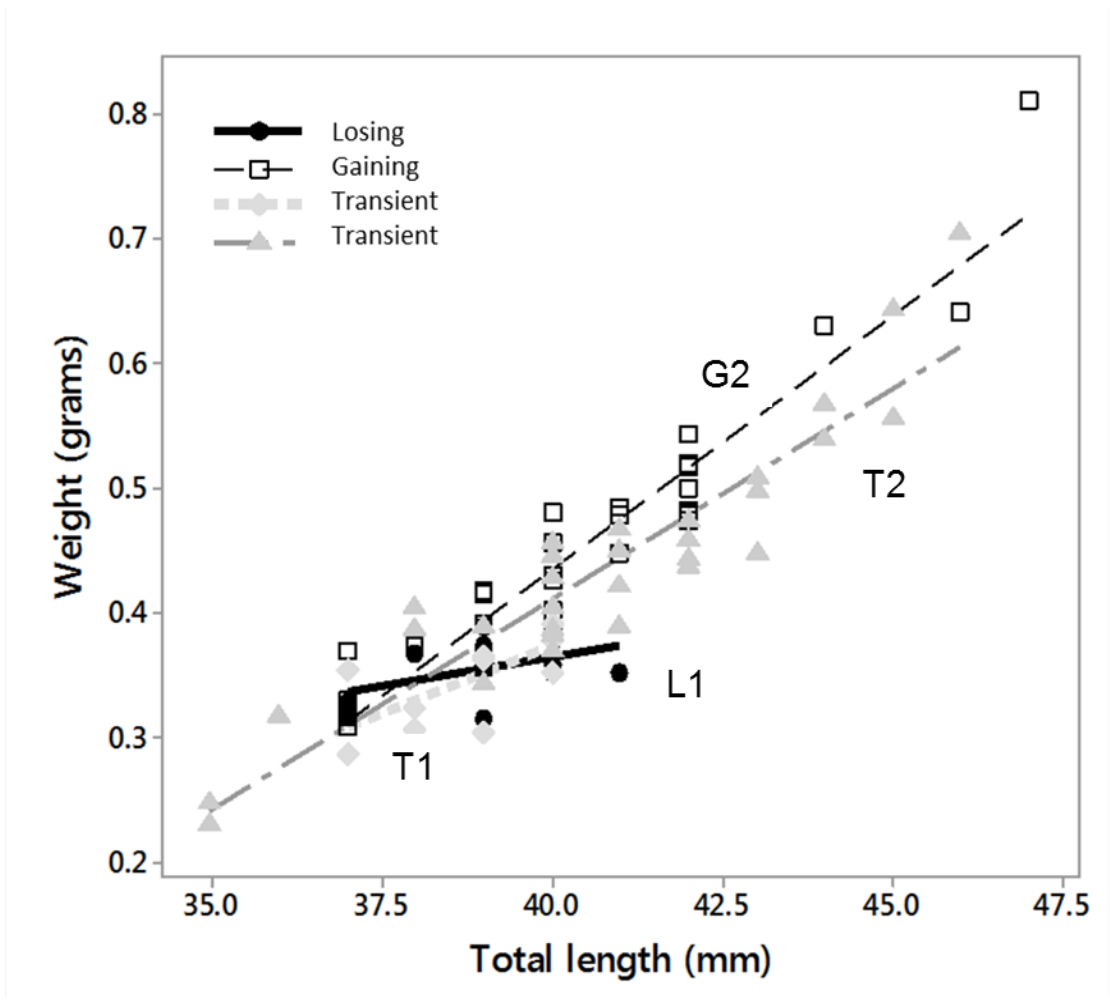


Figure 2.7: Wild post-emergent Chinook salmon length-weight relationships obtained for four of the six sites included in the study. Wild fish were not captured at G1 and L2 even after extensive sampling.



CHAPTER 3 – Understanding the Variability of Temperature Dependence of Stream Metabolism Across a Watershed

Chapter 3 is written in the plural “we” for submittal to the *Ecosystems* journal with co-authors Joseph R. Benjamin, James R. Bellmore, Grace A. Watson, Adrienne Zuckerman, and Alexander K. Fremier.

Introduction

Global mean surface temperature is predicted to increase approximately 0.3°C to 0.7°C for the next twenty years with water temperature expected to rise as air temperature increases (IPCC 2014). This increase in water temperature affects numerous aquatic ecosystem processes, such as ecosystem respiration (ER) and primary production (GPP) with major implications for global carbon budgets and food webs among other ecological concerns (Lopez-Urrutia et al. 2006, Perkins et al. 2010, Demars et al. 2011). The metabolic balance of GPP and ER is likely to shift in favor of ER with increasing temperature in the absence of feedbacks and acclimation because respiration generally responds more strongly to temperature than does to production (Anderson-Teixeira et al. 2012). One of the differences of the response to temperature between terrestrial and aquatic ecosystems is that allochthonous carbon inputs can decouple respiration from photosynthesis in aquatic systems (Valett et al. 2008, Yvon-Durocher et al. 2012) and may alter the metabolic balance of aquatic ecosystems (O’Gorman et al. 2012). Furthermore, in lotic systems, it has been recognized that landscape features influence the temperature dependence of ecosystem respiration (Jankowski et al. 2014). Understanding the temperature dependence on stream

ecosystem processes is currently an active field of research, but has been mostly focused on the temperature dependence of ER. However, further understanding of the variability of temperature dependence of not only ER, but GPP across stream networks is needed as studies that include larger streams and rivers are limited.

The metabolic theory of ecology (MTE) can provide a framework for developing predictions about how temperature influences ecosystem processes (Brown et al. 2004, Sibly et al. 2012, Welter et al. 2015). MTE assumes whole-body metabolism of organisms applies to ecosystem processes (Enquist et al. 2003) and describes temperature dependence as an enzyme activation energy (E) derived from the Arrhenius equation, where metabolic rates increase exponentially with temperature (Brown et al. 2004). MTE predicts a differential temperature dependence of heterotrophic processes of $E_r = 0.65$ eV and autotrophic rates of $E_p = 0.32$ eV. However, deviations from these predictions are indications of spatial and temporal variation in resource availability and quality (Jankowski et al. 2014).

The relationship between metabolism and temperature may vary from canonical expectations when resources change as a direct function of temperature and the supply of a limiting resource co-varies with temperature. Temperature dependence can be higher than expected if the abundance of resources co-varies positively with temperature or can be amplified through positive feedbacks. Conversely, the temperature dependence of an ecosystem process rate can be lower than expected due to a number of possible reasons, including nutrient limitation, acclimation, and changes in microbial abundance, or seasonality (Cross et al. 2015). Nutrient limitation may also suppress temperature dependence when primary producer biomass is high and communities experience reduced access to resources (Welter et al. 2015). In streams, for example, dense benthic algal

communities can result in increased competition for light and nutrients. In addition to potential nutrient limitation, allochthonous contributions from upstream and lateral sources can decrease the effect of temperature on ER (Valett et al 2008).

A considerable amount of work has been carried out on the effect of temperature on GPP and ER in oceans (Lopez-Urrutia et al. 2006, Garcia-Corral et al. 2014), lentic (de Castro and Gaedke 2008) and lotic systems (Acuña et al. 2008, Yvon-Durocher et al. 2010, Demars et al. 2011, Jankowski et al. 2014, Welter et al. 2015). However, the bulk of the research in lotic systems has focused in small streams, experimental settings and limited temporal variability. Here, we aimed to understand how the effects of temperature on GPP and ER vary across a stream network throughout a year. We hypothesized that stream size (drainage area) and channel confinement are predictably associated with the temperature dependence of GPP, mass specific GPP and ER because drainage area and channel confinement can strongly control periphyton biomass accrual, disturbance of streambed and nutrient availability.

Methods

Study Area

We conducted the study in 10 stream reaches (sites) of the Methow River watershed within the Columbia River basin from June 2013 to May 2014 (Figure 4.1). Selected sites were part of a larger habitat monitoring program for the entire Columbia River basin and were representative of the entire watershed (Zuckerman 2015). The Methow River, located in north central Washington State (USA), is generally an alluvial river, but also has some colluvial tributaries. The River is characterized by low nutrient levels and cool water

temperatures (Konrad et al. 2006, Willms and Kendra 1990, Bellmore et al. 2013). The river does not have major impoundments and, as a result, has a largely unaltered, natural flow regime with high flows during May – June, and low flows during August-January. Flows during the study were representative of flows within the historic record at USGS gage 12448500 (Methow River at Winthrop), except for flows in September and October in 2013 which were more than twice as high that the mean average flows of the historic record for those months (1912 to 2014). The riparian corridor is dominated by Douglas-fir (*Pseudotsuga menziesii*) and pine (*Pinus spp.*) in the higher elevation reaches whereas black cottonwood (*Populus trichocarpa*), speckled alder (*Alnus incana*), bigleaf maple (*Acer macrophyllum*), and western red cedar (*Thuja plicata*) are abundant in the lower areas (Bellmore et al. 2013).

Periphyton Biomass, Physical and Chemical Measurements

At each site, we took monthly samples of periphyton biomass of five randomly selected rocks in the active channel at 10 m intervals upstream of the dissolved oxygen sensors. We removed all periphyton from each rock, filtered the slurry, and froze the slurry for later lab analysis for Chlorophyll-*a* (Chl-*a*) and ash free dry mass (AFDM), following Standard Methods (APHA, 2005). To quantify planar surface area, we traced the top surface of each rock on paper (Bergey and Getty 2006). Periphyton samples were taken monthly except on few instances when flows were too high, during spring and early summer, and access to the streambed was unsafe.

We also collected monthly water samples (one per site) at the downstream end of each site to measure ammonium (NH₄-N), nitrate +nitrite (NO₃-N, NO₂-N), and soluble

reactive phosphorus (SRP). Samples were filtered (0.45 μ m), stored frozen and then analyzed using EPA standard methods (United States Environmental Protection Agency 1983) by IEH Analytical Laboratories (Seattle, Washington, USA). For our study, we considered all three dissolved nitrogen species together as dissolved inorganic N (DIN). Detection limits for DIN were 0.01 mg L⁻¹ and for SRP were 0.001 mg L⁻¹.

We measured photosynthetically active radiation (PAR) with a PAR sensor and data logger (sensor model S-LIA-M003, data logger model H21-002, Onset Computer Corporation, Bourne, Massachusetts, USA) at a single, central, open location free of obstructions near Winthrop, WA (Figure 3.1) and corrected for canopy and topographic shade at each site.

For each site, we generated daily discharge estimates using the ratio of daily discharge to bankfull discharge from the closest USGS gages, as suggested in Leopold (1994). Channel confinement (Table 3.1), the ratio of the valley floor width to the bankfull channel width, was calculated with valley floor width data for each stream reach from the Methow River TerrainWorks database (<http://www.terrainworks.com/terrainworks-dataset-locator>) and bankfull channel width data from the CHaMP database. Valley width was calculated at five times bankfull depth (Benda et al. 2007, Burnett et al. 2007). Bankfull width was estimated as the average width of the bankfull polygon calculated from digital elevation models (DEM) at each stream reach. We also used publically available aerial photographs (National Agriculture Imagery Program, NAIP 2009, <http://www.fsa.usda.gov/programs-and-services/aerial-photography/imagery-programs/naip-imagery/index>) to visually verify the validity of estimated widths. We estimated drainage area (Table 4.1), the area that drains to a point on a stream, using StreamStats

(<http://water.usgs.gov/osw/streamstats/>).

Stream Metabolism Estimates

At each stream reach, we measured stream metabolism via the open channel, single-station, diel O₂ method by recording dissolved oxygen (DO) concentrations every ten minutes from June 2013 to May 2014 in the main channel thalweg with an YSI sonde (Yellow Springs, Ohio, USA) outfitted with an optical oxygen probe. Approximately every two weeks, we re-calibrated the sondes in the field in a bucket of air-saturated water using an air pump and air stone (Hall et al. 2015). Prior to data analysis, we corrected our DO readings from drift that occurred during the deployments (Grace and Imberger 2006).

We used the Bayesian Single-station Estimation (BASE) program (Grace et al. 2015) to estimate single-station whole-ecosystem stream metabolism. BASE uses a Markov Chain Monte Carlo (MCMC) method to estimate values for GPP and ER. We evaluated daily models fit using the multiple criteria described in Grace et al. (2015). The criteria includes an R², which quantifies the correlation between modeled and measured DO data, and a posterior predictive check (PPC), which measures the overall fit based on the MCMC iterations. We only used daily models with an R² ≥ 0.6 and a PPC >0.1 or <0.9. The mean R² of our models was 0.92 (±0.08 SD) and mean PPC = 0.63 (±0.13 SD). After applying this set of criteria for model fitting, we deemed 56% of the total days modeled as good fits. Our relatively lower percentage of good fits may be attributed to the inclusion of days characterized by cold water temperatures, low productivity and high turbulence (M. Grace, personal communication). We discarded the poor fitted diel curves and did not include incomplete days or periods where DO probes malfunctioned. The model estimates GPP and

ER in units of $\text{mg O}_2 \text{ l}^{-1} \text{ d}^{-1}$, but were converted to areal rates ($\text{g O}_2 \text{ m}^{-2} \text{ d}^{-1}$) using measured mean stream depth. We used the average of the daily GPP and ER estimates for subsequent statistical analyses. Daily AFDM specific GPP and daily AFDM specific ER rates were estimated by dividing GPP and ER by AFDM.

Statistical Analyses

To assess the effects of temperature on GPP, AFDM specific GPP, ER, and AFDM specific ER, we used repeated measures mixed-effects models (lme function in the R package nlme) with fixed effects of either temperature (inverse temperature in Kelvin, $1/kT$) for each site. Temperature was expressed as $1/kT$ to quantify the temperature dependence of GPP, AFDM specific GPP, ER and AFDM specific ER at each site assuming that all response variables followed the Van't Hoff-Arrhenius relationship

$$e^{-E/kT}$$

where k is the Boltzmann constant $8.61 \times 10^{-5} \text{ eV}$ and 1 eV is $\sim 1.6 \times 10^{-19} \text{ J}$, T is temperature in Kelvin (K), and E is the activation energy E ; in eV. E quantifies the change in reaction rate with temperature (Boltzmann 1872, Arrhenius 1889 as cited by Brown et al. 2004) and is a measure of the minimum amount of chemical energy necessary for a chemical reaction to occur and is measured in eV. A significant ($p < 0.05$) interaction between temperature and the metabolic rate type indicated a significant difference. We compared the temperature dependence of GPP (E_p), mass specific GPP (E_{mp}), ER (E_r), and mass specific ER (E_{mr}) at each site to canonical expectations via linear mixed model regressions. The canonical activation energy values for GPP and ER are -0.32 and -0.65 eV , respectively (Gillooly et al. 2001, Allen et al. 2005). All models considered included a random effect of month on the

intercept to account for non-independence of repeated measurements.

Second, we related temperature dependence estimates (E_p , E_{mp} , E_r , and E_{mr}), one estimate per site ($n=10$) as each energy activation value is the slope of the Arrhenius relationship, across all sites to drainage area and channel confinement to examine the influence of watershed characteristics on the temperature dependence of stream metabolism. We deemed results significant if $p < 0.05$ and marginally significant if p was between 0.05 and 0.1 but of potential ecological importance, given the low sample size (10 sites) and statistical power of our study. This graded approach recognizes that p -values are a continuous measure of evidence and are influenced by small sample size (Gelman 2013).

Results

Stream Metabolism Estimates

There was approximately two orders of magnitude increase across the network for mean GPP, $0.02 \text{ mg O}_2 \text{ m}^{-2} \text{ d}^{-1}$ to $2.39 \text{ mg O}_2 \text{ m}^{-2} \text{ d}^{-1}$ and one order of magnitude increase for mean ER, $0.27 \text{ mg O}_2 \text{ m}^{-2} \text{ d}^{-1}$ and $2.89 \text{ mg O}_2 \text{ m}^{-2} \text{ d}^{-1}$ (Table 3.1). Mean annual GPP and ER increased with drainage area ($r=0.98$, $p<0.0001$; $r=0.96$, $p<0.0001$). Average annual ER was also correlated to channel confinement ($r=0.67$, $p=0.036$). Mean NEP for all sites was negative and ranged from -0.18 ($SD\pm 0.22$) to -1.18 ($SD\pm 0.87$).

Water Temperature and Periphyton Ash Free Dry Mass (AFDM)

Mean daily water temperature (TEMP) varied across sites seasonally, with highest temperatures in the summer and lowest temperatures in the winter. The warmest temperatures were observed at C2, T2 and C1 (from 18.0° to 18.5°C). In contrast, in the

winter BD, EW, L2, and T2 froze either completely or partially from December to February, and M1 had the highest minimum temperatures (Figure 3.2). Mean daily temperature was not strongly associated with either drainage area or channel confinement when all dates were combined. However, when examining seasonal trends, temperature was moderately correlated with drainage area in the spring ($r=0.36$) and winter ($r=0.45$).

Ash free dry mass (AFDM) generally increased with drainage area (Table 3.1). Lowest AFDM was observed in T1 (3.5 ± 1.12) and highest in M2 (15.3 ± 7.64). This change represented approximately a fivefold increase. AFDM also varied seasonally and peaked at different times of year depending on the site, with four sites peaking in the summer (BD, EW, T1, and T2) and six sites in the winter (BV, C1, C2, M1, M2, and M3) (Figure 3.2).

Other Environmental Variables

As expected, mean daily discharge (Q) increased with increasing drainage area and decreasing degree of channel confinement, although there was evidence of some leveling off at the lowest sites. Daily discharge ranged from a mean flow of $0.38 \text{ m}^3 \text{ s}^{-1}$ in BD ($SD \pm 0.17$) to a mean flow of $13.3 \text{ m}^3 \text{ s}^{-1}$ in M2 ($SD \pm 7.46$) (Table 3.1). Mean daily photosynthetic active radiation (PAR) was not associated with either drainage area or channel confinement when all dates were combined. However, PAR exhibited an asymptote pattern in the spring and summer and was moderately correlated with drainage area in the spring ($r=0.39$) and fall ($r=0.31$). Mean DIN and SRP concentrations were not related with drainage area or un-confinement in the basin.

Temperature Dependency of Stream Metabolism

We initially hypothesized that GPP was strongly related to water temperature across the stream network and that stream metabolism would increase with water temperature. However, our results showed that only four sites, BD, EW, T2, and C2, were strongly to moderately fit by an Arrhenius model of temperature dependence and indicated that GPP increased with temperature (negative slopes) (Figure 3.3a). The amount of variance explained for these sites ranged from 24% to 70%. The activation energy coefficient (E_p , or slope of the relationship) of BD was the closest to canonical expectations ($E_p=0.26$ eV). The E_p for EW was almost twice as high as the canonical expectation (0.58 eV), and the remaining two sites were about either one half or one third of the expected value (0.12 and 0.17) (Table 4.2). Sites T1 and M1 had significant relationships too, but their explanatory percentage were low (5 to 10%). Contrary to our expectations, there were four sites, T1, C1, M2, and M3 where GPP decreased with increasing temperature, albeit with a low explanatory power ($R^2 < 10\%$) and not significant except for T1 ($p=0.028$).

The Arrhenius relationship between AFDM specific GPP (E_{mp}) also showed a similar pattern for all the sites (Figure 3.4a), with moderate relationships for the same four sites, BD, EW, T2, and C2 with R^2 ranging from 20% to 70% (Table 3.4). However, in contrast to E_p there only three sites where GPP decreased with increasing temperature. Once we standardized by AFDM, GPP at the M3 site increased marginally with increasing temperature ($R^2=12\%$, $p=0.074$).

For ER, none of the sites were temperature dependent except EW, which only had a weak fit ($R^2=22\%$, $p<0.000$). The E_r value for EW was approximately twice that of the canonical expectation (1.33). Contrary to expectations, the slope was positive indicating that

ER increased with decreasing temperatures. In general, all models had positive slopes suggesting that ER tended to increase when water temperatures decreased except for BD (Figure 3.3b). The results from the Arrhenius relationship between AFDM specific ER (Emr) showed weaker associations for all sites (Figure 3.4b, Table 3.4) including EW (Emp=0.88, R²=17%, p<0.000) and excluding M2, which had a slightly improved association (R²=16%, p=0.041, Table 3.4).

Temperature Dependence Variability Across the Watershed

We found that Ep significantly decreased with drainage area (R²=0.46, p=0.018) but not with channel confinement (R²=0.11, p=0.19, Figure 3.4). In contrast, the Emp relationship with drainage area was weaker (R²=0.37, p=0.050), but improved considerably with channel confinement (R²=0.84, p<0.000).

To examine the relationship between temperature dependence of ER and drainage area, and confinement, we evaluated temperature dependence two ways, one with EW and one without it. The Er for EW was about six times greater than the next site, and it was considered a leverage point. Thus, we removed this site from the regression. When included, this site, reversed the direction of the slope of the temperature dependence vs. drainage area and channel confinement. Once this site was removed, the temperature dependence of ER increased with drainage area and channel confinement, although their relationships were only moderate to marginal (R²=0.34, p=0.057; R²=0.29, p=0.078). In contrast, the Emr relationship with drainage was not significant (R²=0.14, p=0.17), but Emr association with channel confinement improved dramatically (R²=0.55, p=0.014).

Discussion

We found that the effects of temperature on GPP, AFDM specific GPP, ER and AFDM specific ER varied substantially throughout the river network and that these relationships did not always fit the predictions of the metabolic theory of ecology (MTE). The absolute average observed activation energy of GPP (E_p) and AFDM specific GPP (E_{mp}) across the network was 0.21 eV and 0.11 eV, respectively, which was lower than the predicted value of 0.32 eV and lower than those determined in previous studies (Yvon-Durocher et al. 2010, Demars et al. 2011, Welter et al. 2015). The absolute average observed activation energy (E_r) for ER was 0.22 eV and 0.12 eV, and was closer to the predicted GPP activation energy than that of ER, 0.65 eV. These results were considerably lower than those reported by previous studies (Acuña et al. 2008, Demars et al. 2011, Yvon-Durocher et al. 2012, Jankowski et al. 2014, Welter et al. 2015). We had initially anticipated that GPP was strongly related to water temperature, but we found that only four sites were associated with temperature. Our study also revealed that GPP was more temperature dependent than ER at most sites. This finding contradicts the concept that the effect of temperature on ER is greater than the effect of temperature on GPP (Lopez-Urrutia et al. 2006, Anderson-Teixeira and Vitousek 2012). Although we were expecting the AFDM specific rates to be more responsive to temperature, we also determined that the relationships between AFDM specific GPP and AFDM specific ER and temperature were even weaker. Welter et al. (2015) found similar weaker results for mass specific GPP and mass specific ER in the Hengill experimental streams in Iceland which the authors attributed to self-shading and limitation by nutrients or inorganic carbon supply. Lastly, our results suggest that channel confinement and drainage area can influence GPP and ER response to temperature. These findings

highlight the importance of understanding the spatial variability of temperature dependence across a stream network, because understanding the spatial arrangement of this variability is critical to advance our understanding of the effects of climate warming on streams and rivers.

The absence of temperature dependence found for GPP is likely due to co-limitation of resources (Anderson-Teixeira and Vitousek 2012, Cross et al. 2015) through self-shading (upper layers of the periphyton shade bottom layers) and limitation by nutrients or inorganic carbon supply (Cross et al. 2015, Welter et al. 2015). Another potential explanation is that periphyton thickness can buffer the effect of water temperature increase (Acuña et al. 2008). We observed similar conditions to those observed by Acuña et al. (2008), where stable flows from mid-September to March allowed the development of thick layers of periphyton. These sites associated with high periphyton biomass had generally Emp values close to zero.

In the case for ER, temperature was not a good explanatory variable. This finding contradicts the assumption that the effect of temperature on ER is greater than the effect of temperature on GPP. However, this may be explained two ways. The first scenario is related to terrestrial inputs of carbon that co-vary inversely with temperature and can lead to the deviations in temperature dependence (Valett et al. 2008, Yvon-Durocher et al. 2012). This scenario is likely observed in small forested sites like BD. However, after we removed data from the fall as Valett et al. (2008) did (results not shown), we still did not observe the effect of temperature on ER. The second, more probable scenario is associated with sites that support high GPP which in turn results in higher ER due to the combination of autotrophs and heterotrophs respiration in the periphyton mats.

Although it has been recognized that ER in aquatic ecosystems, unlike terrestrial ecosystems, is not constrained by GPP (Yvon-Durocher et al. 2012), during base flow when

terrestrial inputs are low, and periphyton biomass is highest, we can assume steady state (Demars et al. 2011). At steady state, ER is limited by substrate availability and must equal GPP (Yvon-Durocher et al. 2010) if heterotrophs are present to decompose material. GPP may also be constrained by ER where periphyton biomass is high and mature because of positive feedback loops between ER and GPP where GPP is dependent on the nutrients released from the material consumed by heterotrophs. Thus, the sites where the effects of biomass on GPP were significant corresponded to sites where periphyton biomass was highest (in the winter). These sites, due to the stability of the flows during low flow conditions, accumulated biomass until high flows in the spring scoured the streambed. Demars et al. (2011) also noted that there is a difference in GPP response to nutrient supply by new periphyton versus mature periphyton.

Our results also determined that drainage area and channel confinement can influence GPP and ER response to temperature. We found that the effect of temperature on GPP increased with increasing temperature for only four sites (BD, EW, C2; T2); for the other sites, GPP decreased with increasing temperature. Hornbach et al. (2015) determined that the groundwater influence on water temperature at their open sites was likely responsible for the negative association between water temperature and GPP. The sites where we observed negative correlations between temperature and GPP were those located in unconfined sections of the stream network with active hyporheic exchange. This is likely the result of warmer winter temperatures at these sites. These unconfined sites are shallow, wide, have high light availability, and stable stream flows, in addition to large standing biomass stock that becomes available to heterotrophs. These results are also in agreement with findings from Jankowski et al. (2014). Jankowski et al. (2014) determined that the slope of river

networks is important in modifying the response of ER to temperature because of its effect on the accumulation of carbon.

The activation energy of AFDM specific GPP (E_p) relationship with drainage area was slightly weaker, but not the relationship with channel confinement. By removing the influence of biomass accrual and lack of disturbance, we can investigate how GPP and ER were less responsive to temperature than expected. We suggest that sites in confined sections of the watershed are stable, but have higher gradient and lower potential for biomass accrual, so they are more likely subjected to nutrient limitation (Demars et al 2011), whereas the unconfined sites can recycle nutrients and maintain high biomass (Wyatt et al 2012). Although our study was conducted continuously throughout the year, we averaged our results of temperature and biomass effects and we assumed that the average estimates integrate conditions for the entire year. Understanding the variability of E_p and E_r can shed light on how streams adjust to warming temperatures, particularly in the winter when some streams may be most productive. This is relevant, considering that few studies collect year-round data and inferences mostly come from summer studies, although this is changing with the availability of new, more inexpensive technology. As mentioned before, our results were the mean annual average, but we do not anticipate effects of temperature on GPP and ER in the spring or fall because of high terrestrial inputs transported across the watershed. In contrast, we expect that summer estimates may be influenced by potential nutrient limitation depending on the location in the watershed.

A factor that may affect the generality of our results is the presence of *Dydimosphenia germinata* (didymo). This invasive diatom was present in abundance at our sites, particularly in the lower reaches. Dydimosphenia favors cold water and oligotrophic

conditions. Thus, some of the patterns observed here may be a response to the Dydimo production. Lastly, we only included one watershed so inferences from this study may be limited to watersheds similar to other oligotrophic mountain streams.

Our findings have important implications for global carbon cycling and budgets because the expectation is that the metabolic balance of GPP and ER will shift in favor of ER with increasing temperature, as ER generally responds more strongly to temperature than does GPP (Anderson-Teixeira and Vitousek 2012). Stream metabolism contributes to net CO₂ emissions when ER is greater than GPP due to aquatic mineralization of terrestrial organic carbon (Hotchkiss et al. 2015). In this study, our finding that GPP increases with decreasing temperature sheds light on potential mechanisms by which the landscape context can have an effect on CO₂ emissions. Because the temperature dependence of GPP is larger than that of ER, our findings suggest that that carbon emissions in open canopied floodplain rivers although larger than carbon emissions in forested headwaters, could still lead to increased carbon sequestration under future global warming scenarios because in larger streams, most CO₂ emissions are produced directly in the stream itself derived from autochthonous production. Furthermore, it highlights the importance for environmental managers to maintain streams and rivers connected longitudinally, laterally and vertically to the landscape.

References

Acuña V, Wolf A, Uehlinger U, Tockner K. 2008. Temperature dependence of stream benthic respiration in an Alpine river network under global warming. *Freshwater Biology* 53:2076–88. <http://doi.wiley.com/10.1111/j.1365-2427.2008.02028.x> Acuña et al. 2008

Allen AP, Gillooly JF, Brown JH. 2005. Linking the global carbon cycle to individual metabolism. *Functional Ecology* 19:202–13.

Anderson-Teixeira KJ, Vitousek PM. 2012. Ecosystems. Sibly RM, Brown JH, Kodric-Brown A, editors. *Metabolic ecology: A scaling approach*. West Sussex (UK): Wiley-Blackwell. p99-111.

Bellmore JR, Baxter CV, Connolly PJ, Martens K. 2013. The floodplain mosaic: a study of its importance to production of salmon and steelhead. *Ecological Applications* 23:189–207.

Bergey EA., Getty GM. 2006. A review of methods for measuring the surface area of stream substrates. *Hydrobiologia* 556:7–16.

Brown JH, Gillooly JF, Allen AP, Savage VM, West GB. 2004. Toward a metabolic theory of ecology. *Ecology* 85:1771–89.

Burnett KM, Reeves GH, Miller DJ, Clarke S, Vance-Borland K, Christiansen K. 2007. Distribution of salmon-habitat potential relative to landscape characteristics and implications for conservation. *Ecological Applications* 17:66–80.

de Castro F, Gaedke U. 2008. The metabolism of lake plankton does not support the metabolic theory of ecology. *Oikos* 117:1218–26. <http://doi.wiley.com/10.1111/j.0030-1299.2008.16547.x>

Cross WF, Hood JM, Benstead JP, Huryn AD, Nelson D. 2015. Interactions between temperature and nutrients across levels of ecological organization. *Global Change Biology* 21:1025–40. <http://doi.wiley.com/10.1111/gcb.12809>

Demars BOL, Russell Manson J, Ólafsson JS, Gíslason GM, Gudmundsdóttir R, Woodward G, Reiss J, Pichler DE, Rasmussen JJ, Friberg N. 2011. Temperature and the metabolic balance of streams. *Freshwater Biology* 56:1106–21. <http://doi.wiley.com/10.1111/j.1365-2427.2010.02554.x>

Enquist BJ, Economo EP, Huxman TE, Allen AP, Ignace DD, Gillooly JF. 2003. Scaling metabolism from organisms to ecosystems. *Nature* 423:639–42.

García-Corral LS, Barber E, Regaudie-de-Gioux A, Sal S, Holding JM, Agustí S, Navarro N, Serret P, Mozetič P, Duarte CM. 2014. Temperature dependence of planktonic metabolism in the subtropical North Atlantic Ocean. *Biogeosciences* 11:4529–40.

<http://www.biogeosciences.net/11/4529/2014/>

Gelman, A. 2013. Commentary: P Values and Statistical Practice. *Epidemiology* 24(1): 69–72. doi: 10.1097/EDE.0b013e31827886f7.

Gillooly JF, Brown JH, West GB, Savage VM, Charnov EL. 2001. Effects of size and temperature on metabolic rate. *Science* 293: 2248-51.

Grace MR, Imberger SJ. 2006. Stream metabolism: Performing & interpreting Measurements. Water Studies Centre Monash University, Murray Darling Basin Commission and New South Wales Department of Environment and Climate Change. 204 pp.

Grace MR, Giling DP, Hladyz S, Caron V, Thompson RM, McNally R. 2015. Fast processing of diel oxygen curves : estimating stream metabolism with BASE (BAYesian Single-station Estimation). *Limnology and Oceanography:Methods* 13: 103–14. doi: 10.1002/lom.10011

Hall RO, Tank JL, Baker MA, Rosi-Marshall EJ, Hotchkiss ER. 2015. Metabolism, gas exchange, and carbon spiraling in rivers. *Ecosystems* 19: 73-86. doi.org/10.1007/s10021-015-9918-1

Hornbach DJ, Beckel R, Hustad EN, McAdam DP, Roen IM, Wareham AJ. 2015. The influence of riparian vegetation and season on stream metabolism of Valley Creek, Minnesota. *Journal of Freshwater Ecology*:1–20.

<http://www.tandfonline.com/doi/full/10.1080/02705060.2015.1063096>

IPCC. 2014. *Climate Change 2014: Synthesis report. Contribution of working groups I, II and III to the Fifth Assessment Report of the Intergovernmental Panel on Climate Change.* Core Writing Team, Pachauri RK, Meyer LA, editors. Geneva, Switzerland: IPCC. 151 pp.

Hotchkiss ER, Hall Jr RO, Sponseller RA, Butman D, Klaminder J, Laudon H, Rosvall M, Karlsson J. 2015. Sources of and processes controlling CO₂ emissions change with the size of streams and rivers. *Nature Geoscience* 8:696–9.

<http://dx.doi.org/10.1038/ngeo2507>
<http://www.nature.com/ngeo/journal/v8/n9/abs/ngeo2507.html#supplementary-information>
<http://www.nature.com/doi/10.1038/ngeo2507>

Jankowski K, Schindler DE, Lisi PJ. 2014. Temperature sensitivity of community respiration rates in streams is associated with watershed geomorphic features. *Ecology* 95:2707–14.

<http://doi.wiley.com/10.1890/14-0608.1>

Konrad CP. 2006. Location and timing of river-aquifer exchanges in six tributaries to the Columbia River in the Pacific Northwest of the United States. *Journal of Hydrology* 329:444–70.

Leopold LB. 1994. *A view of the river*. Cambridge (MA): Harvard University Press. 298 pp.

Lopez-Urrutia A, San Martin E, Harris RP, Irigoien X. 2006. Scaling the metabolic balance of the oceans. *Proceedings of the National Academy of Sciences* 103:8739–44.

<http://www.pnas.org/cgi/doi/10.1073/pnas.0601137103>

O’Gorman EJ, Pichler DE, Adams G, Benstead JP, Cohen H, Craig N, Cross WF, Demars BOL, Friberg N, Gíslason GM, Gudmundsdóttir R, Hawczak A, Hood JM, Hudson LN, Johansson L, Johansson MP, Junker JR, Laurila A, Manson JR, Mavromati E, Nelson D, Ólafsson JS, Perkins DM, Petchey OL, Plebani M, Reuman DC, Rall BC, Stewart R, Thompson MSA, Woodward G. 2012. Impacts of warming on the structure and functioning of aquatic communities. *Advances in Ecological Research*. Elsevier Vol. 47. p 81–176.

<http://linkinghub.elsevier.com/retrieve/pii/B9780123983152000028>

Perkins DM, Reiss J, Yvon-Durocher G, Woodward G. 2010. Global change and food webs in running waters. *Hydrobiologia* 657:181–98.

Sibly RM, Brown JH, Kodric-Brown A. 2012. *Metabolic Ecology*. (Sibly RM, Brown JH, Kodric-Brown A, editors.). Chichester, UK: John Wiley & Sons, Ltd

<http://doi.wiley.com/10.1002/9781119968535>

Valett HM, Thomas SA, Mulholland PJ, Webster JR, Dahm CN, Fellows CS, Crenshaw CL, Peterson CG. 2008. Endogenous and exogenous control of ecosystem function: N cycling in

headwater streams. *Ecology* 89:3515–27.

Yvon-Durocher G, Allen AP, Montoya JM, Trimmer M, Woodward G. 2010. The temperature dependence of the carbon cycle in aquatic ecosystems. Woodward G, editor. *Advances in Ecological Research*, Vol. 43. Burlington, Massachusetts: Academic Press. p 267-313.

Yvon-Durocher G, Caffrey JM, Cescatti A, Dossena M, Giorgio P Del, Gasol JM, Montoya JM, Pumpanen J, Staehr P a., Trimmer M, Woodward G, Allen AP. 2012. Reconciling the temperature dependence of respiration across timescales and ecosystem types. *Nature* 487:472–6.

Welter JR, Benstead JP, Cross WF, Hood JM, Hurn AD, Johnson PW, Williamson TJ. 2015. Does N₂ fixation amplify the temperature dependence of ecosystem metabolism? *Ecology* 96:603–10. <http://doi.wiley.com/10.1890/14-1667.1>

Willms R, Kendra W. 1990. Methow river water quality survey and assessment of compliance with water quality standards. Washington State Department of Ecology. Environmental Investigations and Laboratory Services Program. Olympia, Washington. USA. 37 pp. Available from <https://fortress.wa.gov/ecy/publications/publications/90e71.pdf> (Accessed 13 September 2015)

Wyatt KH, Turetsky MR, Rober AR, Giroldo D, Kane ES, Stevenson RJ. 2012. Contributions of algae to GPP and DOC production in an Alaskan fen: Effects of historical water table manipulations on ecosystem responses to a natural flood. *Oecologia* 169:821–32.

Tables

Table 3.1: Monthly average estimates for gross primary production (GPP) and ecosystem respiration (ER) in the Methow River basin. Empty cells represent months when sites were not sampled (i.e. high flows, or frozen) or sondes malfunctioned. Sites are organized by drainage area.

Month	BD	EW	BV	T1	T2	C1	M1	C2	M2	M3
<i>Gross primary production</i>										
Jan	0.02	0.02	0.59	0.14		0.55	0.53		4.05	3.49
Feb	0.02	0.03	0.35	0.12	0.13		0.20	0.52		3.77
Mar	0.01	0.02	0.35	0.07	0.13	0.68	0.15	0.75	1.74	
Apr	0.01	0.07	0.59	0.05		0.36	0.22	0.52	1.07	1.58
May				0.02		0.05	0.08			
Jun			0.05	0.05			0.13			
Jul		0.10	0.19	0.04	0.75	0.55	0.07	1.18	2.19	
Aug	0.05	0.07	0.24	0.10	0.68	0.87	0.24	1.27	3.61	2.00
Sep	0.02	0.03	0.12	0.06	0.47	0.48	0.33	0.84	2.04	2.33
Oct	0.01	0.01	0.05	0.05	0.26	0.30	0.15	0.67	1.52	1.78
Nov	0.02	0.02	0.32	0.13	0.30	0.35	0.36	0.75	1.75	1.87
Dec	0.01		0.37	0.09		0.53	0.65		3.93	2.41
Mean (SD)	0.02 (0.02)	0.04 (0.05)	0.29 (0.23)	0.08 (0.07)	0.44 (0.28)	0.52 (0.23)	0.30 (0.22)	0.84 (0.02)	2.26 (1.21)	2.39 (0.80)
<i>Ecosystem respiration (ER)</i>										
Jan	0.07	0.06	0.72	1.35		1.88	1.84		4.51	3.88
Feb	0.04	0.05	0.66	1.14	0.38		1.12	1.28		3.87
Mar	0.09	0.57	1.11	1.18	0.41	1.28	0.55	1.52	2.17	
Apr	0.19	0.28	0.17	0.91		0.84	0.14	1.06	1.29	0.64
May				0.52		0.44	0.26			
Jun			1.09	0.27			0.73			
Jul		0.08	0.25	0.84	0.65	1.20	0.91	1.01	1.94	
Aug	0.19	0.13	0.53	1.24	1.04	1.40	0.86	2.61	2.92	2.08
Sep	0.44	0.27	0.28	1.19	1.05	1.44	1.16	1.91	2.22	2.56
Oct	0.64	0.21	0.83	1.25	1.02	1.31	1.19	2.51	3.12	2.43
Nov	0.39	0.23	0.42	1.58	1.05	0.99	1.77	2.34	2.99	3.04
Dec	0.11		0.85	1.00		1.60	1.86		5.64	4.20
Mean (SD)	0.27 (0.31)	0.22 (0.20)	0.66 (0.39)	1.17 (0.40)	0.91 (0.35)	1.34 (0.50)	1.21 (0.63)	2.02 (0.95)	2.90 (1.53)	2.89 (1.22)

Table 3.2: Average of biological and physical characteristics of sampled sites in the Methow River basin. Chl-a = Chlorophyl-*a*, AFDM=ash free dry biomass, PAR= photosynthetically active radiation, TEMP= temperature, DIN= dissolved inorganic nitrogen, SRP= soluble reactive phosphorus, Q=discharge, CON= channel confinement, DA=drainage area.

<i>Sites</i>	<i>Chl-a</i> mg m ⁻² d ⁻¹	<i>AFDM</i> gm ⁻² d ⁻¹	<i>PAR</i> μ mol m ⁻² s ⁻¹	<i>Temp</i> °C	<i>DIN</i> mg l ⁻¹	<i>SRP</i> mg l ⁻¹	<i>Conf</i> m m ⁻¹	<i>DA</i> km ²	<i>Q</i> cms
BD	13.7	6.1	83	6	0.04	0.008	7	128	0.4
EW	9.2	4	199	7.3	0.05	0.001	11	129	2.2
BV	100.7	15.6	242	6.7	0.3	0.01	7	179	0.5
T1	5.2	3.5	195	6.1	0.07	0.001	25	211	1.9
T2	31.8	10.2	264	10.3	0.08	0.001	15	394	2.4
C1	23.1	9.3	176	5.7	0.04	0.003	22	536	2.1
M1	10.2	5.4	284	7.6	0.05	0.002	32	666	6.3
C2	28.3	11.9	203	8.4	0.05	0.002	13	843	2.6
M2	42.3	15.3	300	7.6	0.1	0.002	28	1669	13.3
M3	44.1	14.7	204	6.8	0.18	0.002	29	1722	10.4

Table 3.3: Estimates of the coefficient estimates, standard errors, p values, and R_m and R_c from the linear mixed models of the relationship between ln-transformed gross primary productivity and ln-transformed ecosystem respiration and $1/kT$, where k is the Boltzmann constant (8.61×10^{-5} eV/K; 1 eV/K= 1.6×10^{-19} J) and T is temperature (K). Both rates were measured in $\text{mg O}_2 \text{ m}^{-2} \text{ d}^{-1}$. Sites in bold are considered temperature dependent.

Site	Estimate	SE	t value	p-value	R_m	R_c
<i>Gross primary production (GPP)</i>						
BD	-0.26	0.003	43	0.000	0.50	0.97
EW	-0.58	0.120	126	0.000	0.57	0.95
BV	-0.28	0.216	159	0.198	0.05	0.90
T1	0.32	0.143	179	0.028	0.10	0.31
T2	-0.17	0.022	95	0.000	0.70	0.77
C1	0.03	0.031	145	0.337	0.02	0.79
M1	-0.25	0.123	218	0.041	0.05	0.84
C2	-0.12	0.033	109	0.000	0.24	0.38
M2	0.02	0.095	86	0.829	0.00	0.98
M3	0.03	0.052	108	0.545	0.01	0.78
<i>Ecosystem respiration (ER)</i>						
BD	-0.08	0.313	43	0.804	0.01	0.54
EW	1.33	0.278	126	0.000	0.22	0.58
BV	0.08	0.050	159	0.122	0.07	0.71
T1	0.05	0.053	179	0.329	0.02	0.41
T2	0.00	0.049	95	0.996	0.00	0.94
C1	0.08	0.042	145	0.064	0.06	0.52
M1	0.17	0.059	218	0.004	0.08	0.75
C2	0.05	0.060	109	0.369	0.02	0.63
M2	0.22	0.116	86	0.058	0.13	0.97
M3	0.12	0.048	108	0.012	0.06	0.92

Table 3.4: Estimates of the coefficient estimates, standard errors, p values, and R_m and R_c from the linear mixed models of the relationship between ln-transformed AFDM specific GPP and ln-transformed AFDM specific ER and $1/kT$, where k is the Boltzmann constant (8.61×10^{-5} eV/K; $1 \text{ eVK} = 1.6 \times 10^{-19}$ J) and T is temperature (K). Both rates were measured in $\text{mg O}_2 [\text{g AFDM}] \text{ d}^{-1}$. Sites in bold are considered temperature dependent.

Site	Estimate	SE	t value	p-value	R_m	R_c
<i>AFDM Specific Gross primary production (AFDM-GPP)</i>						
BD	-0.13	0.002	-64.15	0.000	0.20	0.98
EW	-0.55	0.118	-4.64	0.000	0.40	0.97
BV	-0.15	0.096	-1.62	0.108	0.05	0.97
T1	0.02	0.012	1.40	0.162	0.03	0.28
T2	-0.07	0.010	-7.09	0.000	0.70	0.79
C1	0.01	0.015	0.80	0.427	0.01	0.87
M1	-0.03	0.020	-1.70	0.091	0.04	0.68
C2	-0.06	0.019	-3.10	0.003	0.22	0.61
M2	0.01	0.033	0.29	0.773	0.00	0.98
M3	-0.03	0.019	-1.81	0.074	0.12	0.79
<i>AFDM Specific Ecosystem Respiration (AFDM-ER)</i>						
BD	-0.02	0.132	-0.16	0.871	0.00	0.79
EW	0.88	0.233	3.79	0.000	0.17	0.58
BV	0.00	0.022	0.22	0.826	0.00	0.85
T1	0.04	0.049	0.80	0.427	0.01	0.51
T2	-0.01	0.023	-0.31	0.757	0.00	0.97
C1	0.03	0.020	1.42	0.159	0.04	0.61
M1	0.07	0.041	1.68	0.095	0.01	0.92
C2	-0.01	0.029	-0.22	0.830	0.00	0.85
M2	0.07	0.032	2.07	0.041	0.16	0.97
M3	0.04	0.021	1.98	0.050	0.05	0.94

Figures

Figure 3.1: Map of the Methow River basin. The 10 stream reaches, main tributaries and Columbia River are identified by name. The inset indicates the location of the Methow River in Washington State, USA. Black star represents location of PAR sensor.

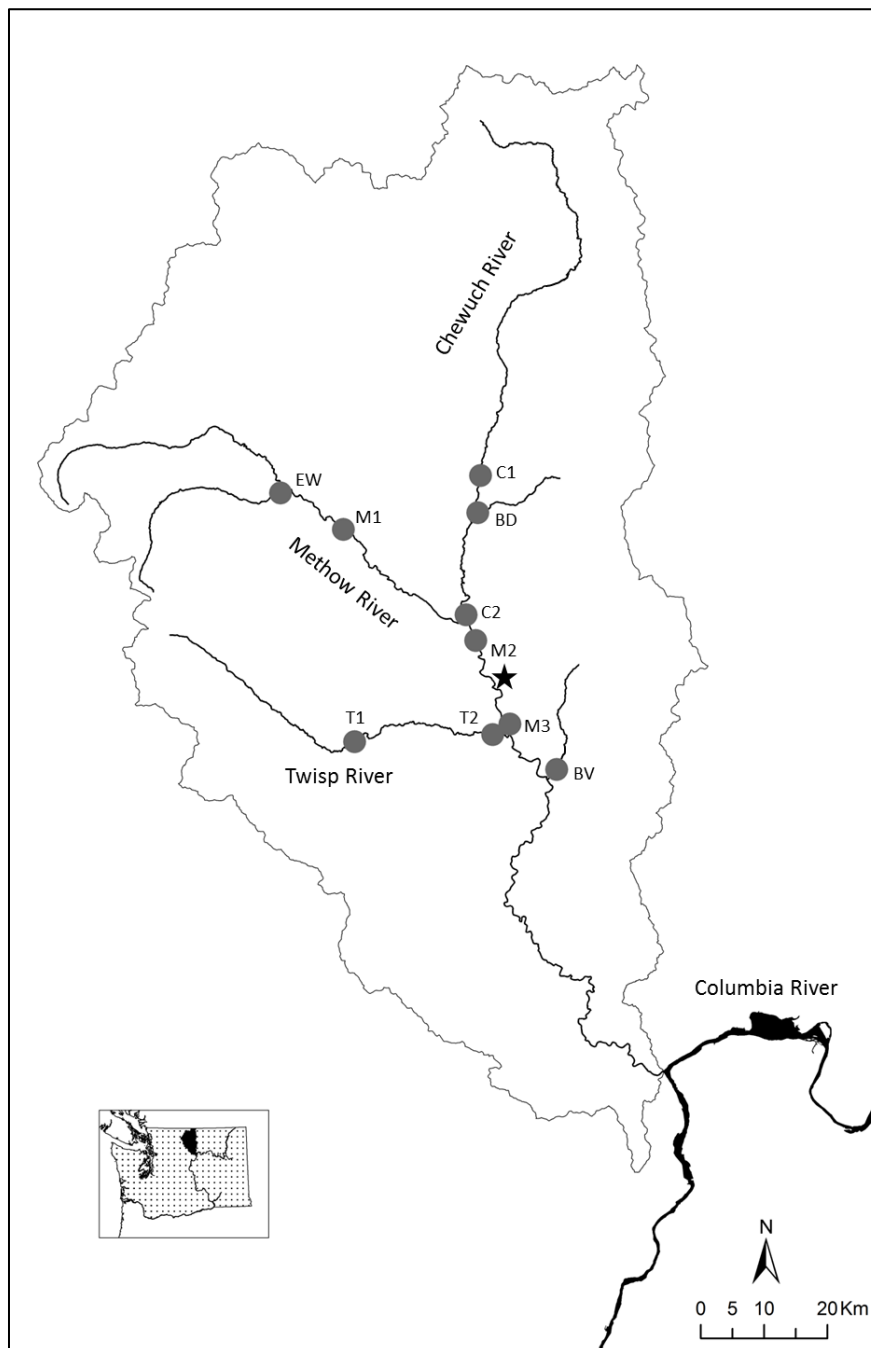


Figure 3.2: (a) Temperature of profile and (b) monthly measured AFDM biomass of the 10 study sites in the Methow River basin. Sites are organized by drainage area from small to large.

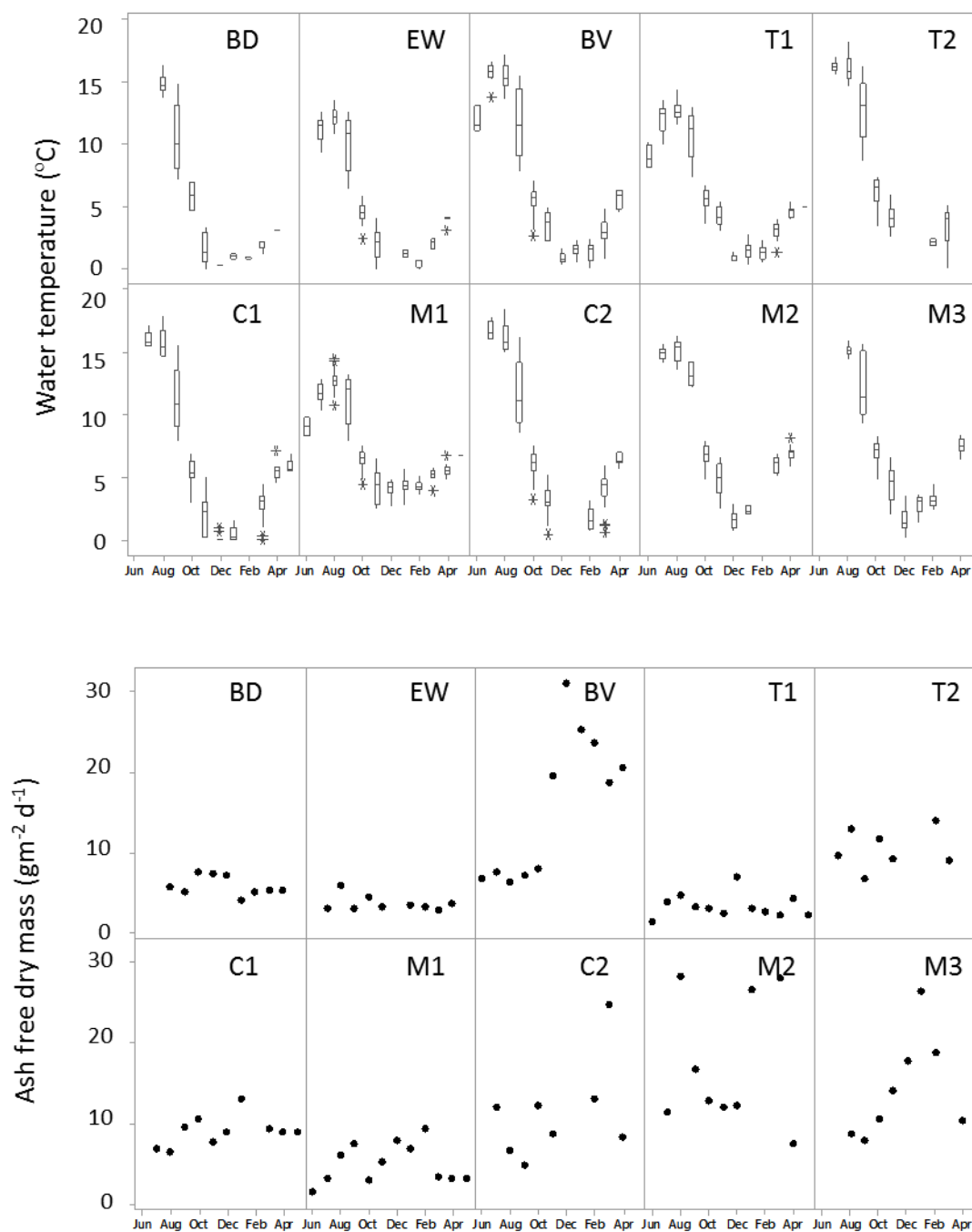


Figure 3.3: (a) Temperature dependence of gross primary production (E_p , originally measured in $\text{mg O}_2 \text{ m}^{-2} \text{ d}^{-1}$) plotted as the relationship between \ln -transformed GPP rate and inverse temperature ($1/kT$). (b) Temperature dependence of ecosystem respiration (E_r , originally measured in $\text{mg O}_2 \text{ m}^{-2} \text{ d}^{-1}$) plotted as the relationship between \ln -transformed ER rate and inverse temperature ($1/kT$). k is the Boltzmann constant ($8.61 \times 10^{-5} \text{ eV/K}$; $1 \text{ eV/K} = 1.6 \times 10^{-19} \text{ J}$) and T is temperature (K). The canonical expectation of GPP and ER are -0.32 and -0.65 , respectively. Sites are organized by drainage area from small to large.

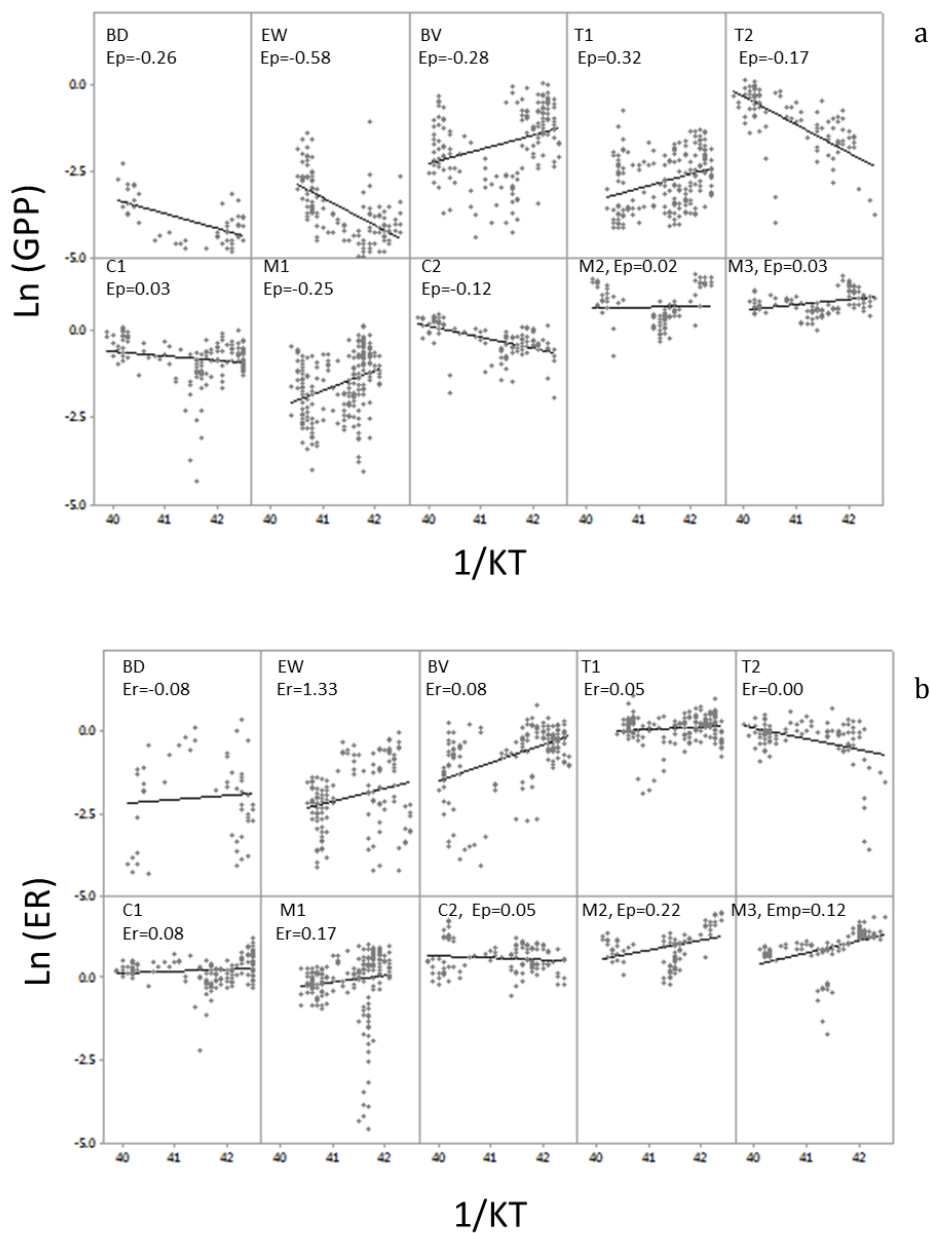


Figure 3.4: (a) Temperature dependence (Emp) of AFDM specific gross primary production (GPP, originally measured in $\text{mg O}_2 [\text{AFDM}] \text{d}^{-1}$) plotted as the relationship between ln-transformed GPP rate and inverse temperature ($1/kT$). (b) Temperature dependence (Emr) of AFDM specific ecosystem respiration (ER, originally measured in $\text{mg O}_2 [\text{AFDM}] \text{d}^{-1}$) plotted as the relationship between ln-transformed ER rate and inverse temperature ($1/kT$). k is the Boltzmann constant ($8.61 \times 10^{-5} \text{ eV/K}$; $1 \text{ eVK} = 1.6 \times 10^{-19} \text{ J}$) and T is temperature (K). The canonical expectation of GPP and ER are -0.32 and -0.65 , respectively. Sites are organized by drainage area from small to large.

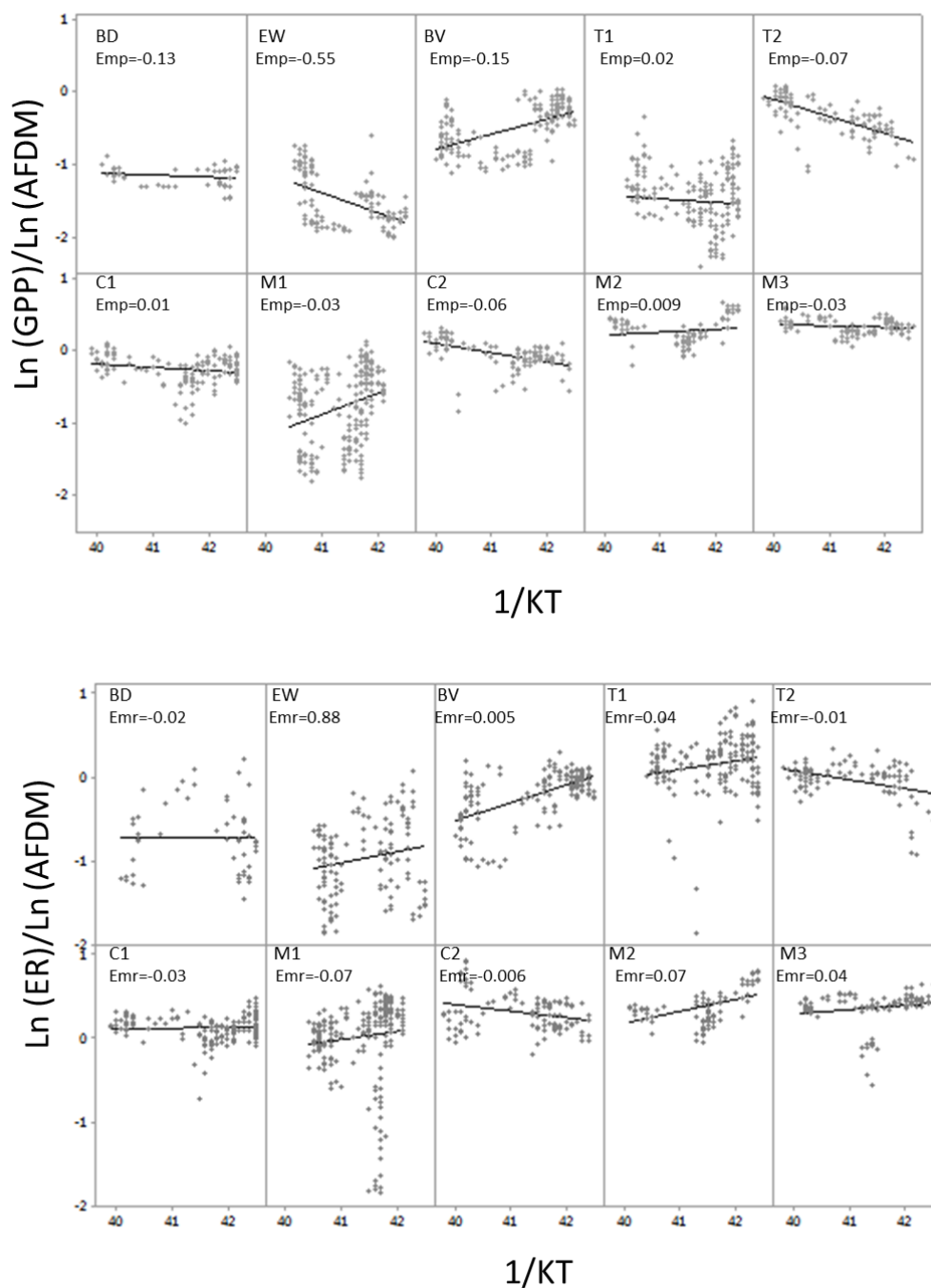


Figure 3.5: Relationship of temperature dependence estimated for individual sites for gross primary production (E_p) vs. (a) drainage area and (b) channel confinement, and ecosystem respiration (E_r) vs. (c) drainage area and (d) channel confinement. * E_r for EW site was not included.

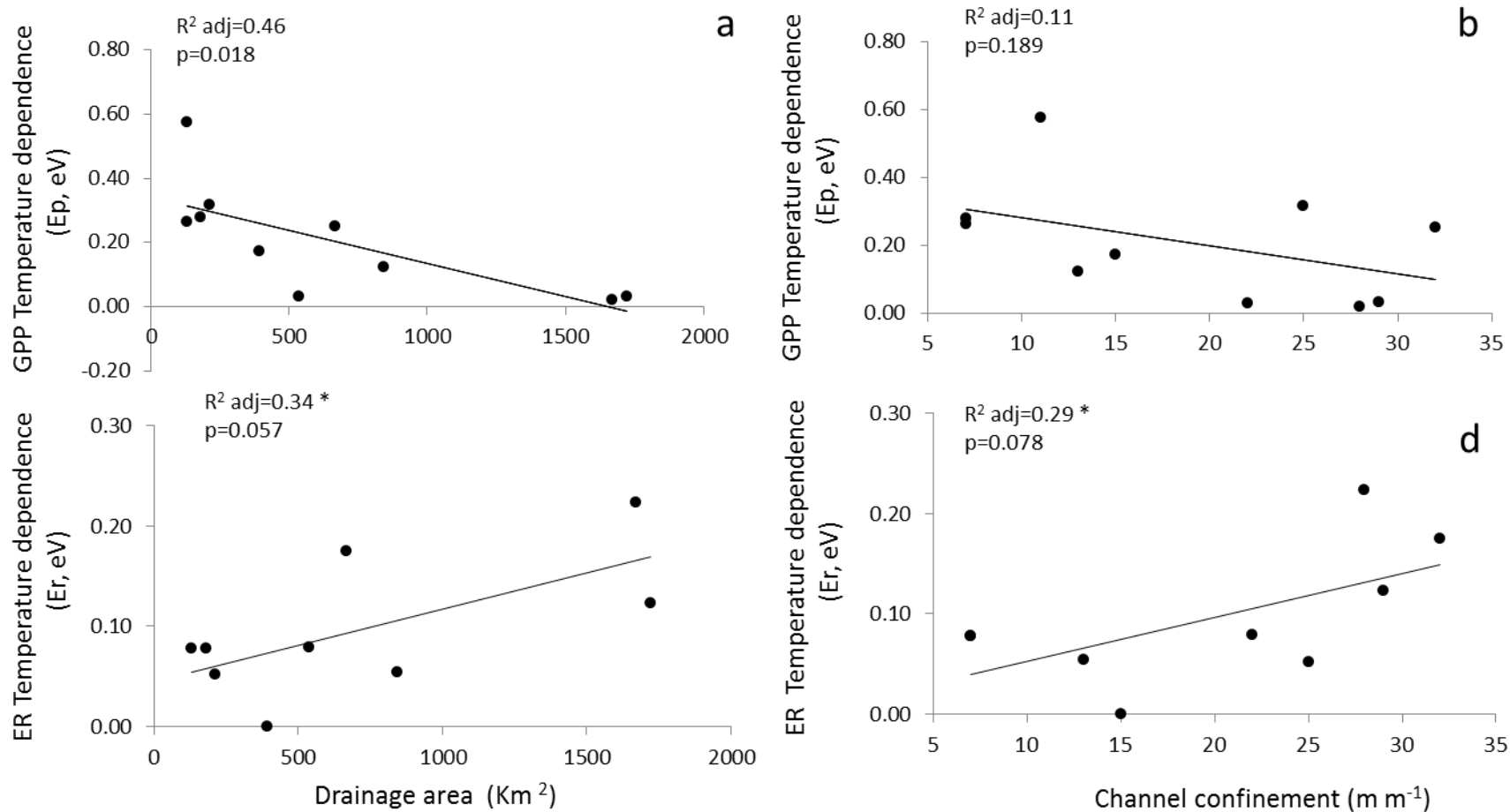
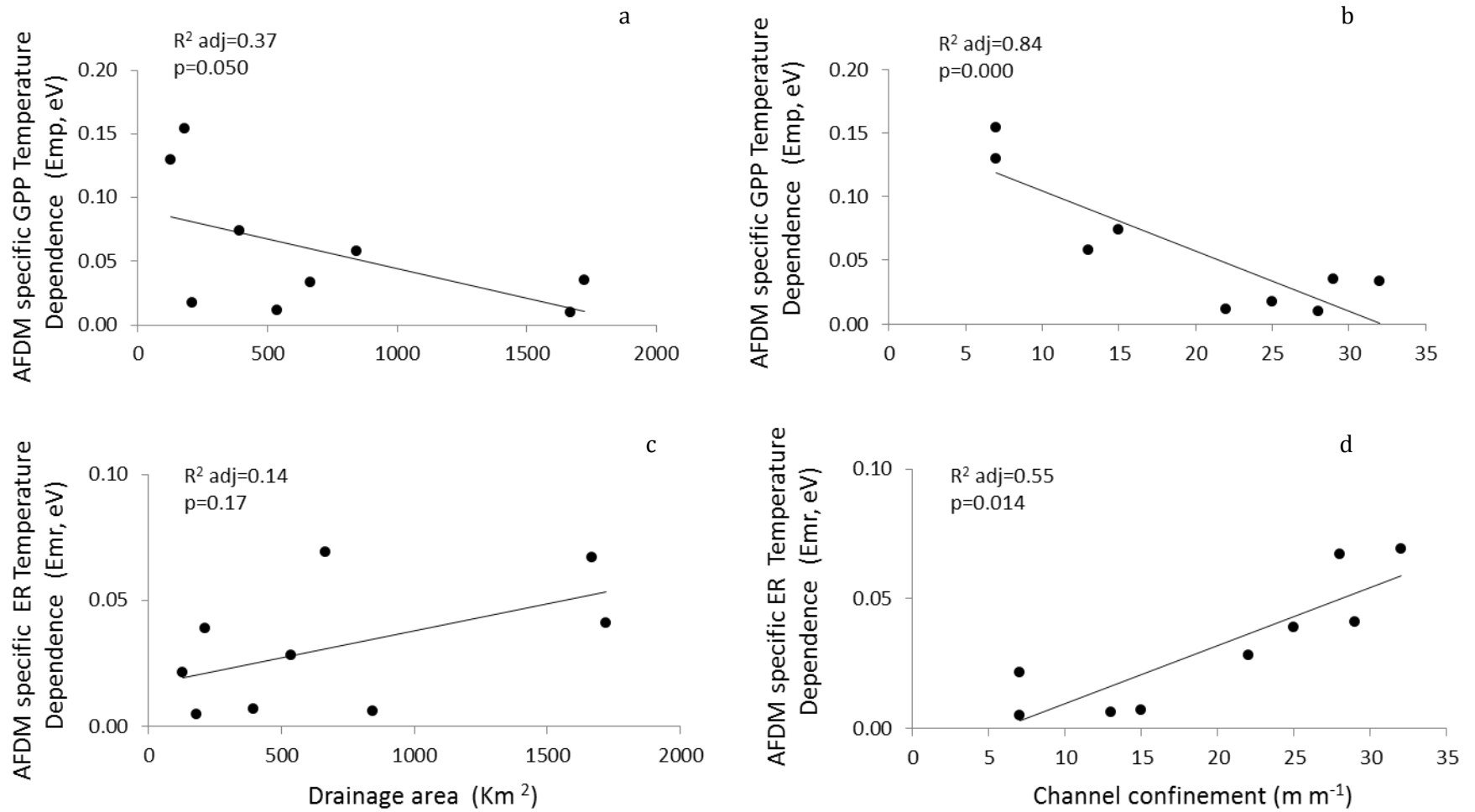


Figure 3.6: Relationship of temperature dependence estimated for individual sites for AFDM specific gross primary production (Emp) vs. (a) drainage area and (b) channel confinement, and AFDM specific ecosystem respiration (Emr) vs. (c) drainage area and (d) channel confinement. * Emp and Emr for EW site were not included.



CHAPTER 4: Stream Metabolism Increases with Drainage Area and Peaks Asynchronously Across a Stream Network

Chapter 4 is written in the plural “we” for submittal to the *Ecosystems* journal with co-authors Joseph R. Benjamin, James R. Bellmore, Grace A. Watson, Adrienne Zuckerman, and Alexander K. Fremier.

Introduction

Stream networks are nested hierarchical habitat mosaics that are connected to the landscape longitudinally, laterally and vertically through hydrology (Fisher and Welter 2005). These dynamic spatial and temporal arrangements in turn influence the structure and function of lotic ecosystems (Poole 2002, Benda et al. 2004). For example, Cross et al. (2013) demonstrated that spatial variability of secondary production in the Colorado River in the Grand Canyon was associated to the position of the major tributaries and Langhans et al. (2008) found that leaf decomposition varied widely across multiple floodplain habitats. An integrative measure of stream structure and function is stream metabolism, which is a measure of the flux of organic carbon flows within a defined stream reach, including both gross primary production (GPP) and ecosystem respiration (ER) (Bernot et al. 2010). GPP is the measure of the total amount of carbon produced via photosynthesis whereas ER represents the amount of carbon respired by both autotrophs and heterotrophs. GPP indicates organic carbon availability for food webs and ER corresponds to carbon consumption (Bernot et al. 2010, Finlay 2011).

Because stream metabolism plays a major role in regulating the supply and temporal

dynamics of basal organic matter resources in lotic systems (Odum, 1956), understanding the underlying processes influencing observed spatial and temporal patterns of GPP and ER is an active field of research and a central goal of stream ecology with applied management implications. A considerable number of studies have examined spatial (Cardinale et al. 2002, Warnars et al. 2007, Finlay 2011, Yates et al. 2013) and temporal variation (Uehlinger and Naegeli 1998, Roberts et al. 2007, Beaulieu et al. 2013) in stream metabolism. However, both spatial and temporal variation of metabolism have seldom been studied simultaneously across a river network (Young and Huryn 1996, Houser et al. 2005, Venkiteswaran et al. 2015) and continuously (but see Izaguirre et al. 2008) and even more rare are studies that include winter conditions (Hart 2013) due to logistic constraints and challenging environmental conditions.

First order controls of metabolism appear system-specific because direct variables controlling stream metabolism (GPP and ER) such as light availability, temperature, nutrients, autotrophic biomass, organic matter supply, and hydrology are affected by factors operating at multiple spatial and temporal scales through their interactions with their landscape setting (Uehlinger 2006, Roberts et al. 2007, Bernot et al. 2010, Tank et al. 2010). Because streams and the landscape they drain are proportional to stream size, drainage area and its geomorphic template integrate environmental conditions (i.e. light, nutrients, and litter fall) and create gradients in resource availability that influence the spatial patterns of GPP and ER (Ogdahl et al. 2010, Finlay 2011). For example, at the watershed scale in montane river networks, the relative importance of allochthonous contributions originating in forested river headwaters decreases in abundance with increasing distance downstream (Vannote et al. 1980). Consequently, streams exhibit changes in organic matter production

and balance as they flow from headwaters to downstream reaches (McTammany et al. 2003).

Hydrologic connectivity and regional climate patterns stimulate synchronous behavior of environmental conditions, particularly in lentic systems (Baines et al. 2000, Ogdahl et al. 2010). However, temporal patterns of stream metabolism may be more controlled by local drivers that differ by location in the watershed (Valett et al. 2008, Ogdahl et al. 2010). The relative abundance and processing of basal organic matter resources varies throughout the year because of seasonality in stream flow, light, temperature, nutrients, and litter fall. High flows in the spring and early summer reduce GPP and ER across the stream network (Uehlinger and Naegeli. 1998), and as flows decline, other environmental conditions, such as light and nutrient availability influence stream metabolism. The relative importance of these factors varies by site. For example, in forested headwaters, light availability becomes the limiting factor (Greenwood and Rosemond 2005) whereas in open canopied streams, nutrients may become limited in the summer as nutrient uptake exhausts supply (Finlay et al. 2011). Valett et al. (2008) suggested that seasonal patterns of stream metabolism differ along a gradient depending on the relative influences of resource subsidies and in-stream autochthonous resources. Thus, changes on the arrangements in resource abundance could lead to asynchrony of basal resources as different environmental conditions control GPP and ER at different times a year.

Our overall objective was to describe the spatial and temporal patterns in stream metabolism across a stream network and examine potential drivers. We asked the following questions: (1) Do GPP and ER increase with stream size and do streams become less heterotrophic with increasing stream size? (2) When are the peaks and troughs of gross primary production and ecosystem respiration? (3) How do environmental conditions change

through the year? and (4) What are the potential drivers of GPP and ER? We hypothesized that GPP and ER increase with stream size and streams become less heterotrophic with increasing stream size. We also hypothesized that GPP and ER were highest when available light and temperature were highest after the high stream flows (summer months); but potential co-limiting environmental conditions, that vary by site, drive seasonal patterns in GPP and ER. To investigate these patterns, we measured dissolved oxygen continuously for 11 months to derive estimates of stream metabolism at 10 stream reaches across a temperate stream network. We also discuss our findings in relation to the dynamic and spatially heterogeneous patterns of stream productivity across the stream network.

Methods

Study Area

The Methow River is an alluvial river in North Central Washington State within the Columbia River basin. It has a large unconfined aquifer, low nutrient levels, cool water temperatures and multiple native anadromous salmonid runs (Konrad et al. 2006, Willms and Kendra 1990, Bellmore et al. 2013). The Methow River basin in north central Washington State (USA) has a catchment area of 4,462 km² and elevations ranging from 2,700 m in the Cascade Mountains to 240 m at the confluence with the Columbia River. The basin has a snowmelt driven hydrology with high-altitude areas on the western side of the basin receiving approximately 2000 mm of precipitation annually and areas in the lower river valley receiving 300 mm (Konrad 2006). The river has a largely unaltered, snowmelt-dominated flow regime with high flows during May – June, and low flows during August-January. Flows during the study were representative of flows within the historic record at

USGS gage 12448500 (Methow River at Winthrop), except for flows in September and October in 2013 which were more than twice as high that the mean average flows of the historic record for those months (1912 to 2014). Due to glacial history valley sediments are mostly unconsolidated sands and gravels. The alluvium and glacio-fluvial sediments deposited during the Quaternary period form the main aquifer. The deposit is almost uninterrupted along the valley bottom to the confluence with the Columbia River. However, some of the upper tributaries such as Boulder Creek, are characterized by colluvial deposits. The riparian corridor is dominated by Douglas-fir (*Pseudotsuga menziesii*) and pine (*Pinus spp.*) in the higher elevation reaches whereas black cottonwood (*Populus trichocarpa*), speckled alder (*Alnus incana*), bigleaf maple (*Acer macrophyllum*), and western red cedar (*Thuja plicata*) are abundant in the lower areas (Bellmore et al. 2013).

Study Design

To examine the spatial and temporal patterns in stream metabolism across a stream network, we continuously measured dissolved oxygen from June 2013 to May 2014 at ten stream reaches in the Methow River basin (Figure 4.1). Gaps in data occurred when flows were too high and sondes were removed, stream reaches froze, or DO sensors malfunctioned. We selected the ten stream reaches from a list of 52 sampling locations that are part of the Columbia River Habitat Monitoring Program (CHaMP; <https://www.champmonitoring.org/>). CHaMP is a fish habitat monitoring implemented across 26 watersheds in the Columbia River basin. We selected the stream reaches using a principal component analysis that summarized the range of environmental conditions that we assumed largely controlled metabolism in the Methow River basin based on the results from a sensitivity analysis carried

out to understand the effects of salmon spawning on periphyton dynamics (Bellmore et al. 2014, Zuckerman 2015). Selection criteria also included ease of winter access, landowner permission, and whether the sites lacked nearby irrigation drains and major groundwater inputs.

Stream Metabolism Measures

Field methods

At each stream reach, we measured stream metabolism via the open channel, single-station, diel O₂ method. We recorded dissolved oxygen (DO) concentrations every 10 minutes from June 2013 to May 2014 in the channel thalweg with an YSI sonde (Yellow Springs, Ohio, USA) outfitted with an optical oxygen probe. Approximately every two weeks, we re-calibrated the sondes in the field in a bucket of air-saturated water using an air pump and air stone (Hall et al. 2015). Prior to data analysis, we corrected our DO readings from drift that occurred during the deployments (Grace and Imberger 2006).

Metabolism estimation

We used the BAYesian Single-station Estimation (BASE) program (Grace et al. 2015) to estimate stream metabolism from the diel DO curves. The BASE program estimates single-station whole-ecosystem metabolism using Bayesian statistics. The batch mode fits data for many days and provides visual and statistical measures of “goodness-of-fit.” In addition to DO data, the BASE program requires inputs of barometric pressure, water temperature and salinity to estimate metabolism. We obtained barometric pressure data (in Hg) recorded every 15 minutes and corrected to sea level from Chief Joseph Dam

Washington Agrimet Cooperative Agricultural weather network station (CJDW <http://www.usbr.gov/pn/agrimet/webagdayread.html>). We corrected barometric pressure data for altitude at each stream reach. We also set salinity values to 0 (Grace and Imberger 2006) because of the low electric conductance in the Methow River (maximum electrical conductance $< 500 \mu\text{S cm}^{-1}$).

The model estimates GPP and ER in units of $\text{mg O}_2 \text{ l}^{-1} \text{ d}^{-1}$, which were converted to areal rates ($\text{g O}_2 \text{ m}^{-2} \text{ d}^{-1}$) using measured mean stream depth. After we ran 8,000 iterations using a Markov Chain Monte Carlo (MCMC) method to estimate values for GPP and ER, we evaluated daily models fit using both an R^2 , which quantifies the correlation between modeled and measured DO data, and a posterior predictive check (PPC), which measures the overall fit based on the MCMC iterations Grace et al. (2015). We only used daily models with an $R^2 \geq 0.6$ and a PPC >0.1 or <0.9 . The mean R^2 of our models was $0.92 (\pm 0.08 \text{ SD})$ and mean PPC = $0.63 (\pm 0.13 \text{ SD})$. After applying this set of criteria for model fitting, we deemed 1,373 days across the ten stream reaches as good fits (56% of the total days modeled). Grace et al. (2015) found that BASE successfully converged and fitted 78% of the DO diel curves included in their evaluation of their model. Our lower percentage may be attributed to the inclusion of days characterized by cold water temperatures, low productivity and high turbulence (M. Grace, personal communication). We discarded the poor fitted diel curves and did not include incomplete days or periods where DO probes malfunctioned. We used the average of the daily GPP and ER estimates for subsequent statistical analyses. We also estimated daily AFDM specific GPP ($\text{g O}_2 \text{ g [AFDM]}^{-1} \text{ d}^{-1}$) by dividing daily GPP by AFDM.

Periphyton Biomass, Physical and Chemical Measurements

At each site, we took monthly samples of periphyton biomass of five randomly selected rocks in the active channel at 10 m intervals upstream of the dissolved oxygen sensors. We removed all periphyton from each rock, filtered the slurry, and froze the slurry for later lab analysis for Chlorophyll-*a* (Chl-*a*, $\text{mg m}^{-2} \text{d}^{-1}$) and for ash free dry mass (AFDM, $\text{g m}^{-2} \text{d}^{-1}$), following Standard Methods (APHA, 2005). To quantify planar surface area, we traced the top surface of each rock on paper (Bergey and Getty 2006). Periphyton samples were taken monthly except on a few instances when flows were too high, during spring and early summer, and access to the streambed was unsafe.

During these monthly sampling events, we collected one water sample at the downstream end of each site. Samples were immediately filtered ($0.45\mu\text{m}$), stored frozen and then analyzed using EPA standard methods (United States Environmental Protection Agency 1983) by IEH Analytical Laboratories (Seattle, Washington, USA) for ammonium ($\text{NH}_4\text{-N}$), nitrate + nitrite ($\text{NO}_3\text{-N}$, $\text{NO}_2\text{-N}$), and soluble reactive phosphorus (SRP). For our study, we considered all three dissolved nitrogen species together as dissolved inorganic N (DIN). Detection limits for DIN were 0.01 mg L^{-1} and for SRP were 0.001 mg L^{-1} .

We measured photosynthetically active radiation (PAR) with a PAR sensor and data logger (sensor model S-LIA-M003, data logger model H21-002, Onset Computer Corporation, Bourne, Massachusetts, USA) at a single, central, open location free of obstructions near Winthrop, WA (Figure 3.1). Readings were recorded every 30 minutes for the duration of the study. This dataset represented the total PAR entering the basin and this amount was adjusted at each site by measuring solar access using a Solmetric Suneye 210 (Solmetric Corporation, Sebastopol, California, USA). We placed the Suneye at the center of

the channel at three locations during an August 2013 visit to each site. Solar access is the amount of site-specific solar insolation available given the shade-causing obstructions (e.g. tree canopy, topographic shading, structures) divided by the solar insolation if there were no shading. The Suneye 210 estimates the solar access percentage for every day of the year by taking into consideration the GPS coordinates to generate a sunpath diagram. We multiplied each PAR measurement taken at the open site by the daily percentage solar access to estimate PAR experienced at each site.

For each site, we generated daily discharge estimates using the ratio of daily discharge to bankfull discharge from the closest USGS gages. This ratio was multiplied by the bankfull discharge at the un-gaged stream reach to create an adjusted dataset of mean daily discharge, as suggested by Leopold (1994). We obtained gage daily discharge from four nearby USGS gages (12448000, 12448500, 12448998, 12449500).

To determine estimates of channel confinement (Table 4.1), the ratio of the valley floor width to the bankfull channel width, we obtained valley floor width data for each stream reach from the Methow River TerrainWorks database (<http://www.terrainworks.com/terrainworks-dataset-locator>) and bankfull channel width data from the CHaMP database. Valley width was calculated at five times bankfull depth (Benda et al. 2007, Burnett et al. 2007). Bankfull width was estimated as the average width of the bankfull polygon calculated from digital elevation models (DEM) at each stream reach. We also used publically available aerial photographs (National Agriculture Imagery Program, NAIP 2009, <http://www.fsa.usda.gov/programs-and-services/aerial-photography/imagery-programs/naip-imagery/index>) to visually verify the validity of estimated widths.

We estimated drainage area (Table 4.1), the area that drains to a point on a stream,

using StreamStats (<http://water.usgs.gov/osw/streamstats/>). StreamStats use digital elevation data from the National Elevation Dataset (NED) to determine drainage-basin boundaries.

Statistical Analyses

To determine whether GPP, AFDM specific GPP, and ER increased and stream reaches became increasingly less heterotrophic with stream size, we used Pearson correlations between metabolism and drainage area. We also determined seasonal patterns of GPP AFDM specific GPP, and ER two ways. First, we plotted daily metabolism and compared them across the network. Second, we standardized stream metabolism by estimating the Z-scores of GPP and ER per each site and month (Valett et al. 2008). A Z-score is a statistical measurement of a score's relationship to the mean in a group of scores. A Z-score of 0 means the score is the same as the mean. A Z-score can also be positive or negative, indicating whether it is above or below the mean and by how many standard deviations. We then plotted the monthly average of daily metabolism to develop generalized curves of observed patterns.

Lastly, we inferred potential environmental drivers using a linear mixed modeling approach (Zuur et al. 2009) with the nlme package for mixed effects modeling (R Development Core Team 2013). At each scale for the linear mixed models, the explanatory variables were AFDM, SRP, DIN, TEMP, PAR and Q and the dependent variable were ER and GPP. However, for, ER models, we also included GPP. For the across site analysis of GPP and ER, we included stream reach and month as random effects to account for the repeated measures. For the individual site analysis, we only included month as a random effect. We inspected deviations from the analysis assumptions using model diagnostic plots

and accounted for heteroscedasticity by including variance functions (Pinheiro and Bates 2000; Zuur et al. 2009). We did not find evidence of multicollinearity among explanatory variables (variance inflation factor < 3); hence all variables were considered. We used the Akaike's Criterion corrected for small sample sizes (AICc) to select the best models and retained models that had a delta < 2 . We estimated $R^2_{\text{GLMM}(m)}$, marginal R^2 , for fixed factors and $R^2_{\text{GLMM}(c)}$ conditional R^2 for both fixed and random factors $R^2_{\text{GLMM}(m)}$ using the R function 'r.squaredGLMM' from the package 'MuMIn' (Bartoń 2015).

Before conducting the linear mixed modeling, we tested predictor variables for multicollinearity in two ways. First, we compared Pearson correlations between metabolism and predictor variables. Second, we estimated the variance inflation factor (vif) and deemed that a $\text{vif} > 10$ indicated multicollinearity (Fox and Weisberg 2011). Removal of collinear variables is necessary because correlated predictors may not give valid results about any individual predictor, or about which predictors are redundant with respect to others. We also tested normality with the Shapiro–Wilk test. All statistical analyses were performed in R (R Core Team, 2013) and deemed results significant if $p < 0.05$.

Results

Does Stream Metabolism Increase with Drainage Area?

Stream metabolism (GPP, mass-specific GPP, and ER) varied widely across the 10 stream reaches. Daily GPP and daily $|\text{ER}|$ ranged from 0 to 5.22 $\text{mg O}_2 \text{ m}^{-2} \text{ d}^{-1}$ and 0.009 to 7.48 $\text{mg O}_2 \text{ m}^{-2} \text{ d}^{-1}$ (Appendix 1-Table 1). On average, there was approximately two orders of magnitude increase across the network for mean GPP, 0.02 $\text{mg O}_2 \text{ m}^{-2} \text{ d}^{-1}$ to 2.39 $\text{mg O}_2 \text{ m}^{-2} \text{ d}^{-1}$ and one order of magnitude increase for mean $|\text{ER}|$, 0.27 $\text{mg O}_2 \text{ m}^{-2} \text{ d}^{-1}$ and 2.89 $\text{mg O}_2 \text{ m}^{-2} \text{ d}^{-1}$.

$\text{O}_2 \text{ m}^{-2} \text{ d}^{-1}$ (Table 4.1, Figures 4.2a and 4.2b). Mean annual GPP, mass-specific GPP, and $|\text{ER}|$ increased with drainage area ($r=0.98$, $p<0.0001$; $r=0.67$, $p<0.0001$; $r=0.96$, $p<0.0001$, Appendix 1 – Table 1). Average annual ER was also correlated to channel confinement ($r=0.67$, $p=0.036$). Gross primary production (GPP) and mass-specific GPP increased with drainage area in all seasons (Figure 4.2 for GPP, mass-specific GPP not shown) ($r>0.90$ and $p<0.0001$ for GPP and $r>0.60$, $p<0.0001$ for mass-specific GPP). In contrast, ecosystem respiration ($|\text{ER}|$) was significantly correlated with drainage area in all seasons (r coefficients ranged from 0.86 to 0.96) except in the spring ($r=0.60$, $p=0.087$; Figure 4.2b) when we observed lower than expected $|\text{ER}|$ values at the largest stream reach.

Does Heterotrophy Decrease with Drainage Area?

Stream reaches were mostly heterotrophic with mean annual NEP ranging from -0.18 (SD=0.22) in to -1.18 (SD=0.87) from smallest to largest stream reach (Figure 4.2c, Table 4.1). Although we expected NEP to increase with drainage area in all seasons and NEP relationship with drainage area became increasingly negative (heterotrophic) as fall progressed, this relationship was only significant in the fall, $r=-0.70$, $p=0.025$ (Figure 4.2c). However, we did observe positive NEP (autotrophy) at some stream reaches occasionally in all seasons, except in the fall. In addition, GPP and ER were positively correlated with each other at most sites except for two of the smallest stream reaches, BD and EW (Figure 4.3, $r=0.70$, $p<0.0001$, all sites combined) where allochthonous carbon contributions were likely large.

When are the Peaks and Troughs of Gross Primary Production and Ecosystem Respiration?

Gross primary production (GPP) and mass-specific GPP exhibited three temporal patterns across the stream network, although, these patterns were more pronounced for mass-specific GPP (Figures 4.4a and 4.4b, Appendix 2 –Figures 1 and 2). For the first pattern, a subset of stream reaches (BD, EW, C2, and T2) revealed peaks during the summer months and most of these stream reaches either froze completely or partially from December to February. For the second set of stream reaches (M1, T1, M3), GPP peaked during the winter. The third pattern included stream reaches that displayed multiple peaks (BV, C1, and M2). Temporal patterns at these three sites seem to correspond to a blend of the other two groupings.

Ecosystem respiration peaks exhibited two temporal patterns. ER either peaked in the fall (BD, EW, C2, and T2) or the winter (BV, T1, M1, C1, M2, and M3), depending on the site (Figure 4.4b, Appendix 2 –Figure 3).

How Do Environmental Conditions Change Through the Year?

Generally, decreasing daily discharge (Q) in late summer coincided with increasing light availability (PAR) and increased water temperatures across the basin (Figure 4.5). Water temperature followed a similar trajectory, highest in the spring and summer and lowest in the winter, for all three GPP groups (Figure 4.5). DIN concentrations in the multiple peaks group was highest and tended to increase in the winter (Figure 4.5). SRP was generally very low, but peaked in the summer and spring for the multiple peaks group and peaked in the winter for the winter group (Figure 4.5).

What are the Potential Drivers of GPP and ER?

Overall, daily discharge was the most important environmental driver for all stream reaches regardless of temporal groupings except at T1 where PAR and SRP were the best predictors (Table 4.2). Water temperature (TEMP) was also a significant driver for most stream reaches where GPP peaked in the summer. In contrast, GPP was negatively associated with daily PAR in stream reaches that peaked in winter. Lastly, although DIN and SRP associations were not significant in most stream reaches, associations in the summer peak group were positive in one reach (T2, $p=0.007$), whereas associations in the winter and multiple peaks groups were negative (BV, $p=0.008$; T1, $p=0.029$). These relationships may suggest that streams that peak in the winter and spring may experience high nutrient uptake in the summer and thus may be nutrient limited or co-limited in the summer. BV, a multiple peak site, was the only stream reach where GPP was positively associated with AFDM ($p<0.0001$).

The ER linear mixed models for individual stream reaches confirmed patterns observed between ER and GPP (Figure 4.3). Ecosystem respiration (ER) was positively associated with GPP in all stream reaches except BD and EW. Daily discharge (Q) had the most influence in BD whereas negative associations with nutrients (DIN and SRP) appear to be equally important in EW (Table 4.3).

The across sites linear mixed model for GPP accounted for approximately 44% of the variability of the fixed effects (Table 4.4) and AFDM was the best explanatory variable. In contrast, Q was the most consistent variable influencing GPP at the stream reach level and was used as a measure of stream reach disturbance. Q at the across sites model may not be a good measure of disturbance and it may relate to light penetration better or it may not be that

important when looking across sites. Instead, AFDM was likely a close surrogate of disturbance as periphyton accrual may indicate stable conditions. Thus, the strongest association in the across sites GPP model was between AFDM and GPP ($p < 0.0001$). AFDM roughly explained twice as much of GPP as SRP (second most important variable, opposite direction). The negative association with SRP may indicate an increase of nutrient uptake by primary producers take up more nutrients with increasing GPP.

The “best” across sites ER model explained approximately 52% of the fixed effects variability (Table 4.4). Results from this model reflected the individual stream reach models, as GPP was the best explanatory variable of ER ($p < 0.0001$) account for most of the variability.

Discussion

We found that there was substantial variation in GPP and ER across the network and throughout the year, but within the range reported in other studies in temperate streams (Hoellein et al. 2013, Hall et al. 2015). We confirmed that GPP and ER increased with drainage area as predicted by the River Continuum Concept RCC (Vannote et al. 1980) and that the stream network was largely heterotrophic except for few days in the spring and summer. We also determined three main seasonal patterns for GPP and two for ER. We found that some stream reaches peaked in the summer, others in the winter and some had multiple peaks. We confirmed our hypothesis that stream metabolism was controlled by local drivers that differ by location in the watershed and changes in seasonal hydrology (Bernal et al. 2013). The spatial arrangement and temporal patterns of discharge, temperature, light and nutrients and their relative importance resulted in asynchrony of the

peaks of GPP and ER despite consistent regional climatic conditions across the stream network. This asynchrony of ecosystem processes promotes stability across the watershed (Moore et al. 2015). Our findings also demonstrated the importance of designing studies that incorporate extensive spatial and temporal coverage across stream networks because inferences obtained from limited snapshots in the summer can either underestimate or overestimate metabolism measurements depending on the location of the watershed.

Larger drainage areas yielded higher stream metabolism. The size of the landscape relative to the stream reach likely yielded more nutrients that stimulated GPP and ER (Hoellein et al. 2013) and potentially yielded higher insolation and warmer water temperatures (Lamberti and Steinman 1997). In relatively pristine watersheds, like the Methow River, drainage area has been recognized as the best predictor of spatial variability of GPP (Finlay 2011). This watershed characteristic integrates multiple relevant environmental conditions such as nutrients and temperature and creates natural gradients in resource availability that in turn drive the spatial organization of river food web productivity (Lamberti and Steinman 1997, Finlay 2011).

Contrary to our expectations, we did not find a clear pattern of NEP increasing with drainage area except for few instances in the spring and summer. However, the lower stream reaches were stable, wide and shallow reaches that stimulated periphyton biomass accrual which in turn may have driven most ER during our study despite stream reaches being mostly heterotrophic. However, the strength of the correlation between GPP and ER decreased considerably during the autumn leaf fall when allochthonous carbon likely became the primary source of carbon in the stream network (Valett et al. 2008). Autochthonous carbon in streams not only fuels short-term microbial production and biogeochemical

cycling, but provide longer-term resources for consumers (Hotchkiss and Hall 2015).

Our results also demonstrated distinct asynchrony of peak primary production across the stream network. To our knowledge, only one study has reported this pattern of asynchrony for benthic GPP (Ogdahl et al. 2010). We conjecture that this may be due to the limited number of studies that have examined both temporal and spatial patterns of GPP across a stream network (Young and Huryn 1996, Houser et al. 2005, Ogdahl et al. 2010, Venkiteswaran et al. 2015). These results contradicted our expectations that GPP peaks would occur during spring and summer seasons when light availability and water temperature are likely highest. This pattern of asynchrony in GPP peaks, suggest seasonal shifts in the degree to which potential co-limiting factors influenced GPP and that the patterns arise because of different controlling factors become more or less important in different environmental contexts.

We developed three conceptual models to describe temporal patterns of GPP we observed. One pattern peaks in the summer, another one peaks in the winter and a third peaks multiple times (Figure 4.6). However, all GPP valleys were associated with stream disturbance. Streambed disturbance due to the high flow events in the spring and late summer suppressed GPP across the network. Reduction of GPP and to some extent of ER reflects that more productive sites have more periphyton biomass and therefore they are more affected by scour (Uehlinger 2006). Although, our sampling did not include the highest flow events due to logistical constraints, it included periods when high flows were receding in the spring and early summer and during leaf fall when flows were likely transporting large amounts of terrestrial carbon.

We found that the stream reaches that peaked in the summer had positive associations

with water temperature, but did not find positive associations with PAR. We initially hypothesized that GPP and ER are highest when light and temperature are highest in the summer after the high stream flows. The Methow River is a typical temperate stream network with seasonal synchrony of light and temperature. Disentangling the effects of temperature vs. light on metabolism is complex and mostly done through experiments or modeling (see Huryn et al. 2014). Light likely mediated stream temperatures, particularly in the smaller forested stream reaches included in the study. In addition, DIN and SRP concentrations at all stream reaches were characteristic of oligotrophic conditions (Minshall et al. 2014). However, the positive associations of SRP with GPP in T2 were tied to elevated SRP concentrations in the summer.

The winter group was associated mostly with a lack of disturbance as the build-up of periphyton biomass may have contributed to positive feedbacks by recycling nutrients and extending the period of high gross productivity until high flow events in the spring “reset the clock”. Additionally, we found that for this winter group, GPP tended to be greater at low water temperatures than at higher temperatures. Kendrick and Huryn (2015) found similar results during the spring and fall, and determined that temperature was a poor predictor of metabolism, suggesting that other factors such as nutrient availability, high Chl-*a* biomass and/or algal taxonomic composition were driving this response.

GPP peaks in winter or shoulder seasons (spring and fall) may have been driven by potential co-limitation of either light or nutrients in the summer as nutrient uptake increases with temperature (Rasmussen et al. 2011). Increased nutrient uptake can potentially deplete nutrient resources and depress GPP during warmer months. The negative associations we found between SRP and GPP suggested high phosphorus demand strengthening the

likelihood of nutrient limitation or co-limitation. However, higher nitrogen recycling in larger stream reaches (Ensign and Doyle 2006) likely stimulated GPP and may have allowed GPP to peak in the cooler months instead. Co-limitation through self-shading can occur where upper layers of the periphyton mat shade the bottom layers, and limitation by nutrients or inorganic carbon supply can also occur when high biomass accrual prevent nutrient accessibility (Cross et al. 2015, Welter et al. 2015). Evidence of self-shading in our study was strengthened by the negative associations between PAR and GPP as periphyton biomass accrual increased with stable flow conditions during base flow (August to March). Future work should consider measurements of nutrient uptake because they are better indicators of biological activity at the time of measurement (Hoellein et al. 2013). Water samples for nutrients were only taken once a month and these samples could have been taken at times where nutrients in the water column were uncharacteristically high or low. The third group is a blend of the winter and summer peak groups where disturbance and nutrient limitation appeared to be the driving factors.

We also developed two conceptual models to describe mechanisms by which environmental factors were associated with each ecosystem respiration peak (Figure 4.7). As with the GPP groups, both ER groups were associated with stream disturbance, Q. However, different mechanisms were at play. For the fall peak group, Q was positively associated with ER and corresponded to high ER in the summer during high flows that likely carried large amounts of terrestrial carbon from the adjacent riparian corridor. In contrast, the negative associations between ER and Q in T1 are likely associated with high autotrophic respiration.

GPP and ER were coupled in most stream reaches except for the smallest stream reaches where there were large contributions of terrestrial carbon, and high ER was associated with

low GPP. The strong coupling of GPP and ER suggests that during base flow conditions (September through March), autochthonous carbon was an important source of organic carbon fueling ER. Furthermore, this tight relationship was likely maintained by the production of labile carbon, its rapid consumption by bacteria, and subsequent release of nutrients for further primary production (Townsend et al. 2011). Finlay et al (2011) found that autotrophs strongly altered stream-water nutrient concentration stoichiometry in lower portions of the South Fork Eel River due to the large standing stock and rapid metabolism made available by high light availability and stable stream flow. Thus, this recycling of nutrients maintained relatively high rates of productivity after water column nutrients were depleted (Wyatt et al. 2012). Nutrient recycling is complex and rates may be influenced by the algal community found in the stream network. Although identifying algal communities was beyond the scope of our analysis, we observed *Didymosphenia geminata* (didymo), an invasive alga that thrives in cold, oligotrophic conditions, to be abundantly present in over half of the stream reaches. The semi-labile nature of the didymo stalks (Aboal et al. 2012) that thrive under oligotrophic conditions (Bothwell et al. 2014) may affect the availability of labile carbon for bacterial consumption. Labile carbon is readily available in a scale time of hours to days whereas semi-labile carbon turnover is in a scale of weeks or months (Piontek et al. 2011). Semi-labile organic matter is consumed by heterotrophic bacteria, when the input of labile compounds is not sufficient to meet the bacterial carbon and energy requirements (Piontek et al. 2011) and consumption is most efficient in areas with low nutrient concentrations (Romaní and Sabater 2000). Thus, we anticipate didymo to play a significant role in nutrient recycling and carbon consumption.

In general, results for individual stream reaches confirmed relationships inferred from

observed patterns along the gradients of daily temperature, light availability, and discharge, as well as monthly nutrient concentrations (Figure 4.7). We anticipated, higher GPP in the forested streams in the spring (Roberts et al. 2007), but we observed that summer values were highest instead. High disturbance from increased discharge due to snowmelt in addition to potential high water turbidity may have contributed to low GPP observed in the spring. As high flows receded, water turbidity may have decreased and water temperature increased, in turn increasing photosynthetic activity.

We acknowledge that top-down effects (e.g. grazing, nutrient excretion) could have been an important factor responsible for some of the GPP and ER patterns observed. Zuckerman (2015) measured invertebrate biomass in six of the ten stream reaches in this study and the only stream reach where grazing was likely to play an important role controlling periphyton biomass was T1. Other top-down effects on GPP we did not examine in our study were the potential influence of nutrient recycling through excretion or spawning. Fish and other animals can create hotspots of nutrient recycling in streams (McIntyre et al. 2008, Griffiths and Hill 2014) even at low numbers. Benjamin et al. (2016) determined that low densities of spawning salmon in the Methow River can increase GPP by 46% during spawning. Spawning generally occurs in lower stream reaches in the Methow River, thus short pulses of DIN and SRP may have contributed to the winter peaks in the lower stream reaches.

Although the spatial patterns observed in our study were consistent with predictions of the river continuum concept (Vannote et al. 1980, Minshall et al. 1992), our study was limited to one stream network, and the strength of our inferences may be limited by the geomorphic and hydrologic context of the watershed.

Because ecosystem metabolism is an integrative descriptor of the sources and sinks of

carbon (Marcarelli et al. 2011), our study allowed us to understand how autochthonous carbon, a high quality source of energy for consumers, is distributed across space and time in a stream network. Considering that stream networks are interacting hierarchical mosaics of habitat heterogeneity, understanding how asynchrony of peak gross production may have an effect on higher trophic levels has implications on management, planning conservation and restoration efforts. The importance of asynchrony among patches for maintaining the stability of meta-communities has been supported by multiple empirical studies (LeCraw et al. 2014). For example, asynchrony of peak GPP may reverse the productivity gradient and the direction of the energy transfer between contiguous habitats, subsidizing habitats reciprocally (Nakano and Murakami 2001). In addition, because GPP has a rapid turnover, it has the potential of fueling heterotrophic production through the immediate release of biologically available DOC, downstream export to areas of lower productivity, or it can be stored (Hotchkiss and Hall 2015).

Asynchrony of ecosystem processes also highlights the importance of sampling throughout the year and capturing the temporal variability of the system. It has been generally assumed that stream productivity is low during the winter, but we found the opposite to be true in at least half of the streams sampled in our study. Thus, predictions derived solely from summer estimates can either overestimate metabolism in smaller streams or underestimate metabolism in larger unconfined streams.

Lastly, Moore et al. (2015) suggested that rivers act as a natural portfolio because the structure of free-flowing river networks stabilizes their biotic and abiotic processes through the integration of asynchronous dynamics. Thus, we need to understand the relationship of spatial heterogeneity to ecosystems functions such as GPP and ER so we can understand and

predict the consequences of human alterations on spatial patterns as these modifications have the potential effect of not only homogenizing and simplifying stream and river networks, but influencing the way stream dynamics interact across the network which in turn can make stream networks less stable.

References

- Aboal M, Marco S, Chaves E, Mulero I, García-Ayala A. 2012. Ultrastructure and function of stalks of the diatom *Didymosphenia geminata*. *Hydrobiologia* 695:17–24.
- Bernal S, von Schiller D, Sabater F, Martí E. 2013. Hydrological extremes modulate nutrient dynamics in Mediterranean climate streams across different spatial scales. *Hydrobiologia* 719:31–42.
- Baines SB, Webster KE, Kratz TK, Carpenter SR, Magnuson JJ. 2000. Synchronous behavior of temperature, calcium, and chlorophyll in lakes of Northern Wisconsin. *Ecology* 81: 815-25.
- Bartoń K. 2015. MuMIn: Multi-model inference. R package version 1.15.1.
- Beaulieu JJ, Arango CP, Balz DA, Shuster WD. 2013. Continuous monitoring reveals multiple controls on ecosystem metabolism in a suburban stream. *Freshwater Biology* 58:918–37.
- Bellmore JR, Baxter CV, Connolly PJ, Martens K. 2013. The floodplain mosaic: a study of its importance to production of salmon and steelhead. *Ecological Applications* 23:189–207.

Bellmore JR, Fremier AK, Mejia F, Newsom M. 2014. The response of stream periphyton to Pacific salmon: Using a model to understand the role of environmental context. *Freshwater Biology* 59:1437–51.

Benda L, Poff NL, Miller D, Dunne T, Reeves G, Pess G, Pollock M. 2004. The network dynamics hypothesis: How channel networks structure riverine habitats. *Bioscience* 54: 413-27. Doi: 10.1641/0006-3568(2004)054[0413:TNDHHC]

Benda L, Miller D, Andras K, Bigelow P, Reeves G, Michael D. 2007. NetMap: A new tool in support of watershed science and resource management. *Forest Science* 53:206–19.

Benjamin JR, Bellmore JR, Watson GA. 2016. Response of ecosystem metabolism to low densities of spawning Chinook Salmon. *Freshwater Science* 35:000–000.

<http://www.journals.uchicago.edu/doi/10.1086/686686>

Bergey EA., Getty GM. 2006. A review of methods for measuring the surface area of stream substrates. *Hydrobiologia* 556:7–16.

Bernot MJ, Sobota DJ, Hall RO, Mulholland PJ, Dodds WK, Webster JR, Tank JL, Ashkenas LR, Cooper LW, Dahm CN, Gregory S V., Grimm NB, Hamilton SK, Johnson SL, McDowell WH, Meyer JL, Peterson B, Poole GC, Maurice Valett HM, Arango C, Beaulieu JJ, Burgin AJ, Crenshaw C, Helton AM, Johnson L, Merriam J, Niederlehner BR, O'Brien JM, Potter JD, Sheibley RW, Thomas SM, Wilson K. 2010. Inter-regional comparison of land-use effects on stream metabolism. *Freshwater Biology* 55:1874–90.

Bothwell ML, Taylor BW, Kilroy C. 2014. The Didymo story : the role of low dissolved phosphorus in the formation of *Didymosphenia geminata* blooms. *Diatom research* 29:229–

36. <http://dx.doi.org/0269249X.2014.889041>

Brown JH, Gillooly JF, Allen AP, Savage VM, West GB. 2004. Toward a metabolic theory of ecology. *Ecology* 85:1771–89.

Burnett KM, Reeves GH, Miller DJ, Clarke S, Vance-Borland K, Christiansen K. 2007. Distribution of salmon-habitat potential relative to landscape characteristics and implications for conservation. *Ecological Applications* 17:66–80.

Cardinale BJ, Palmer MA., Swan CM, Brooks S, Poff NL. 2002. The influence of substrate heterogeneity on biofilm metabolism in a stream ecosystem. *Ecology* 83:412–22.

Cross WF, Baxter C V., Rosi-Marshall EJ, Hall RO, Kennedy TA, Donner KC, Wellard Kelly HA, Seegert SEZ, Behn KE, Yard MD. 2013. Food-web dynamics in a large river discontinuum. *Ecological Monographs* 83:311–37. <http://doi.wiley.com/10.1890/12-1727.1>

Cross WF, Hood JM, Benstead JP, Hury AD, Nelson D. 2015. Interactions between temperature and nutrients across levels of ecological organization. *Global Change Biology* 21:1025–40. <http://doi.wiley.com/10.1111/gcb.12809>

Ensign SH, Doyle MW. 2006. Nutrient spiraling in streams and river networks. *Journal of Geophysical Research: Biogeosciences* 111:1-13.
<http://doi.wiley.com/10.1029/2005JG000114>

Finlay JC. 2011. Stream size and human influences on ecosystem production in river networks. *Ecosphere* 2:art87. doi:10.1890/ES11-00071.1

Finlay JC, Hood JM, Limm MP, Power ME, Schade JD, Welter JR. 2011. Light-mediated thresholds in stream-water nutrient composition in a river network. *Ecology* 92:140–50.

Fisher SG, Welter JR. 2005. Flowpaths as integrators of heterogeneity in streams and landscapes. Lovett GM, Jones CG, Turner MG, Weathers KG, editors. *Ecosystem function in heterogenous landscapes*. New York. Springer. p. 311-28.

Fox J, Weisberg S. 2011. *An {R} companion to applied regression*, second edition. Thousand Oaks (CA): Sage Publications. 472 pp.

Grace MR, Imberger SJ. 2006. *Stream metabolism: Performing & interpreting Measurements*. Water Studies Centre Monash University, Murray Darling Basin Commission and New South Wales Department of Environment and Climate Change. 204 pp.

Grace MR, Giling DP, Hladyz S, Caron V, Thompson RM, McNally R. 2015. Fast processing of diel oxygen curves : estimating stream metabolism with BASE (BAYesian Single-station Estimation). *Limnology and Oceanography:Methods* 13: 103–14. doi: 10.1002/lom.10011

Greenwood JL, Rosemond AD. 2005. Periphyton response to long-term nutrient enrichment in a shaded headwater stream. *Canadian Journal of Fisheries and Aquatic Sciences* 62:2033–45. <http://www.nrcresearchpress.com/doi/abs/10.1139/f05-117>

Griffiths NA, Hill WR. 2014. Temporal Variation in the Importance of a Dominant Consumer to Stream Nutrient Cycling. *Ecosystems* 17:1169–85. <http://link.springer.com/10.1007/s10021-014-9785-1>

Hall RO, Tank JL, Baker MA, Rosi-Marshall EJ, Hotchkiss ER. 2015. Metabolism, gas exchange, and carbon spiraling in rivers. *Ecosystems* 19: 73-86. doi.org/10.1007/s10021-015-9918-1

Hart AM. 2013. Seasonal variation in whole stream metabolism across varying land use types. Masters thesis. Virginia Polytechnic Institute and State University. Blacksburg, Virginia, USA.

Hoellein TJ, Bruesewitz DA, Richardson DC. 2013. Revisiting Odum (1956): A synthesis of aquatic ecosystem metabolism. *Limnology and Oceanography* 58:2089–2100.
http://www.aslo.org/lo/toc/vol_58/issue_6/2089.html

Hotchkiss ER, Hall Jr RO, Sponseller RA, Butman D, Klaminder J, Laudon H, Rosvall M, Karlsson J. 2015. Sources of and processes controlling CO₂ emissions change with the size of streams and rivers. *Nature Geoscience* 8:696–99.
<http://dx.doi.org/10.1038/ngeo2507>
<http://www.nature.com/ngeo/journal/v8/n9/abs/ngeo2507.html#supplementary-information>
<http://www.nature.com/doifinder/10.1038/ngeo2507>

Hotchkiss ER, Hall Jr RO. 2015. Whole-stream ¹³C tracer addition reveals distinct fates of newly fixed carbon. *Ecology* 96:403–16.

Houser JN, Mulholland PJ, Maloney KO. 2005. Catchment disturbance and stream metabolism: patterns in ecosystem respiration and gross primary production along a gradient of upland soil and vegetation disturbance. *Journal of the North American Benthological Society* 24:538-52

Huryn AD, Benstead JP, Parker SM. 2014. Seasonal changes in light availability modify the temperature dependence of ecosystem metabolism in an arctic stream. *Ecology* 95:2826–39.

Izaguirre O, Agirre U, Bermejo M, Pozo J, Elosegi A. 2008. Environmental controls of whole-stream metabolism identified from continuous monitoring of Basque streams. *Journal of the North American Benthological Society* 27: 252-68. doi: <http://dx.doi.org/10.1899/07-022.1>

Jankowski K, Schindler DE, Lisi PJ. 2014. Temperature sensitivity of community respiration rates in streams is associated with watershed geomorphic features. *Ecology* 95:2707–14.
<http://doi.wiley.com/10.1890/14-0608.1>

Kendrick MR, Huryn AD. 2015. Discharge, legacy effects and nutrient availability as determinants of temporal patterns in biofilm metabolism and accrual in an arctic river. *Freshwater Biology* 60: 2323–36.

Konrad CP. 2006. Location and timing of river-aquifer exchanges in six tributaries to the Columbia River in the Pacific Northwest of the United States. *Journal of Hydrology* 329:444–70.

Lamberti GA, Steinman AD. 1997. A comparison of primary production in stream ecosystems. *Journal of the North American Benthological Society* 16:95–103.

Langhans SD, Tiegs SD, Gessner MO, Tockner K. 2008. Leaf-decomposition heterogeneity across a riverine floodplain mosaic. *Aquatic Sciences* 70:337–46.
<http://link.springer.com/10.1007/s00027-008-8062-9>

LeCraw RM, Kratina P, Srivastava DS. 2014. Food web complexity and stability across habitat connectivity gradients. *Oecologia* 176:903–15.

Leopold LB. 1994. *A view of the river*. Cambridge (MA): Harvard University Press. 298 pp.

McIntyre PB, Flecker AS, Vanni MJ, Hood JM, Taylor BW, Thomas SA. 2008. Fish distributions and nutrient cycling in streams: can fish create biogeochemical hotspots. *Ecology* 89:2335–46. <http://doi.wiley.com/10.1890/07-1552.1>

Marcarelli AM, Baxter CV, Mineau MM, Hall RO. 2011. Quantity and quality: Unifying food web and ecosystem perspectives on the role of resource subsidies in freshwaters. *Ecology* 92:1215–25.

McTammany ME, Webster JR, Benfield EF, Neatrour MA. 2003. Longitudinal patterns of metabolism in a southern Appalachian river. *Journal of the North American Benthological Society* 22:359–70.

Minshall GW, Petersen RC, Bott TL, Cushing CE, Cummins KW, Vannote RL, Sedell JR. 1992. Stream Ecosystem Dynamics of the Salmon River, Idaho: An 8th-Order System. *Journal of the North American Benthological Society* 11:111–37.

Moore J, Beakes MP, Nesbitt HK, Yeakel JD, Patterson D a, Thompson L a, Phillis CC, Braun DC, Favaro C, Scott D, Carr-Harris C, Atlas WI. 2015. Emergent stability in a large, free-flowing watershed. *Ecology* 96:340–7.

Nakano S, Murakami M. 2001. Reciprocal subsidies: Dynamic interdependence between terrestrial and aquatic food webs. *Proceedings of the National Academy of Sciences of the*

United States of America 98:166–70.

WOS:000166222600034\nhttp://www.pubmedcentral.nih.gov/articlerender.fcgi?artid=14562
&tool=pmcentrez&rendertype=abstract

Odum HT. 1956. Primary production in flowing waters. *Limnology and Oceanography* 1:
102-17.

Ogdahl ME, Lougheed VL, Stevenson RJ, Steiman AD. 2010. Influences of multi-scale
habitat on metabolism in a coastal Great Lakes watershed. *Ecosystems* 13: 222-38.

Pinheiro JC, Bates DM. 2000. *Mixed-effect models in S and S-Plus*. New York. Springer.
528 pp.

Piontek J, Händel N, De Bodt C, Harlay J, Chou L, Engel A. 2011. The utilization of
polysaccharides by heterotrophic bacterioplankton in the Bay of Biscay (North Atlantic
Ocean). *Journal of Plankton Research* 33:1719–35.

Poole GC. 2002. Fluvial landscape ecology: Addressing uniqueness within the river
discontinuum. *Freshwater Biology* 47:641–60.

R Development Core Team. 2013. *R: A language and environment for statistical computing*.
R Foundation for Statistical Computing, Vienna, Austria. R 2.15.2 GUI

Rasmussen JJ, Baattrup-Pedersen A, Riis T, Friberg N. 2011. Stream ecosystem properties
and processes along a temperature gradient. *Aquatic Ecology* 45:231–42.

<http://link.springer.com/10.1007/s10452-010-9349-1>

Romaní AM, Sabater S. 2000. Variability of heterotrophic activity in Mediterranean stream biofilms: A multivariate analysis of physical-chemical and biological factors. *Aquatic Sciences* 62:205–15.

Roberts BJ, Mulholland PJ, Hill WR. 2007. Multiple scales of temporal variability in ecosystem metabolism rates: Results from 2 years of continuous monitoring in a forested headwater stream. *Ecosystems* 10:588–606.

Tank J, Rosi-Marshall E, Griffiths NA, Entekin SA, Stephen ML. 2010. A review of allochthonous organic matter dynamics and metabolism in streams. *Journal of the North American Benthological Society* 29:118–46. <http://www.jstor.org/stable/10.1899/08-170.1>

Townsend SA, Webster IT, Schult JH. 2011. Metabolism in a groundwater-fed river system in the Australian wet/dry tropics: tight coupling of photosynthesis and respiration. *Journal of the North American Benthological Society* 30:603–20.

Uehlinger U, Naegeli MW. 1998. Ecosystem metabolism, disturbance, and stability in a prealpine gravel bed river. *Journal of the North American Benthological Society* 17:165–78. <Go to ISI>://000075262700003

Uehlinger U. 2006. Annual cycle and inter-annual variability of gross primary production and ecosystem respiration in a floodprone river during a 15-year period. *Freshwater Biology* 51:938–50.

Uehlinger U, Naegeli MW. 1998. Ecosystem metabolism, disturbance, and stability in a prealpine gravel bed river. *Journal of the North American Benthological Society* 17:165–78. <Go to ISI>://000075262700003

Valett HM, Thomas SA, Mulholland PJ, Webster JR, Dahm CN, Fellows CS, Crenshaw CL, Peterson CG. 2008. Endogenous and exogenous control of ecosystem function: N cycling in headwater streams. *Ecology* 89:3515–27.

Vannote RL, Minshall GW, Cummins KW, Sedell JR, Cushing CE. 1980. The river continuum concept. *Canadian Journal of Fisheries and Aquatic Sciences* 37:130–37.

Venkiteswaran JJ, Schiff SL, Taylor WD. 2015. Linking aquatic metabolism, gas exchange, and hypoxia to impacts along the 300-km Grand River, Canada. *Freshwater Science* 34:1216–32. <http://www.journals.uchicago.edu/doi/10.1086/683241>

Warnaars, TA, Hondzo M, Power ME. 2007. Abiotic controls on periphyton accrual and metabolism in streams: Scaling by dimensionless numbers, *Water Resources Research* 43, W08425, [doi:10.1029/2006WR005002](https://doi.org/10.1029/2006WR005002).

Welter JR, Benstead JP, Cross WF, Hood JM, Hury AD, Johnson PW, Williamson TJ. 2015. Does N₂ fixation amplify the temperature dependence of ecosystem metabolism? *Ecology* 96: 603-10.

Willms R, Kendra W. 1990. Methow river water quality survey and assessment of compliance with water quality standards. Washington State Department of Ecology. Environmental Investigations and Laboratory Services Program. Olympia, Washington. USA. 37 pp. Available from <https://fortress.wa.gov/ecy/publications/publications/90e71.pdf> (Accessed 13 September 2015)

Wyatt KH, Turetsky MR, Rober AR, Girollo D, Kane ES, Stevenson RJ. 2012.

Contributions of algae to GPP and DOC production in an Alaskan fen: Effects of historical water table manipulations on ecosystem responses to a natural flood. *Oecologia* 169:821–32.

Yates AG, Brua RB, Culp JM, Chambers PA. 2013. Multi-scaled drivers of rural prairie stream metabolism along human activity gradients. *Freshwater Biology* 58:675–89.

Young RG, Huryn AD. 1996. Interannual variation in discharge controls ecosystem metabolism along a grassland river continuum. *Canadian Journal of Fisheries and Aquatic Sciences* 53:2199–2211.

Zuckerman A. 2015. Seasonal variation in empirical and modeled periphyton at the watershed scale. Masters thesis. University of Idaho, Moscow, Idaho, USA.

Zuur AF, Ieno EN, Walker N, Saveliev AA, Smith GM. 2009. Mixed effects models and extensions in ecology with R. New York, NY: Springer New York

<http://link.springer.com/10.1007/978-0-387-87458-6>

Tables

Table 4.1: Annual average metabolic rates and average of biological and physical characteristics of the 10 sampled stream reaches in the Methow River basin. Standard deviations are in parentheses. GPP=gross primary production, ER=ecosystem respiration, NEP=net ecosystem production, Chl-a =Chlorophyll-a, AFDM=ash free dry biomass, PAR=photosynthetically active radiation, TEMP=temperature, DIN=dissolved inorganic nitrogen, SRP=soluble reactive phosphorus, CON=channel confinement, DA=drainage area, Q=discharge.

Site	GPP	ER mgO ₂ m ⁻² d ⁻¹	NEP	Chl- <i>a</i> mg m ⁻² d ⁻¹	AFDM gm ⁻² d ⁻¹	PAR μ mol m ⁻² s ⁻¹	TEMP °C	DIN mg l ⁻¹	SRP mg l ⁻¹	CON	DA km ²	Q m ³ s ⁻¹
BD	0.02 (0.02)	0.27 (0.31)	-0.25 (0.32)	13.7 (2.7)	6.07 (1.10)	83 (100)	6.0 (5.9)	0.04 (0.02)	0.008 (0.0040)	7	128	0.38 (0.17)
EW	0.04 (0.05)	0.22 (0.20)	-0.18 (0.22)	9.2 (3.9)	4.02 (1.20)	199 (142)	7.3 (4.4)	0.05 (0.02)	0.001 (0.0002)	11	129	2.17 (1.06)
BV	0.29 (0.23)	0.66 (0.39)	-0.37 (0.38)	100.7 (67.9)	15.57 (8.35)	242 (141)	6.7 (5.7)	0.30 (0.08)	0.010 (0.0029)	7	179	0.47 (0.36)
T1	0.08 (0.07)	1.17 (0.40)	-1.09 (0.36)	5.2 (2.4)	3.45 (1.12)	195 (162)	6.1 (4.4)	0.07 (0.03)	0.001 (0.0007)	25	211	1.94 (1.90)
T2	0.44 (0.28)	0.91 (0.35)	-0.48 (0.32)	31.8 (16.2)	10.17 (2.47)	264 (160)	10.3 (5.4)	0.08 (0.02)	0.001 (0.0003)	15	394	2.39 (0.91)
C1	0.52 (0.23)	1.34 (0.50)	-0.82 (0.43)	23.1 (9.8)	9.32 (2.02)	176 (133)	5.7 (5.7)	0.04 (0.02)	0.003 (0.0026)	22	536	2.14 (2.52)
M1	0.30 (0.22)	1.21 (0.63)	-0.91 (0.50)	10.2 (4.6)	5.43 (2.04)	284 (227)	7.6 (3.6)	0.05 (0.02)	0.002 (0.0005)	32	666	6.30 (4.89)
C2	0.84 (0.34)	2.02 (0.95)	-1.18 (0.87)	28.3 (12.4)	11.91 (6.93)	203 (148)	8.4 (5.5)	0.05 (0.02)	0.002 (0.0005)	13	843	2.55 (1.21)
M2	2.26 (1.21)	2.90 (1.53)	-0.64 (0.91)	42.3 (31.3)	15.33 (7.64)	300 (183)	7.6 (4.6)	0.10 (0.03)	0.002 (0.0007)	28	1669	13.33 (7.46)
M3	2.39 (0.80)	2.89 (1.22)	-0.50 (0.91)	44.1 (22.7)	14.69 (6.61)	204 (137)	6.8 (4.8)	0.20 (0.04)	0.002 (0.0011)	29	1722	10.35 (5.50)

Table 4.2: Coefficient estimates, standard errors, percent of the explained variance for fixed (R^2_m) and random and fixed effects combined (R^2_c) for GPP models for each site (all dates combined).

		Value	Std.Error	DF	t-value	p-value	Rm	Rc
Summer Peak	BD						0.91	0.96
	(Intercept)	-4.4074	0.13931	42	-31.64	0.000		
	TEMP	0.05612	0.01	42	5.61	0.000		
	Log(Q)	-0.4536	0.09855	42	-4.6	0.000		
	EW						0.65	0.95
	(Intercept)	-3.581	0.157	125	-22.88	0.000		
	TEMP	0.103	0.016	125	6.35	0.000		
	Log(Q)	-0.563	0.107	125	-5.27	0.000		
	C2						0.41	0.49
	(Intercept)	0.584	0.05	108	11.64	0.000		
	Log(Q)	-0.238	0.038	108	-6.19	0.000		
	TEMP	0.024	0.005	108	5.39	0.000		
Winter Peak	T2						0.83	0.83
	(Intercept)	1.615	0.34	94	4.75	0.000		
	TEMP	0.03	0.002	94	16.12	0.000		
	Log(P)	0.22	0.049	5	4.47	0.007		
	Log(Q)	-0.099	0.03006	94	-3.28	0.002		
	M1						0.45	0.6
	(Intercept)	0.627	0.059	217	10.56	0.000		
	Log(Q)	-0.035	0.009	217	-3.73	0.000		
Multiple Peaks	Log(PAR)	-0.066	0.011	217	-5.89	0.000		
	T1						0.37	0.47
	(Intercept)	-2.552	0.665	179	-3.84	0.000		
	Log(P)	-0.275	0.108	10	-2.55	0.029		
	Log(PAR)	-0.411	0.055	179	-7.52	0.000		
Multiple Peaks	M3						0.30	0.71
	(Intercept)	1.784	0.106	108	16.86	0.000		
	Log(Q)	-0.263	0.042	108	-6.28	0.000		
	BV						0.75	0.88
	(Intercept)	-10.53	1.3	158	-8.1	0.000		
	Log(AFDM)	1.922	0.322	8	5.97	0.000		
	Log(N)	-1.229	0.353	8	-3.48	0.008		
	TEMP	0.172	0.027	158	6.35	0.000		
	Log(Q)	-1.431	0.218	158	-6.58	0.000		
	C1						0.31	0.70
(Intercept)	0.457	0.035	145	13.07	0.000			
Log(Q)	-0.127	0.021	145	-5.96	0.000			
Multiple Peaks	M2						0.20	0.97
	(Intercept)	1.752	0.113	86	15.5	0.000		
	Log(Q)	-0.245	0.032	86	-7.63	0.000		

Table 4.3: Coefficient estimates, standard errors, percent of the explained variance for fixed effects (R^2_m) and random and fixed effects combined (R^2_c) for ER models for for each site (all dates combined).

	Value	Std.Error	DF	t-value	p-value	Rm	Rc	
Fall Peak	BD					0.95	0.95	
	(Intercept)	0.330	0.023	42	14.51	0.000		
	Log(PAR)	-0.078	0.010	42	-7.92	0.000		
	Log(Q)	1.374	0.002	42	875.59	0.000		
	EW						0.44	0.86
	(Intercept)	-14.097	7.680	126	-1.84	0.069		
	Log(N)	-1.328	0.515	6	-2.58	0.042		
	TEMP	-0.188	0.024	126	-7.85	0.000		
	Log(P)	-1.453	1.231	6	-1.18	0.283		
	C2						0.16	0.66
	(Intercept)	0.579	0.094	109	6.14	0.000		
	Log(GPP)	0.698	0.078	109	8.95	0.000		
T2						0.37	0.87	
(Intercept)	0.765	0.063	95	12.18	0.000			
Log(GPP)	0.222	0.027	95	8.09	0.000			
Winter Peak	BV					0.19	0.83	
	(Intercept)	0.293	0.073	159	4.01	0.000		
	Log(GPP)	0.725	0.076	159	9.56	0.000		
	T1						0.29	0.48
	(Intercept)	1.011	0.047	178	21.30	0.000		
	Log(GPP)	0.075	0.012	178	6.13	0.000		
	Log(Q)	-0.171	0.019	178	-9.16	0.000		
	C1						0.48	0.63
	(Intercept)	-0.592	0.322	145	-1.84	0.068		
	Log(GPP)	0.959	0.084	145	11.40	0.000		
	Log(AFDM)	0.464	0.144	8	3.22	0.012		
	M1						0.38	0.91
	(Intercept)	1.078	0.162	217	6.67	0.000		
	Log(GPP)	0.492	0.041	217	11.92	0.000		
	Log(Q)	-0.318	0.040	217	-7.98	0.000		
	M2						0.65	0.99
	(Intercept)	0.434	0.084	86	5.17	0.000		
	Log(GPP)	0.759	0.043	86	17.45	0.000		
M3						0.46	0.97	
(Intercept)	0.776	0.114	107	6.79	0.000			
Log(GPP)	0.622	0.056	107	11.09	0.000			
TEMP	-0.035	0.005	107	-7.27	0.000			

Table 4.4: Coefficient estimates, standard errors, percent of the explained variance for fixed effects (R^2_m) and random and fixed effects combined (R^2_c) for across sites GPP and ER models.

	Value	Std.Error	DF	t-value	p-value	Rm	Rc
GPP (All stream reaches)						0.44	0.99
(Intercept)	-6.902	0.812	1276	-8.5	0.000		
Log(AFDM)	1.212	0.135	81	8.95	0.000		
Log(Q)	-0.264	0.025	1276	-10.54	0.000		
TEMP	0.035	0.005	1276	6.97	0.000		
Log(P)	-0.577	0.113	81	-5.12	0.000		
ER (All stream reaches)						0.52	0.81
(Intercept)	0.604	0.172	1276	3.51	0.001		
Log(GPP)	0.302	0.011	1276	28.55	0.000		
TEMP	-0.025	0.003	1276	-8.57	0.000		
Log(P)	-0.086	0.027	82	-3.22	0.002		

Figures

Figure 4.1: Map of the Methow River basin. The 10 stream reaches, main tributaries and Columbia River are identified by name. The inset indicates the location of the Methow River in Washington State, USA. Black star represents location of PAR sensor.

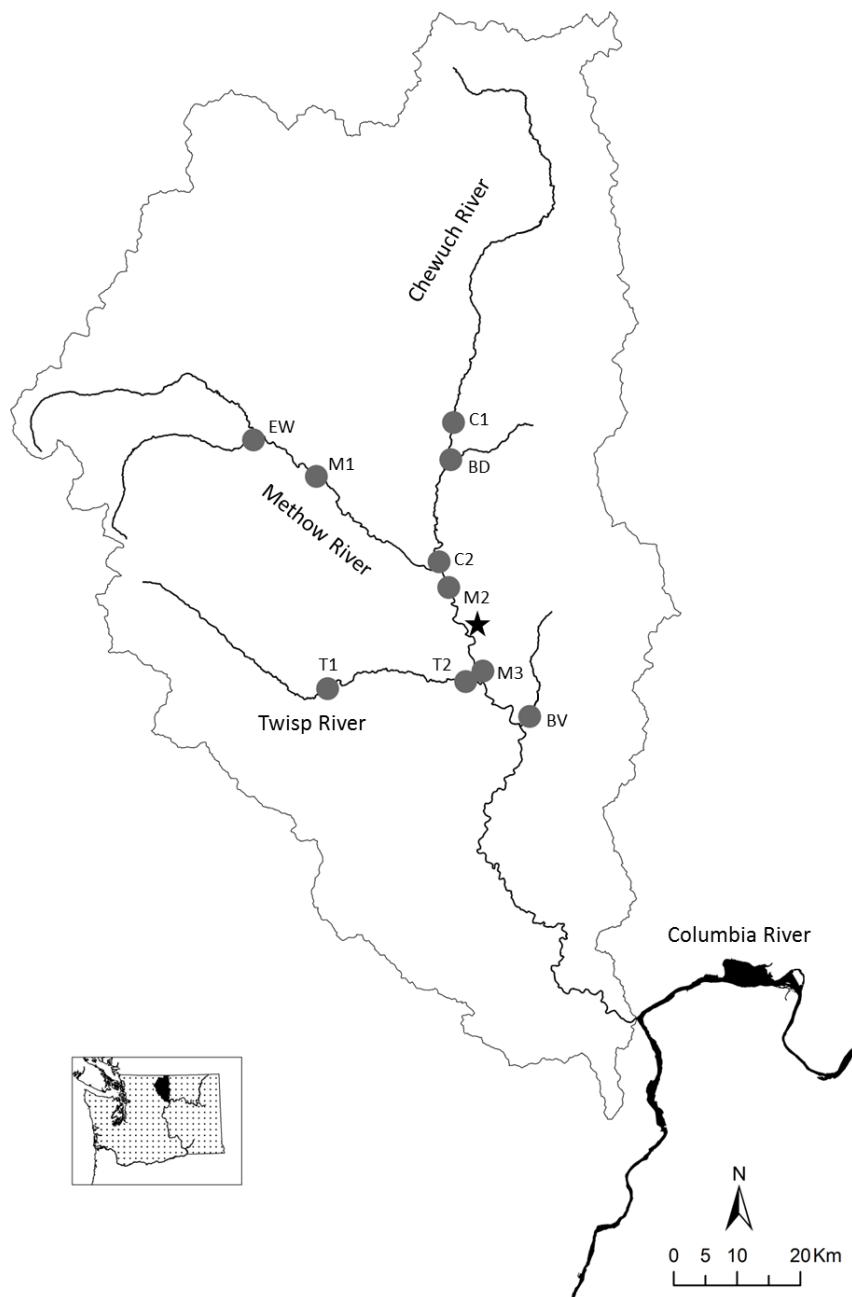


Figure 4.2: Seasonal patterns of GPP (a),ER (b),NEP) (c). Stream reaches were ordered from smallest to largest drainage area.

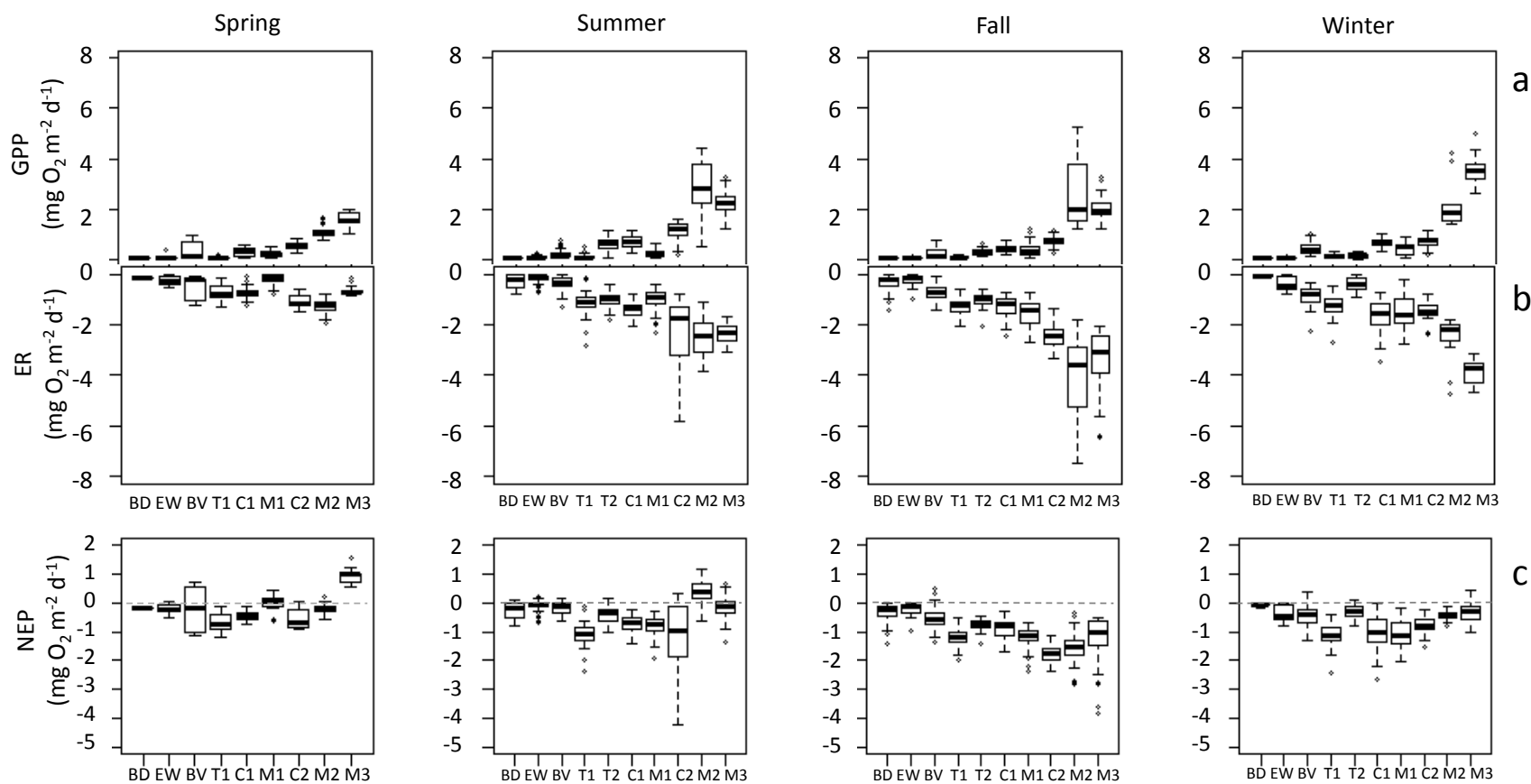


Figure 4.3: Plots of daily gross primary productivity (GPP) vs. daily ecosystem respiration (ER) for our ten stream reaches. Line is $GPP = ER$. Net ecosystem production (NEP) is average NEP for the entire sampling period June 2013-May 2014.

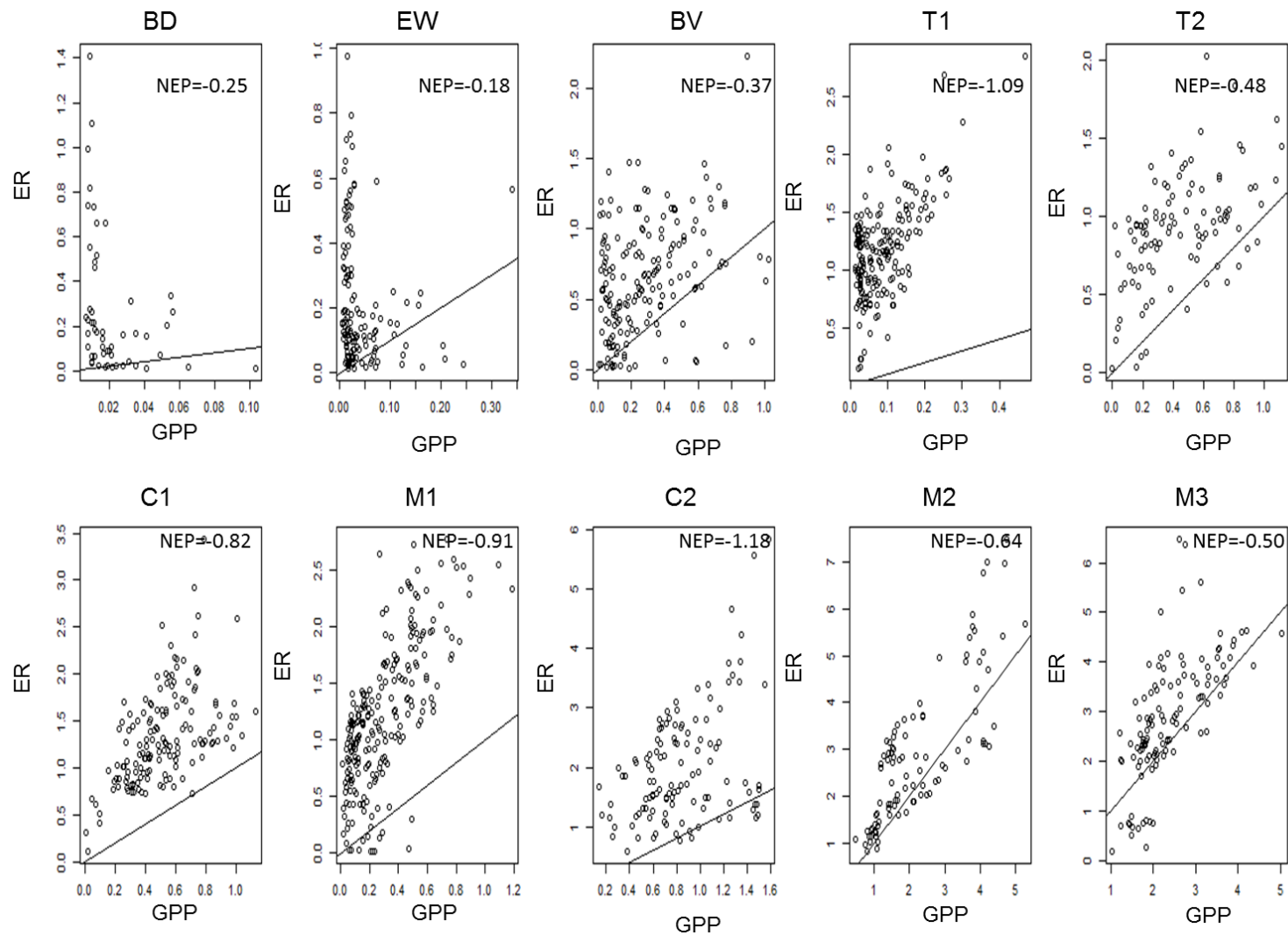


Figure 4.4: Generalized curves of observed patterns of gross primary production (GPP) and ecosystem respiration (ER) across the stream network. Mean monthly metabolism values were standardized by calculating mean z-scores for each site. Groups were classified according to their peaks: summer, winter and multiple for GPP (a), and AFDM specific GPP (b), and fall and winter for ER (c). The red line crosses 0 representing the mean.

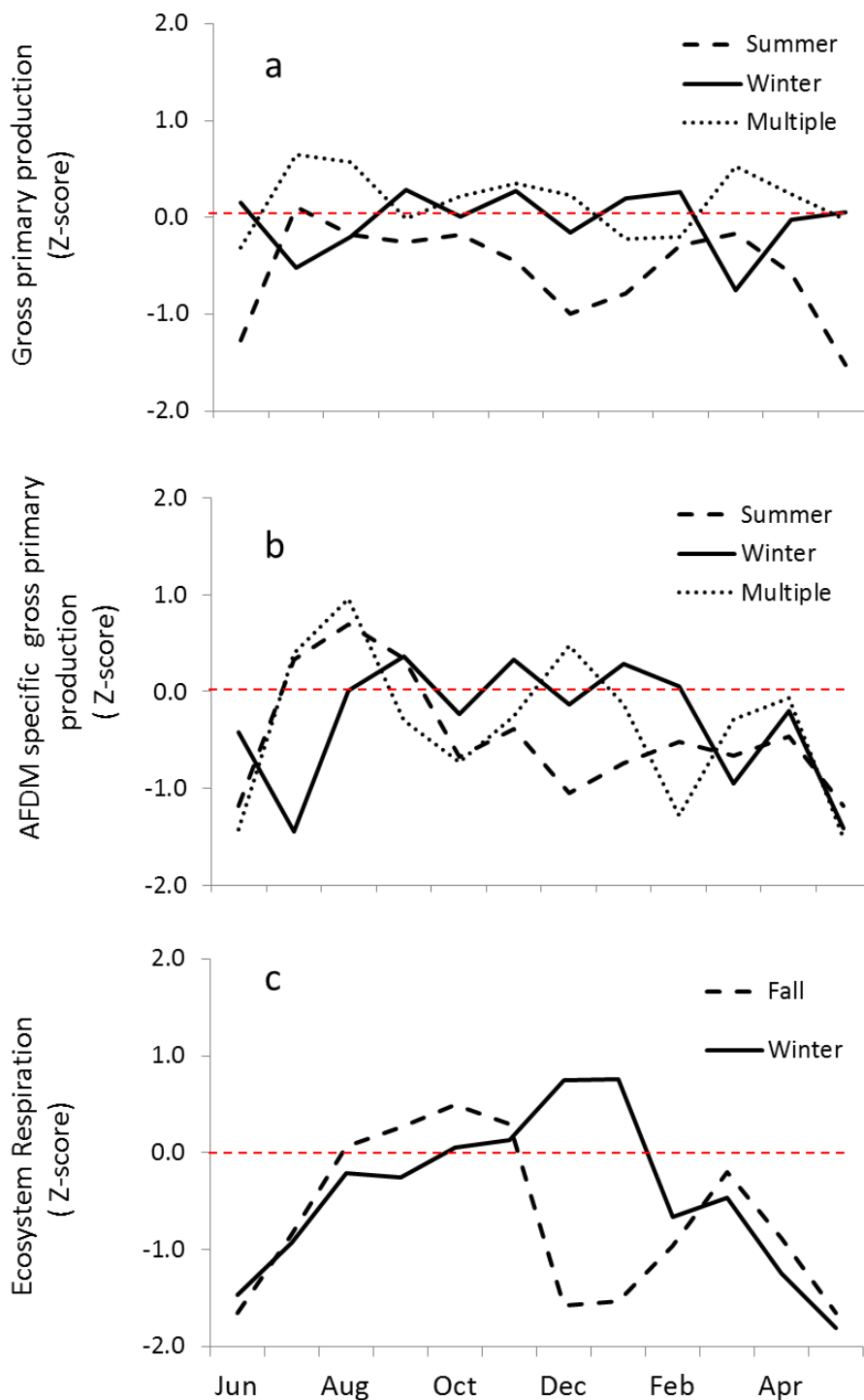


Figure 4.5: Mean environmental conditions for the three temporal patterns observed in GPP. Summer group includes stream reaches that peak in the summer. Winter group includes stream reaches that peak in the winter. Multiple peaks group has multiple peaks.

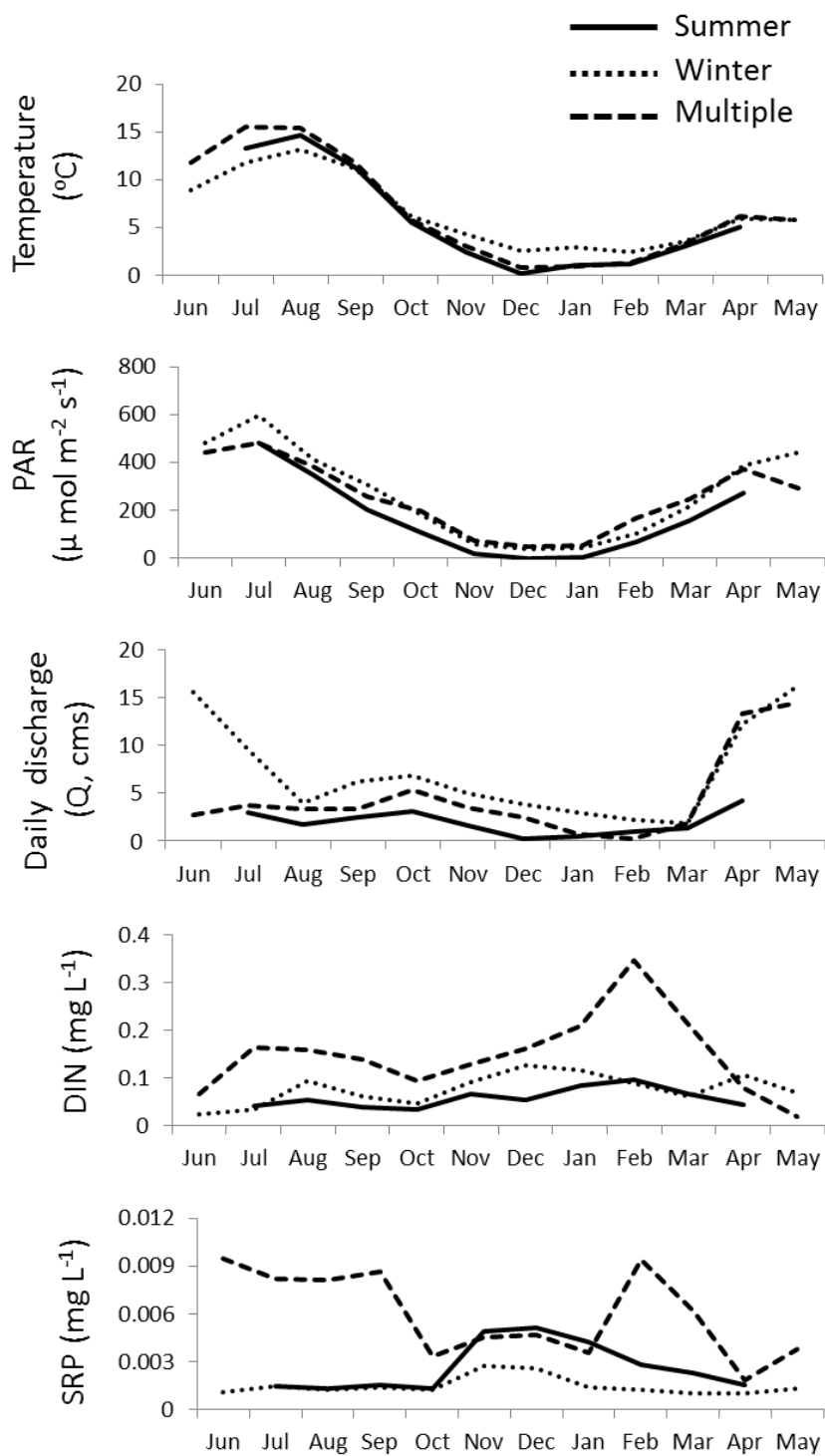


Figure 4.6: Conceptual model of environmental drivers of GPP for streams that peak in the summer (a), peak in the winter (b) and multiple peaks (c).

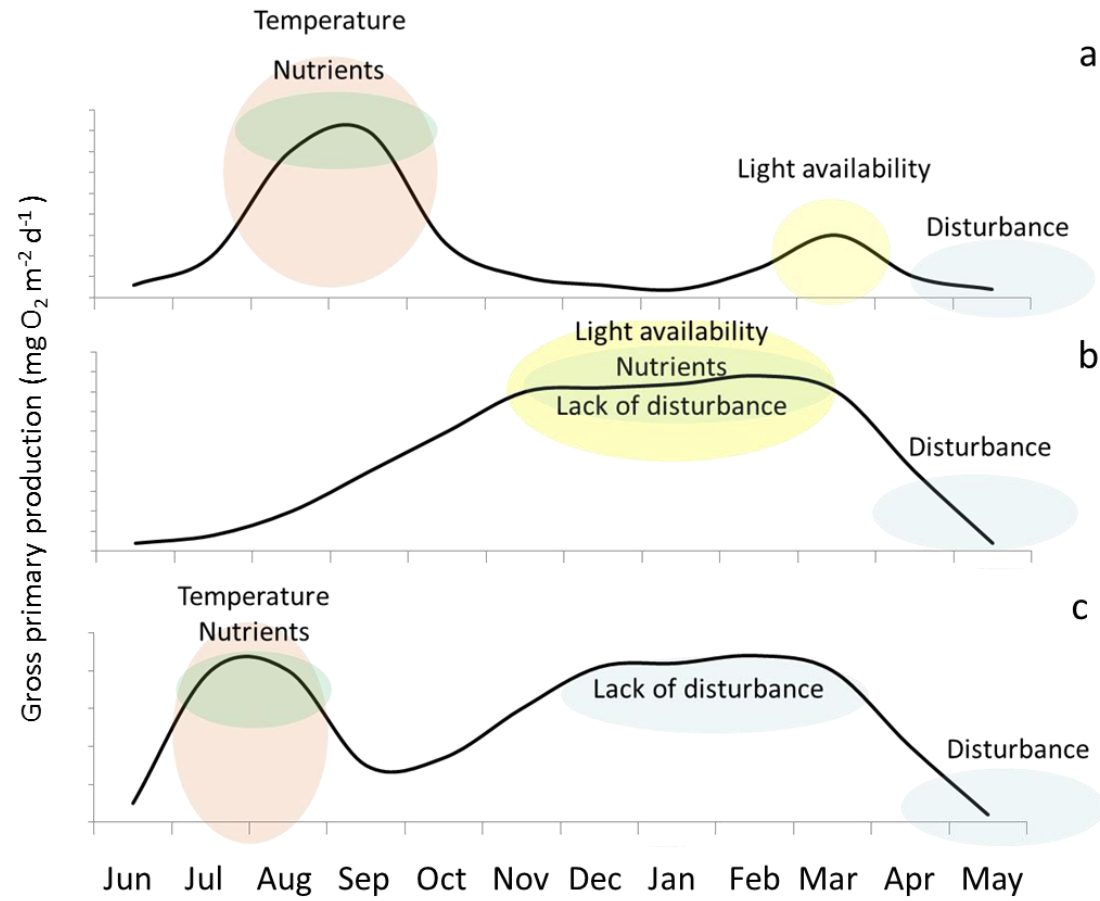
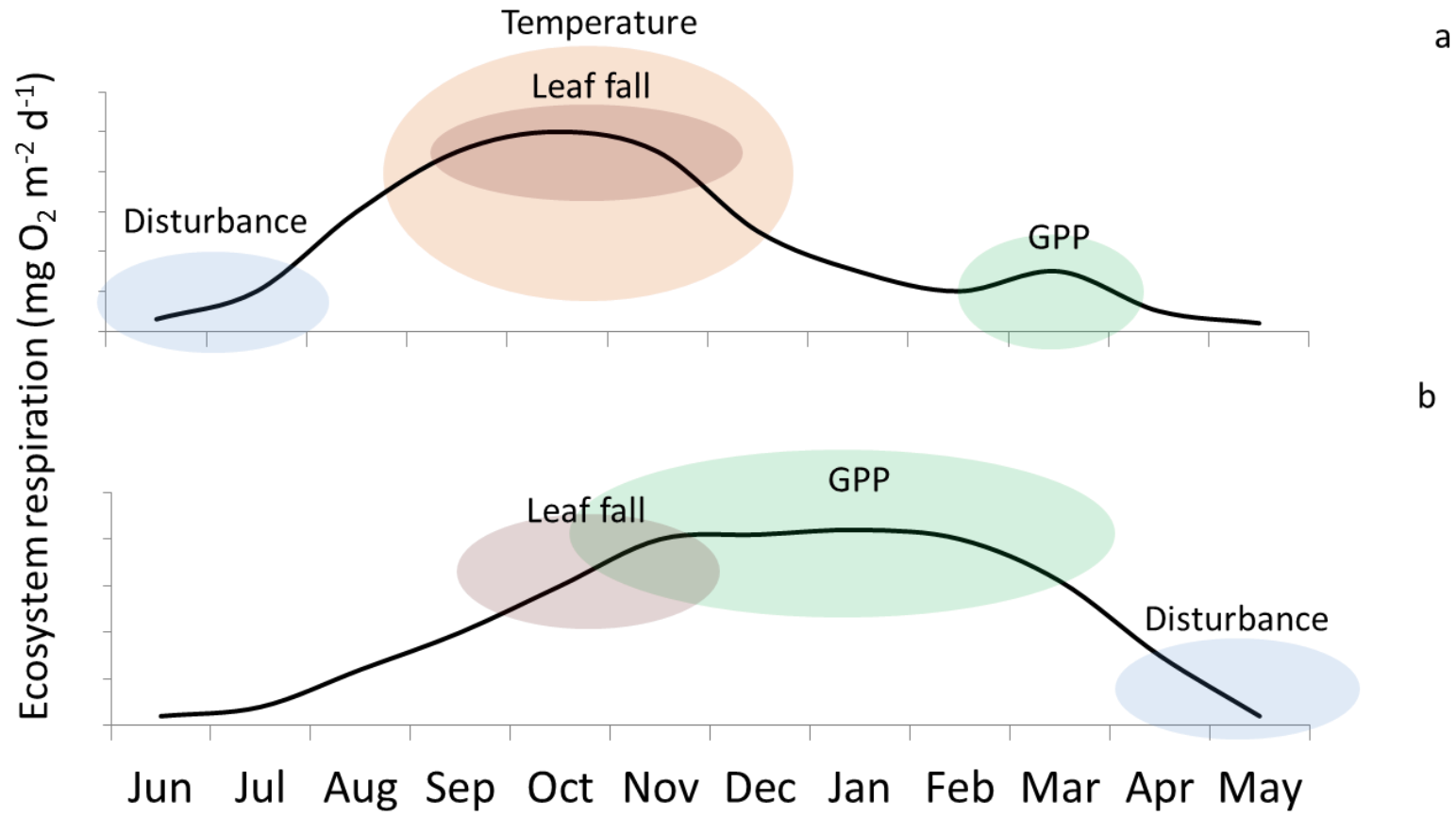


Figure 4.7: Conceptual model of environmental drivers of ecosystem respiration for streams that peak in the fall (a) and winter (b).



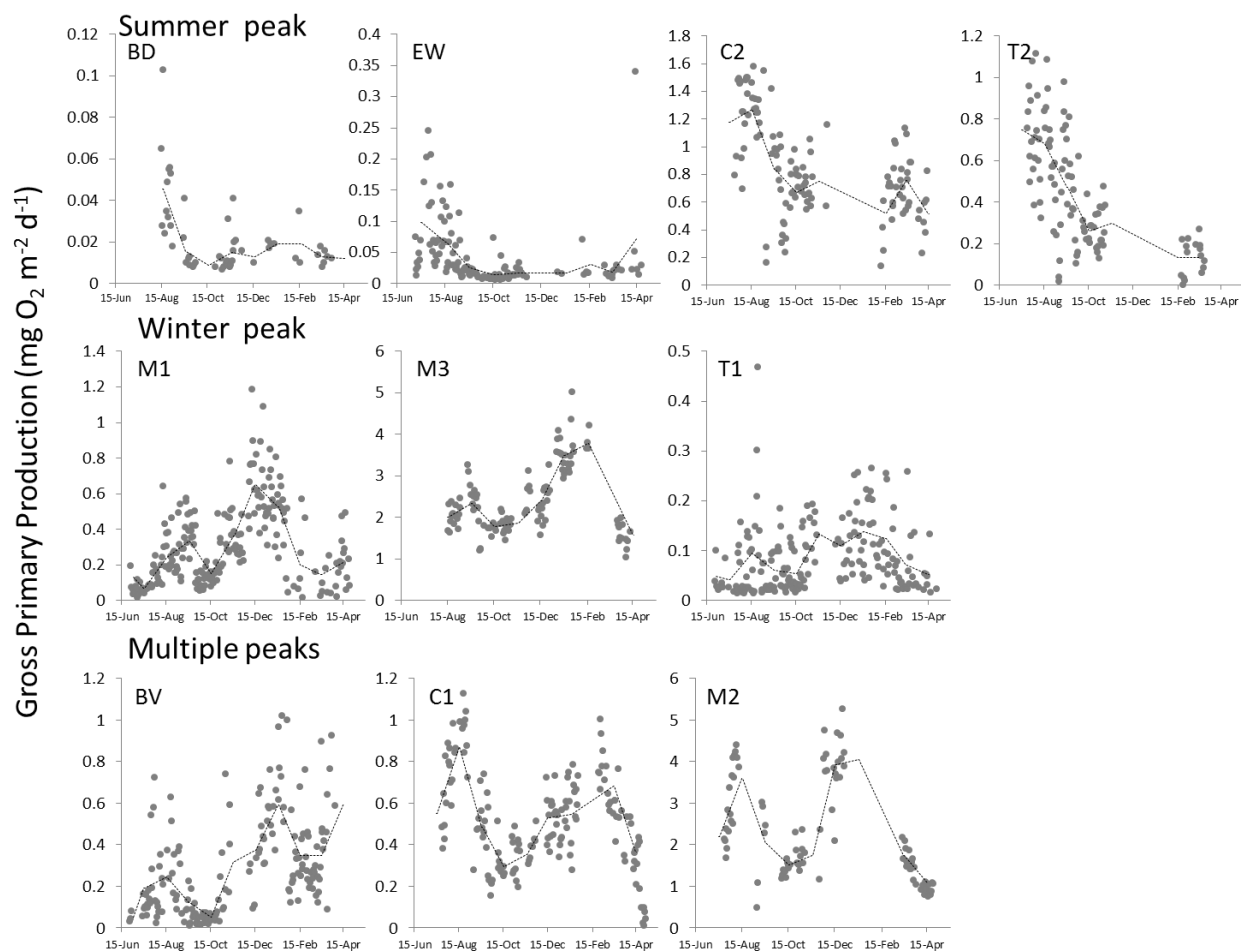
Appendix 1

Appendix 1 -Table 1: Correlation matrix for untransformed mean annual GPP, ER, and covariates. Pearson correlation coefficients and p- values. GPP=gross primary production, |ER|=absolute value of ecosystem respiration, NEP=net ecosystem production, Chl-a =Chlorophyll-a, AFDM=ash free dry biomass, PAR=photosynthetically active radiation, TEMP=temperature, DIN=dissolved inorganic nitrogen, SRP=soluble reactive phosphorus, CON=channel confinement, DA=drainage area, Q=discharge. Bold represents significant correlations.

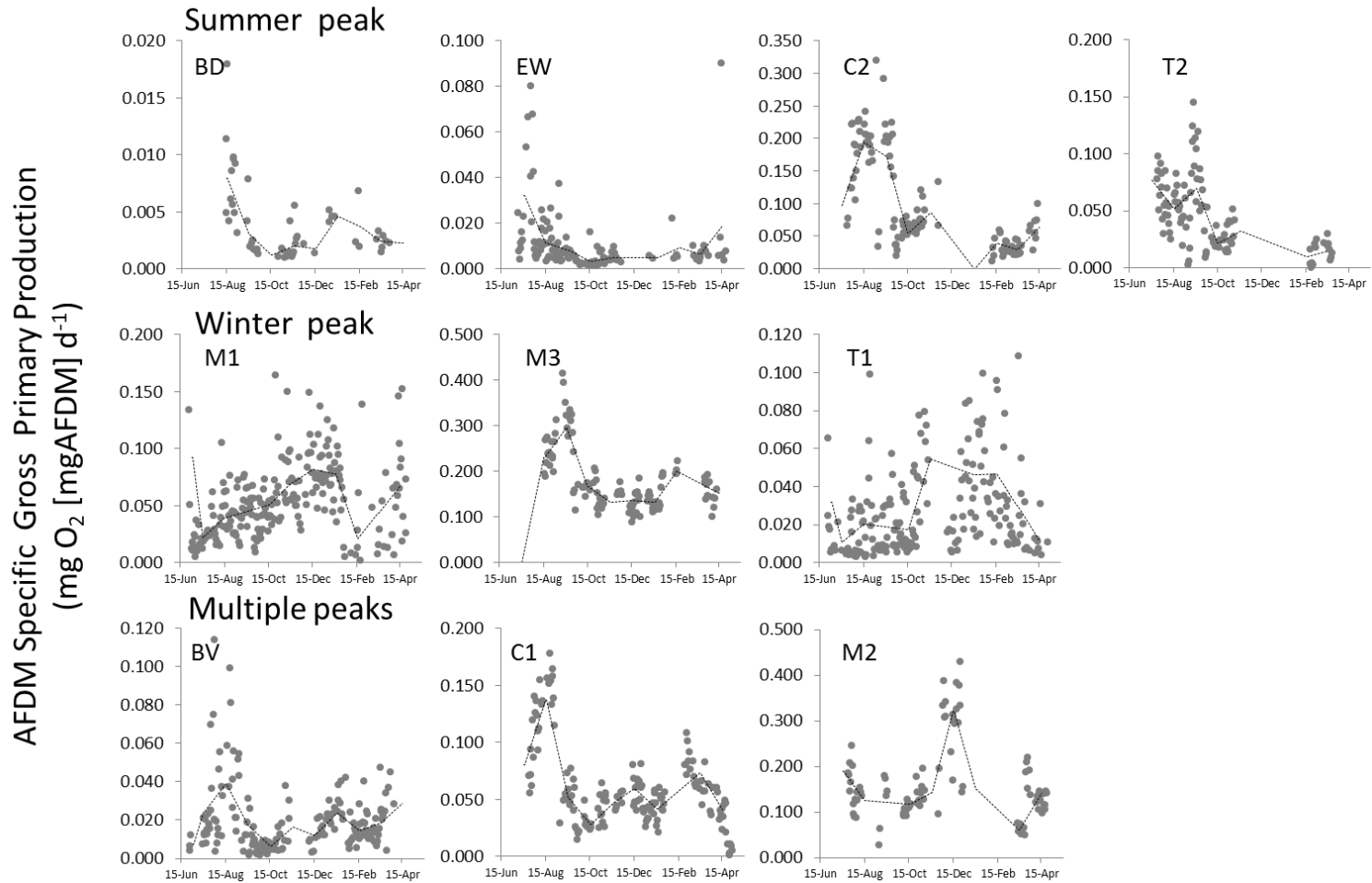
Variable	GPP	ER mg O ₂ m ² d ⁻¹	NEP	Chl-a mg m ⁻²	AFDM g m ⁻²	PAR μmol m ² s ⁻¹	Temp °C	DIN mg l ⁻¹	SRP mg l ⁻¹	Conf	DA Km ²
ER	0.93										
p-value	0.000										
NEP	-0.051	-0.406									
p-value	0.889	0.244									
Chl-a	0.28	0.157	0.275								
p-value	0.433	0.664	0.442								
AFDM	0.72	0.628	0.081	0.82							
p-value	0.019	0.052	0.825	0.004							
PAR	0.365	0.409	-0.213	0.304	0.375						
p-value	0.300	0.241	0.555	0.393	0.286						
Temp	0.097	0.095	-0.025	0.041	0.191	0.56					
p-value	0.790	0.794	0.945	0.910	0.597	0.093					
DIN	0.265	0.132	0.31	0.93	0.68	0.265	-0.081				
p-value	0.459	0.717	0.384	0.000	0.031	0.460	0.825				
SRP	-0.248	-0.378	0.424	0.62	0.283	-0.355	-0.399	0.56			
p-value	0.490	0.281	0.222	0.056	0.428	0.315	0.254	0.091			
Conf	0.535	0.67	-0.488	-0.276	0.022	0.488	-0.054	-0.158	-0.59		
p-value	0.111	0.036	0.152	0.440	0.952	0.153	0.882	0.663	0.073		
DA	0.98	0.96	-0.187	0.16	0.634	0.411	0.12	0.141	-0.338	0.65	
p-value	0.000	0.000	0.604	0.660	0.049	0.238	0.740	0.698	0.340	0.043	
Q (m ³ s ⁻¹)	0.90	0.85	-0.084	0.061	0.466	0.546	0.116	0.086	-0.391	0.74	0.93
p-value	0.000	0.002	0.818	0.866	0.175	0.102	0.749	0.814	0.264	0.015	0.000

Appendix 2

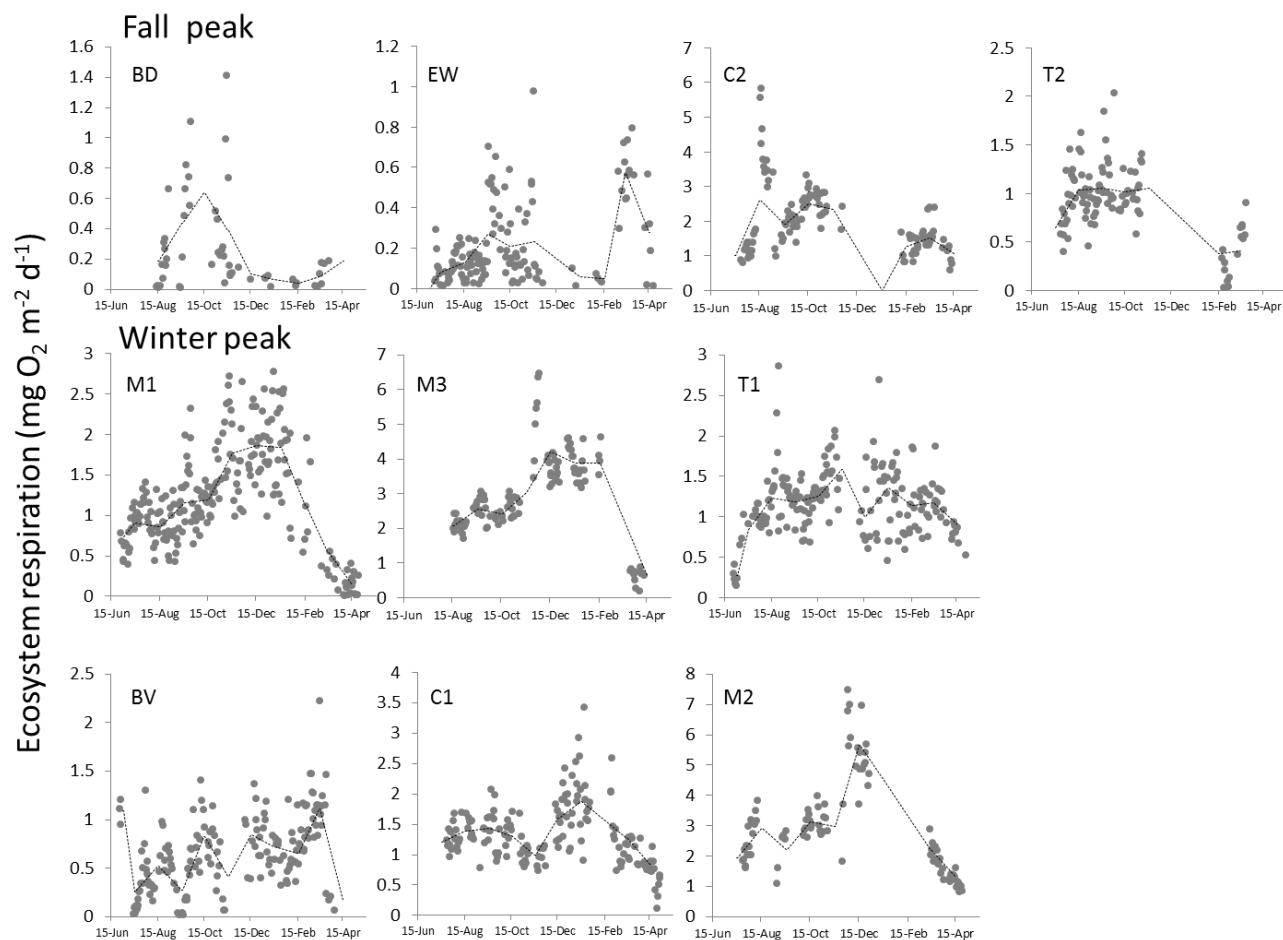
Appendix 2-Figure 1: Daily gross primary production (GPP) measured across 10 sites within the Methow River network. GPP are in $\text{mg O}_2 \text{ m}^{-2} \text{ d}^{-1}$. Gray line represents moving average. Stream reaches, BD, EW, C2 and T2 were partially frozen from mid December to mid February.



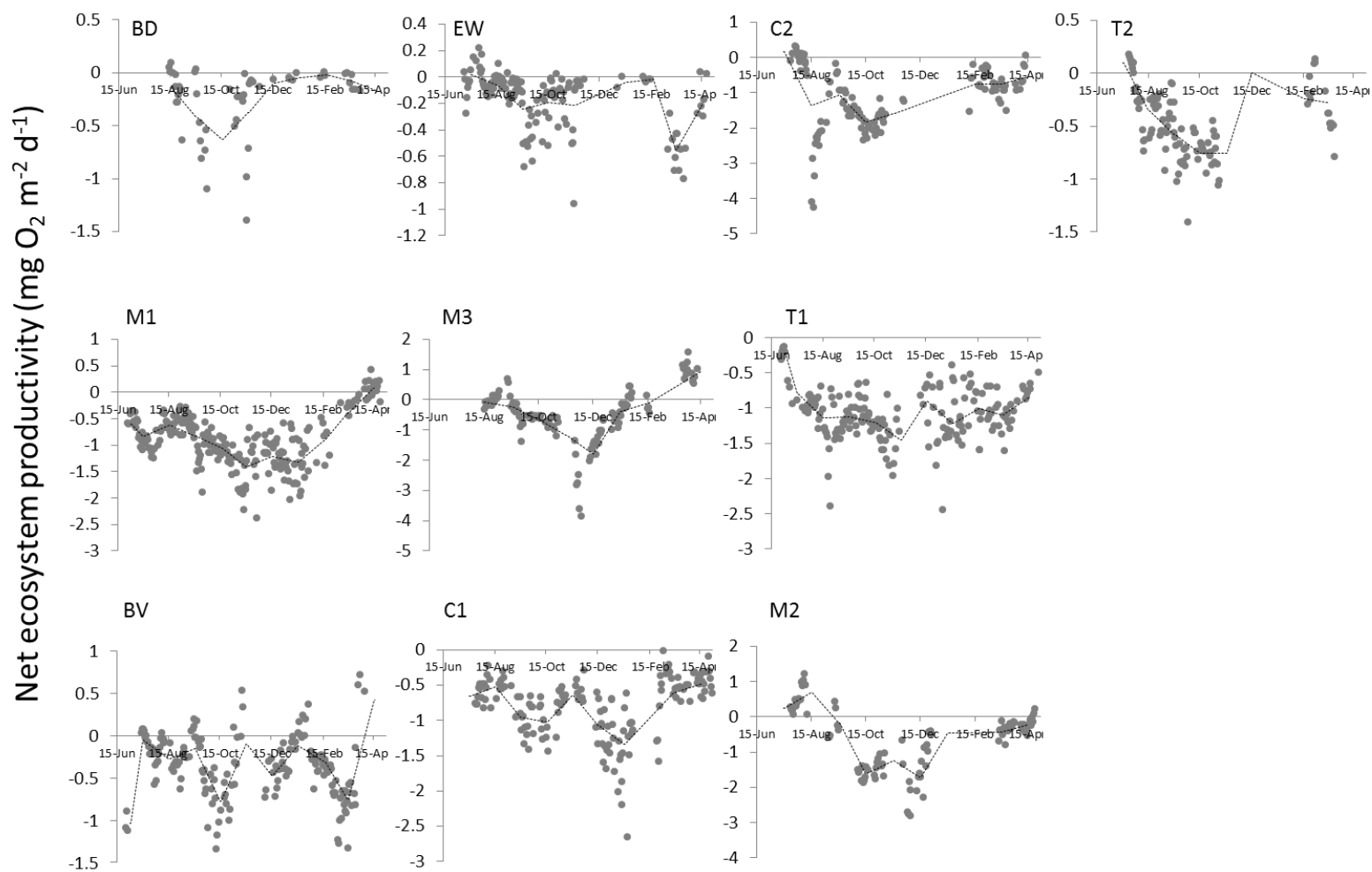
Appendix2-Figure 2: Daily AFDM specific gross primary production measured across 10 sites within the Methow River network. GPP are in $\text{mg O}_2 \text{ g[AFDM]} \text{ d}^{-1}$. Gray line represents moving average. Stream reaches, BD, EW, C2 and T2 were partially frozen from mid December to mid February.



Appendix2-Figure 3: Daily ecosystem respiration (ER) measured across 10 sites within the Methow River network. |ER| are absolute values in $\text{mg O}_2 \text{ m}^{-2} \text{ d}^{-1}$. Gray line represents moving average. Stream reaches, BD, EW, C2 and T2 were partially frozen from mid December to mid February.

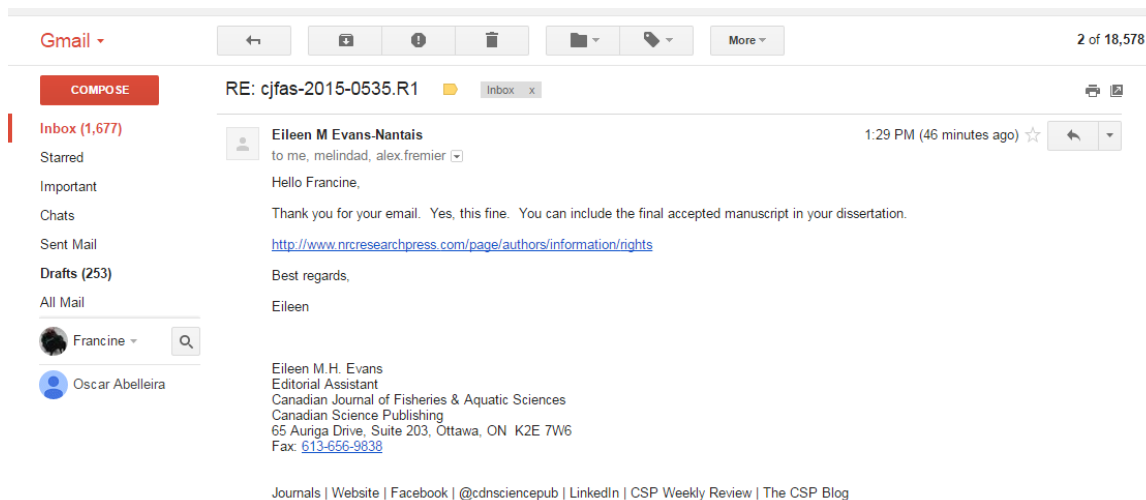


Appendix2-Figure 4: Daily net ecosystem production (NEP) measured across 10 sites within the Methow River network. NEP are in $\text{mg O}_2 \text{ m}^{-2} \text{ d}^{-1}$. Gray line represents moving average. Stream reaches, BD, EW, C2 and T2 were partially frozen mid-December to mid February.



Appendix 3

Email confirmation of Chapter 2 for publication rights in the Canadian Journal of Fisheries and Aquatic Sciences.



Information from the link included in the email above:

Authors' rights:

As of 2009, copyright of all articles in NRC Research Press journals remains with the authors. Copyright of all articles published prior to 2009 is held by Canadian Science Publishing (operating as NRC Research Press) or its licensors (also see our Copyright and Reuse of Content information).

Under the terms of the license to publish granted to NRC Research Press, authors retain the following rights:

To post a copy of their submitted manuscript (pre-print) on their own website, an institutional repository, a preprint server, or their funding body's designated archive (no embargo period). Publication on a preprint server prior to submitting to an NRC Research Press journal does not constitute “prior publication”.

To post a copy of their accepted manuscript (post-print) on their own website, an institutional repository, a preprint server, or their funding body's designated archive (no embargo period). Authors who archive or self-archive accepted articles are asked to provide a hyperlink from the manuscript to the Journal's website.

Authors, and any academic institution where they work at the time, may reproduce their manuscript for the purpose of course teaching.

Authors may reuse all or part of their manuscript in other works created by them for non-commercial purposes, provided the original publication in an NRC Research Press journal is acknowledged through a note or citation.

These authors' rights ensure that NRC Research Press journals are compliant with open access policies of research funding agencies, including the Canadian Institutes of Health Research, the Natural Sciences and Engineering Research Council of Canada, the US National Institutes of Health, the Wellcome Trust, the UK Medical Research Council, l'Institut national de la santé et de la recherche médicale in France, and others.

In support of authors who wish or need to sponsor open access to their published research articles, NRC Research Press also offers a Gold Open Access (OpenArticle) option.

The above rights do not extend to copying or reproduction of the full article for commercial purposes. Authorization to do so may be obtained by clicking on the "Reprints & Permissions" link in the Article Tools menu of the article in question or under license by Access Copyright. The Article Tools menu is accessible through the full-text article or abstract page.